MESENCHYMAL STEM CELLS AND SECRETED FRIZZLED RELATED PROTEIN 2; ENHANCING THE HEALING POTENTIAL

By

Maria Paula Alfaro

Dissertation

Submitted to the Faculty of the

Graduate School of Vanderbilt University

in partial fulfillment of the requirements

for the degree of

DOCTOR OF PHILOSOPHY

In

Pathology

May, 2011

Nashville, Tennessee

Approved:

Ethan Lee M. D., Ph. D.
Antonis Hatzopoulos Ph. D.
Andries Zijlstra Ph. D.
Jeffrey Davidson Ph. D.
Larry Swift Ph. D., Chair

To my amazing family, the bright reflection of God’s beauty

ACKNOWLEDGEMENTS

I hope that those of you who have touched my life truly know how appreciative I am of your love and support. Without you this work would not be possible.

God's first gift to me was to place me in my parents' arms at birth. Thank you, mom and dad, for your seemingly infinite love for me. Your sacrifices and hard work have made my life wonderful and rich. Thank you for the opportunities you have allowed me to experience and for enjoying them with me. My most fervent wish is to make you proud and to see you smiling. ¡Los amo, son los mejores papitos del mundo!

My fantastic husband is who makes my everyday happy. Thank you dear for your joy and love and for accepting to go through life next to me; I am blessed to have you by my side. Our beautiful daughter is the most awe inspiring gift I have ever gotten. I wish to make both of you proud as well.

The encouragement I have gotten from the rest of my family surpasses what I deserve. I learn from each and every one of you and will continue to grow from the substance you add to my life. Our family is an incalculable treasure.

Particularly as it pertains to my scientific and professional growth, I am forever grateful to Dr. Pampee Young. I cannot imagine a better mentor, a fantastic role-model who has successfully pushed me to be the best I can be.

I am obliged to also mention the funding sources: R01-HL088424 (P. Young), HL08842402S1 (P. Young), RO1-GM081635 (E. Lee), 2RO1AG006528-

21 (J. Davidson); VA merit award (P. Young); GI SPORE P50CA95103 (E. Lee); and AHA 09PRE2010035 (M. Alfaro).

TABLE OF CONTENTS

LIST OF TABLES

LIST OF FIGURES

LIST OF NOMENCLATURE

ALK - anaplastic lymphoma receptor tyrosine kinase
Ang-1 – Angiopoietin 1
ANOVA – Analysis of Variance
BM – Bone Marrow
BMP – Bone Morphogenic Protein
BrdU - Bromodeoxyuridine (5-bromo-2-deoxyuridine)
CAM – Chick Chorioallantoic Membrane
CD – Cluster of Differentiation
CM – Conditioned Media
CRD – Cystein Rich Domain
CTGF – Connective Tissue Growth Factor
CXCR - Chemokine, CXC Motif, Receptor
DAPI - 4',6-diamidino-2-phenylindole
Dkk1 – Dickkopf-related protein 1
DNA – Deoxyribonucleic Acid
EF – Ejection Fraction
ELISA - Enzyme-linked immunosorbent assay
FACS – Fluorescent Activated Cell Sorting
FGF – Fibroblast Growth Factor
FITC – Fluorescein
FPR – N-formyl Peptide Receptor
FS – Fractional Shortening
GFP – Green Fluorescent Protein
GO – Gene Ontology
GVHD – Graft Versus Host Disease
HEK – Human Embryonic Kidney
HGF – Hepatocyte Growth Factor
HLA – Human Leukocyte Antigen
HO1- Hemeoxygenase 1
HSC – Hematopoietic Stem Cell
ID – DNA-binding protein inhibitor
IF – Immunofluorescence
IGF1 – Insulin-like Growth Factor 1
IL – Interleukin
IL-1RN – Interleukin 1 Receptor Antagonist
IV – Intravenous
L – Lumen
LC – Liquid Chromatography
LiCl – Lithium Chloride

LIF – Leukemia Inhibiting Factor
Lin – Lineage
LRP - Lipoprotein Receptor-Related Protein
LV – Left Ventricle
LVIDD – Left Ventricular Internal Diameter Diastole
LVIDS – Left Ventricular Internal Diameter Systole
MHC – Major Histocompatibility Complex
MI – Myocardial Infarction
MS – Mass Spectroscopy
MSC – Mesenchymal Stem Cell
MT1-MMP – Membrane Tethered 1-Matrix Metalloprotease
N/T – No Treatment
NOD/SCID – Non Obese Diabetic/Severe Combined Immunodeficient
ns – not significant
OD – Optical Density
PBS – Phosphate Buffered Saline
PE – Phycoerythrin
PECAM-1 - Platelet Endothelial Cell Adhesion Molecule
PGE2 – Prostaglandin 2
PlGF – Platelet-derived Growth Factor
PPAR-γ – Peroxisome proliferator-activated receptor-gamma
pSMAD 1/5/8 – phosphorylated Smads 1, 5 and 8
PVA – Poly-vinyl Alcohol
qRT-PCR – quantitative Real Time Polymerase Chain Reaction
REPAIR-AMI - Reinfusion of Enriched Progenitor cells And Infarct Remodeling in Acute Myocardial Infarction
SCA – Stem Cell Antigen
SCF – Stem Cell Factor
SD – Standard Deviation
SDF1-α – Stromal Derived Factor 1-alpha
SEM – Standard Error Mean
sFRP – secreted Frizzled-Related Protein
shRNA – Short Hairpin Ribonucleic Acid
siRNA – silencing Ribonucleic Acid
SP – Sponge
Szl – Sizzled
TCA – Trichloro Acetic Acid
TGF-β1 – Transforming Growth Factor-beta 1
TNF-α – Tumor Necrosis Factor-alpha
VEGF – Vascular Endothelial Growth Factor
WT – Wild Type
Xlr – Xolloid-related
β-gal – beta galactosidase

β-gluc – Beta-glucuronidase
Δ% - Percent Difference

CHAPTER I

LESSONS FROM GENETICALLY ALTERED MESENCHYMAL STEM CELLS (MSCs); CANDIDATES FOR IMPROVED MSC-DIRECTED MYOCARDIAL REPAIR

Introduction

The regenerative and reparative potential of Mesenchymal Stem Cells (MSCs) make them attractive candidates for numerous cell-directed therapies. The variant degree of tissue repair by transplanted MSCs has been assessed in several published reports. There are many gaps in the knowledge of MSC biology and the underlying reasons for their disparate effectiveness in tissue repair. This chapter examines successful pre-clinical models of MSC-directed repair, particularly of myocardial repair, in an attempt to shed light into the events dictating MSC therapeutic efficacy. The reparative advantage of genetically altered MSCs will be described. This overview will elucidate possible molecular mechanisms that can influence MSC engraftment, differentiation, self-renewal, and ultimately increase wound repair.

Mesenchymal Stem Cell Characterization

MSCs are a heterogeneous population of fibroblastoid cells isolated by their ability to form adherent colonies following low density tissue culture plating conditions [1-3]. There are variable methodologies for the initial isolation of the MSCs[1, 4]. Physical dissociation of the starting tissue may or may not be

followed by immuno-depletion of unwanted cells to attain a starting population [5]. Once isolated, MSCs can be expanded *in vitro* in serum-containing media to attain a characteristic spindle-like shape [4]. Although bone marrow (BM)-derived MSCs will be the focus of this review, reviews concerning MSCs isolated from adipose tissue [6] umbilical cord blood [7, 8] and fetal tissues [9] are available. Regardless of the source, MSCs retain the pluripotent ability to differentiate into distinct mesenchymal lineages, particularly the adipogenic, chondrogenic and osteogenic [10, 11].

Table 1 contains a short list of cell surface markers that characterize the antigenic phenotype of murine BM-derived MSCs; their categories and the appropriate references are included. To separate the MSCs from any hematopoietic contaminants of the BM, most investigators have agreed that murine MSCs must not express the protein tyrosine phosphatase CD45 ($CD45^-$) or markers of hematopoietic lineages such as B-cells or T-cells (Lin^-). MSCs must also express the Stem Cell Antigen 1 ($Sca1^+$) as well as the cell adhesion molecule, HCAM ($CD44^+$).

A large amount of data is available which characterizes human MSCs [11, 12]. The minimal criteria to define human MSCs have been established by the Mesenchymal and Tissue Stem Cell Committee of the International Society for Cellular Therapy. Human MSCs must express CD105, CD73 and CD90, and lack expression of CD45, CD34, CD14 or CD11b, CD79alpha or CD19 and HLA-DR surface molecules [13].

Table 1 – Antigenic Phenotype of Murine MSCs

	Identity	Expression	References
Adhesion Molecule	CD44, CD106	+	[1, 3, 14-16]
	CD9, CD54, CD62P, CD138	+	[14, 16]
	CD31	-	[1, 2, 14, 15]
	CD62L	-	[14]
	CD29	+	[1, 3, 15]
	CD48	-	[1, 15]
Hematopoietic Marker	CD90	-	[14, 15]
	CD90, CD11b, CD34,	-	[1, 15, 16]
	CD45	-	[1, 2, 14-16]
	Lineage (CD4, CD5, CD8, B220, Mac-1, Gr-1)	-	[2, 17]
Growth factor receptor	CD105, CD117, CD126, Flk-1	+	[14]
	CD117, CD135	-	[1, 15]
Other	CD81	+	[1, 15]
	SCA-1	+	[1-3, 14-16]
	Nucleostemin	+	[15]
	Oct-4	-	[15]

Abbreviation: Cluster of Differentiation (CD)

The above description of the isolation, epitope identification and expansion of MSCs points to the fact that there is variability in the definition of MSCs. Variations in the biological activities of these cells are present between isolates and passages [18-20]. The consensus reached to define human MSCs is addressing this point; however, no such consensus exists for the murine MSC field. Moreover, the description of the nature of MSCs has relied on the *in vitro* characterization of these cells due to the lack of a definitive antigen *in vivo.*

Do MSCs Exist *in vivo*?

A large body of evidence has emerged which document the presence of stem cells within the neural crest of the vertebrate embryo. *In vitro* analysis of a subset of these stem cells has demonstrated that they have mesenchymal properties. These studies suggest the identification of the source of MSCs in the developing embryo and several reviews on these are available [21, 22]. Signaling cascades involved in the *in vivo* generation of these neural crest mesenchymal progenitor cells have been identified [23, 24].

In the adult, a hypothesis which equates MSCs to pericytes or vascular-associated mesenchymal cells has been proposed [25-27]. The work of Simmons *et al.* demonstrated that bone marrow-derived cells isolated by virtue of their STRO-1 positivity had MSC qualities [25]. This work has since been validated, demonstrating the *in vitro* differentiation capabilities of this fibroblastoid population [25, 28]. The STRO-1^+ cells were localized to blood vessel walls of human bone marrow sections, strengthening the perivascular hypothesis [29]. Pericytes were detected in several human tissues (all known sources of MSCs) and when isolated gave rise to MSCs *in vitro* [27]. Interestingly, these pericytes expressed several known MSC markers in their native *in vivo* state [27]. Although proof of endogenous MSCs or MSC-like pericytes has been documented, their role in tissue repair is not understood. Among other things, it is still unclear whether these tissue resident cells migrate to sites of injury or solely secrete factors that contribute to wound healing [30].

Main Clinical Applications

The National Library of Health provides information about ongoing clinical trials at http://clinicaltrials.gov [31]. Currently, there are 73 clinical trials in which bone marrow-derived MSCs are to be administered as therapy for a variety of human conditions. Table 2 contains a list of these conditions, the number of trials engaged in the particular disease, and the method of administration of MSCs.

Table 2 –MSCs as Therapy, Current Clinical Trials and their Method of Administration (Clinicaltrials.gov)

Condition	Number of Trials	Administration
Graft Versus Host Disease	14	Intravenous (I.V.)
Myocardial Infarction	10	Intramyocardial, Transedocardial Injection, I.V.
Organ Transplant/Rejection	6	I.V.
Articular Cartilage Defects	5	Surgical Implantation, Intraarticular Injection
Multiple Sclerosis	3	I.V., Intra-thecal Injection
Cirrhosis	3	I.V., Intra-arterial
Crohn's Disease	3	I.V.
Ventricular Dysfunction	2	Intramyocardial, Transedocardial Injection
Degenerative Disk Disease	2	Surgical Implantation
Type I Diabetes	2	I.V.
Type II Diabetes	2	Intramuscular Injection, I.V.
Systemic Lupus Erythematosus	2	I.V.
Bone Neoplasms	1	Surgical Implantation
Cronic Obstructive Pulmonary Disease	1	I.V.
Parkinson's Disease	1	Implanted into Striatum
Primary Sjogren's Syndrome	1	I.V.
Ischemic Stroke	1	I.V.
Systemic Sclerosis	1	I.V.
Critical Limb Ischemia	1	Intramuscular Injection
Osteonecrosis of Femoral Head	1	I.V.
Multiple System Atrophy	1	Intra-arterial
Tibial Fracture	1	Surgical Implantation
Amyotrophic Lateral Sclerosis	1	Intramuscular Injection
Tibia or Femur Pseudo-arthritis	1	Surgical Implantation
Adult Periodontitis	1	Surgical Implantation
Non-malignant Red Blood Cell Disorders	1	I.V.
Neuroblastoma	1	I.V.
Osteodysplasia	1	I.V.
Epidermolysis Bullosa	1	I.V.
Osteogenesis Imperfecta	1	I.V.
TOTAL	**73**	

Homing to Sites of Injury

The data included in Table 1 clearly demonstrate that the primary form of MSC transplantation, in 20 out of 30 conditions (67%), is intravenous. This form of administration takes advantage of the homing capacity of MSCs. Clinicians are relying on the ability of MSCs to travel through the vasculature and localize within injured tissue [32-34].

The effectiveness of homing ability varies between published pre-clinical reports. One explanation for this was delineated by Rombouts *et al.* by demonstrating that GFP-tagged murine MSCs lose their homing abilities in a syngeneic mouse model following prolonged *in vitro* expansion [14]. Recently, several groups have shown that regulation of the CXC Chemokine Receptor 4 (CXCR4) and its ligand, Stromal-Derived Factor 1-alpha (SDF1-α), play an important role in the motility of human and rodent MSCs [35, 36]. Shi *et al.* demonstrated that incubation of MSCs in medium containing five cytokines (Flt-3 ligand, SCF, IL-6, HGF and IL-3) resulted in up-regulation of both cell surface and intracellular CXCR4 [35]. Tail vein injection of cytokine-cultured, and thus CXCR4-expressing, MSCs into sub-lethally irradiated NOD/SCID mice increased the homing to the bone marrow by seven fold; albeit an increase in detection from 0.03% to 0.2% of the injected cells only 24 hours post-transplant [35]. This indicates that even in optimized conditions the efficacy of targeting is far less than 1%. The *in vitro* culture conditions in which the MSCs are expanded have an effect on the expression of CXCR4; 1-day exposure to hypoxia (1% oxygen tension) was sufficient to increase CXCR4 and CX3CR1 mRNA and protein

levels enough to positively impact MSC migration and engraftment in a xenograft chick embryo model; this, however, was only an increase in engraftment from 0.3% to 0.9% [37].

There are other ligands and receptors involved in MSC migration besides the SDF1-α and CXCR4 axis. Hepatocyte Growth Factor (HGF) and its receptor c-met increase the migration ability of MSCs *in vitro [38]* and have been implicated in the recruitment of MSCs to the site of injury [39]. Human MSCs express the N-formyl peptide receptor (FPR) suggesting they are able to migrate to inflammatory sites where N-formylated peptides are present in the same way immune cells home to injury [40].

Migrating to the site of injury is only part of the challenge MSCs face for clinical application. MSCs must be able to traverse the 3-dimensional connective tissue. Type I collagen is the dominant extracellular matrix molecule found in mammalian tissues [41] and so MSCs must be capable of proteolytic degradation of this component to invade and extravasate into the tissue. The membrane-tethered 1 matrix metalloproteinase (MT1-MMP) has been recently shown to be involved in human MSC trafficking, *in vitro* and *in vivo* [42]. MSCs were able to traverse type I collagen matrices 2-D and 3-D *in vitro* systems, and this activity was blocked completely by siRNA silencing of MT1-MMP. The chick chorioallantoic membrane (CAM) was used to confirm these results *in vivo*. Within 2 days of their placing on top of the membrane, hMSCs invaded the CAM surface and were detected in the underlying stroma; MT1-MMP silencing abrogated their invasive capabilities [42].

Understanding the genes/proteins involved in MSC homing, and their ability to remodel the collagenous extracellular matrix, will ultimately help increase their therapeutic efficiency. The CXCR4/SDF1-α signaling components seem to be important in the recruitment of MSCs. MT1-MMP seems involved in the degradation and penetration of type I collagen tissue barriers. Further work is needed to elucidate the regulation of the 'homing' signature necessary for improved migration, invasion and extravasation of MSCs into targeted tissues.

Immuno-modulatory Properties

Further observation of Table 2 provides an interesting find. Fourty four percent (32/73) of the current clinical trials are utilizing MSCs for their immuno-modulatory properties. In conditions like graft versus host disease (GVHD), Crohn's Disease, Primary Sjogren's Syndrome, Organ Transplantation/Rejection, Systematic Sclerosis, Type I Diabetes, Systemic Lupus Erythematosus, Multiple Sclerosis, Neuroblastoma, and Non-malignant Red Blood Cell disorders, MSCs are being transplanted as treatment by themselves or as adjunct therapy.

The biology behind the effects of MSCs on the immune system is mostly unknown; however, a few experimental models have elucidated some of the key molecular players involved in the anti-inflammatory role of MSCs. One of these models is a rat renal transplantation model where MSCs injections increased overall survival of the recipient animals due, in part, to a decrease in interleukin-1α (IL-1), tumor necrosis factor α (TNF-α), and transforming growth factor (TGF)-β1[43]. The authors of this work remind us that there are still unknowns as they

note that adjunct Cyclosporine A (a powerful immunosuppressant, non-steroidal) treatment further increases the survival of the rats and further diminishes the levels of the inflammatory cytokines [44].

Other models have shown a similar effect of MSCs on the down-regulation of the immune function. Such is a rodent model of interstitial lung disease, where bleomycin (a cytotoxic glycopeptide antibiotic)[45] treatment induces pulmonary fibrosis and concomitant inflammation[46]. Following induction of the disease, Ortiz *et al*. treated the mice with MSCs and demonstrated a decrease in the levels of two important pro-inflammatory cytokines: TNF α and IL-1α[15]. This group demonstrated the anti-inflammatory capacity of MSCs in this setting due to the expression of interleukin-1 receptor antagonist (IL-1RN). These results were confirmed by *in vitro* assays in which MSC-conditioned media decreased the proliferation of an IL-1 responsive T-cell population[15].

Studies using an experimental autoimmune encephalomyelitis model demonstrated that MSCs were able to suppress T-cell activation *in vitro* and *in vivo*, and this effect was partially reversible by the addition of IL-2[16]. In this case, the authors suggest that the limited expression of MHC class II molecules as well as lack of co-stimulatory molecules, such as CD80, CD86, and CD40, on MSCs may be the reason behind the T-cell inactivation. A more detailed study on secreted factors in MSC conditioned media demonstrated that neither IL-10, TGF-β1, nor prostaglandin E2 (PGE2) were responsible for the T-cell inhibition[47].

The roles of MSCs in immune suppression have been partially described and the molecular mechanism behind this capacity remains elusive. Further studies on the effects of IL-1RN on T-cells might give insight into how MSCs inhibit inflammation and prevent T-cell activation.

Myocardial Infarction (MI) Therapy

The second most common application for MSCs in the clinic is treatment for ventricular dysfunction and myocardial repair [31]. Although ten current trials are underway utilizing MSCs in the setting of MI very little clinical data have been gathered. A private company, Osiris Therapeutics recently published clinical results demonstrating that MSC transplantation proved a safe therapy with increased benefits (increased left ventricular ejection fraction and reversed remodeling) compared to the placebo-treated group [48]. Although these data are exciting, it is important to note that this study had a relatively small sample size (n=53), a follow-up time of only 6 months, and is the first to show an overall statistical improvement in heart function in all MSC-treated patients (global symptom score p=0.027). Because the available clinical data are scarce, many investigators are trying to dissect the necessary events, and the molecular mechanism that drive them, for MSCs to positively affect the heart following MI.

Possible Mechanisms of MSC-Mediated Repair

Figure 1 shows the possible results of the transplanted cells within the site of injury. Regardless of whether the mechanism of repair reflects their differentiation (direct contribution) or paracrine effects, the MSCs must be able to successfully reach the wound, survive and expand within it. This section will focus on the molecular mechanisms thought to be involved in these events by looking at the effects of genetically altered MSCs in pre-clinical models of myocardial repair.

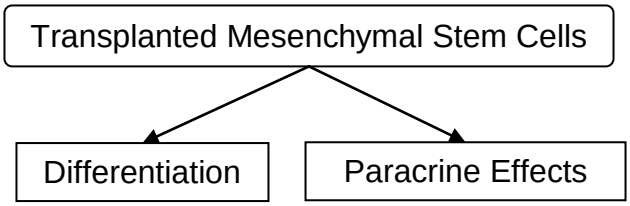

Figure 1. Possible Effects of MSCs on Injured Tissue

Cardiogenic Differentiation of MSCs within Infarcted Myocardium

As early as 1999, researchers noticed that MSCs could be differentiated *in vitro* (by 5-azacytidine treatment) into beating, MEF-2A and MEF-2D expressing cardiomyocytes [49]. More recent work has demonstrated that these cells express functional adrenergic and muscarinic ($ß_1$, $ß_2$, M_1, and M_2) receptors after 5-azacytidine treatment *in vitro* [50]. Instead of using this potentially toxic inhibitor of DNA methylation to derive cardiomyocytes from MSCs, Behfar *et al*.

developed a “cardiogenic cocktail” [51]. This mix of trophic factors include TGF-β1, Bone morphogenetic protein 2 (BMP2), IGF1, Fibroblast growth factor 4 (FGF4), Interleukin-6, Leukemia inhibitory factor (LIF), α-Thrombin, Vascular endothelial growth factor A (VEGF-A), TNF-α, and Retinoic acid. The cocktail was able to drive the nuclear expression of cardiac Nkx2.5 and MEF-2C providing insight into the molecular mechanisms and signaling pathways that govern MSC cardiogenic differentiation [51]. This *in vitro* phenomenon suggested MSCs could be a novel therapy used to regenerate damaged cardiac tissue and it prompted investigators to look for the *in vivo* differentiation of MSCs into cardiomyocytes following their administration.

GFP-tagged Lin^- c-kit^+ MSCs injected into the peri-infarct area following coronary artery ligation were fully incorporated into the myocardium and seemed to give rise to new, regenerated tissue after only 9 days [17]. These results seem unique as several studies of this nature revealed that the level of *in vivo* cardiogenic differentiation of MSCs is very low [34, 52] or completely lacking [53]. Instead of MSC-derived regeneration of the heart, researchers have shown a fusion event of MSCs with injured cardiomyocytes [54].

Despite the low levels of direct contribution of the MSCs to the myocardium, MSCs have a positive effect in the function and remodeling of injured myocardium [55, 56], albeit to varying degrees. It is widely accepted that the most probable effect of the MSCs in the site of injury is to supply the wound with soluble factors that enhance the repair process.

Secreted Factors Involved in Cardiac Reperfusion by MSCs

An ischemic environment is a direct consequence of coronary artery occlusion [57]. The severity of the occlusion may lead to myocardial death and necrosis [58]. Neovascularization nourishes the wounded tissue with the necessary nutrients and oxygen supply to prevent further tissue damage and increase repair [59]. Several reports have demonstrated that MSCs induce VEGF expression, and therefore, neovascularization in ischemic myocardium [60-62]. *In vitro* analysis of MSC-conditioned media (MSC-CM) demonstrated that MSCs themselves secrete a variety of angiogenic factors, among them VEGF and Placental growth factor (PlGF); and that these are up-regulated in response to hypoxic culture conditions [63]. Together, these studies suggest that MSCs may play a role on the reperfusion of the infarcted myocardium.

Matsumo *et al.* reported that the adenoviral overexpression of VEGF by MSCs (VEGF-MSCs) increases capillary density (approximately 2-fold) in the VEGF-MSC-treated hearts 28 days post MI. In this study, the MSCs were followed by beta-galactosidase expression and the number of dual alpha smooth muscle actin and LacZ positive cells was increased approximately 4-fold in the treatment group. These authors suggest that the trans-differentiation of MSCs to endothelial progeny led to a significant increase in cardiac function and a significant decrease in infarct size in the VEGF-MSC-treated group [64].

Erythropoietin (Epo) is involved in neovascularization of damaged tissue [65, 66] and thus increased vascular density was observed in the infarcted hearts treated with Epo-overexpressing-MSCs [53]. Without data to indicate endothelial

trans-differentiation of MSCs, the authors conclude the MSCs were accessory to the newly formed blood vessels. The secretion of trophic factors, especially Epo, was what ultimately improved cardiac function post MI.

Increased Myocardial Survival in Response to the MSC Secretome

The MSC-secreted factors seem to have more than just pro-angiogenic effects; MSC treatment reduces the apoptotic index within the peri-infarct area [67, 68]. *In vitro*, cultured cardiomyocytes have improved survival in hypoxic conditions when treated with MSC-CM [55] or in co-culture experiments [68-70]. An important pro-survival factor, Akt, has been shown to be expressed by MSCs in response to hypoxia [68]. Overexpression of Akt in MSCs (Akt-MSCs) increased their survival compared to control but importantly, injection of their MSC-CM to the myocardium following MI had a significantly positive effect on the apoptotic index of the cardiomyocytes [71].

Microarray analysis performed on the CM obtained from Akt-MSCs documented the presence of sFRP2 [71]. Both rat cardiomyocytes *in vitro*, as well as infarcted mice cardiomyocytes *in vivo*, had decreased apoptosis when treated with CM from the Akt-MSCs. The pro-survival effect on the cardiomyocytes was due to sFRP2 since CM from “Akt-MSCs minus sFRP2” (knocked down sFRP2 expression by siRNA in Akt-MSCs) did not have the same pro-survival effect in either setting. The decrease in cardiomyocyte apoptosis post-MI due to Akt-MSC-CM led to decreased infarct size [71]. It is important to

note that the authors looked at infarct size 72 hours post treatment and that they did not assess any functional cardiac parameters.

When Heme-oxygenase 1 (HO1) was overexpresseed by MSCs (HO1-MSCs), similar effects as the ones described above were observed [72]. This group saw significant decrease in the *in vitro* apoptotic index of the HO1-MSCs compared to the control-MSCs. *In vivo*, HO1-MSC-treated infarcted hearts had increased capillary density but this was attributed to the increase of VEGF by the HO1-MSCs. Transgene expression led to a significant decrease in the apoptotic index of cardiomyocytes in the treatment hearts. HO1-MSC treatment following MI led to a smaller infarct size, decreased ventricular remodeling and increased cardiac function 28 days post-MI. There was no mention of engraftment or differentiation by the MSCs in this report. The authors conclude that the most important role of the transgene was its anti-apoptotic and anti-oxidant effects on the cardiomyocytes [72].

Enhancing MSC Survival in the Wound

Retroviral expression of the pro-survival gene Akt-1 decreased the apoptotic index of MSCs *in vitro*. [73] The authors transplanted the Akt-MSCs, or GFP-MSCs as a control, directly onto the rat myocardium following MI. Although the transgene expression decreased the apoptosis of the MSCs *in vivo,* this analysis was performed 24 hours after the injection. No long-term effect on MSC survival was established. The degree of the incorporation of the MSCs into the tissue was not discussed despite observation of MSC-derived cardiomyocytes.

Improved cardiac function due to Akt-MSC treatment was determined at 2 weeks post-MI, albeit using an *ex-vivo* Langendorff model [73].

Jiang *et al.* tested the *in vivo* efficacy of MSCs transduced with a retroviral vector to express both Akt and Ang-1 [52]. The animals in this study underwent permanent coronary occlusion and were treated with an intramyocardial injection of MSCs. Although the authors claim transgene expression afforded the MSC with increased engraftment, these data were not presented in their publication. Expression of Akt and Ang-1 by MSCs increased blood vessel density within the peri-infarct area and led to a statistical increase in heart function (fractional shortening and ejection fraction) compared to the control media treatment group.

Retroviral overexpression of Epo by MSCs increased the survival both *in vitro* and *in vivo* in a murine subcutaneous implantation model of Matrigel-embedded MSCs [53]. Although assessment of the Epo-MSC- and control-MSC-treated hearts 7 and 14 days post MI did not demonstrate an increase in MSC engraftment or in the MSC-derived cardiac progeny, there was improved cardiac function related with Epo-MSC treatment.

Improving MSC Self-renewal

Whether MSCs work by direct regeneration or through paracrine modulation, MSCs are unable to have a significant effect on the repair process unless a critical mass is attained within the wound (*i.e.* enhanced engraftment). The levels of engraftment of MSCs in pre-clinical models of myocardial repair are low [34, 35, 37]. Few clinical data on the engraftment of MSCs are available that

address long term engraftment. In one example, fewer than 1% donor cells were detected four to six weeks post-infusion on osteogenesis imperfecta patients [74]. Recently, our group demonstrated that retroviral overexpression of sFRP2 by MSCs (sFRP2-MSCs) increased the *in vitro* proliferation [75] and survival of MSCs by modulation of both the BMP and Wnt signaling cascades [76]. This phenomenon provided the MSCs with a survival advantage also observed *in vivo*. Although sFRP2-MSCs showed long-term engraftment within infarcted myocardium approximately 2.5-fold greater than a GFP-MSC control 30 days post-MI [75], the observed degree of engraftment was still modest. The amount of engraftment observed was much greater in another model of tissue repair [75] suggesting engraftment also depends on the wound context. Achieving a critical mass of MSCs by improving their survival and self-renewal capacity should increase their numbers in the damaged tissue.

Conclusion

This chapter described the mechanisms by which MSCs are thought to increase repair by looking closely at their effects on myocardial repair. The involvement of several genes on the ability of the MSCs to home to the site of injury, engraft within the myocardium, give rise to new myocytes/fuse with existing cells and/or increase the vascular content within the wound were discussed. These genes and their documented effects are depicted in Figure 2; the overall division is that of autocrine effects (affecting the MSCs themselves) or paracrine effects (affecting the wounded/infracted tissue). Although much more

work needs to be done to fully understand MSC biology and their reparative capacities, the goal remains to find a gene or set of genes that could have both autocrine and paracrine effects so as to increase MSC-directed repair.

The next chapters will include an in-depth discussion of the activity of sFRP2 on MSC-directed wound and myocardial repair. The molecular mechanism of this protein will be presented and its effects on MSC biology assessed. Ultimately, this compilation aims to demonstrate that sFRP2 enhances the reparative potential of MSCs.

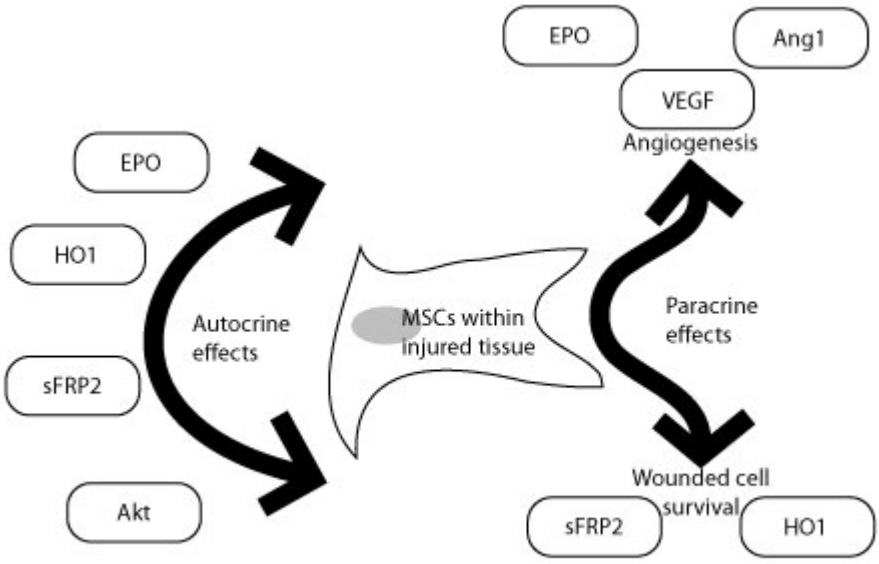

Figure 2. Lessons from Genetically Altered MSCs

CHAPTER II

THE WNT MODULATOR SFRP2 ENHANCES MESENCHYMAL STEM CELL ENGRAFTMENT, GRANULATION TISSUE FORMATION AND MYOCARDIAL REPAIR

Introduction

Cell-based therapies, using MSCs for organ regeneration, are being pursued for cardiac disease, orthopedic injuries and biomaterial fabrication. The molecular pathways that regulate MSC-mediated regeneration or enhance their therapeutic efficacy are, as stated in the previous chapter, poorly understood. We compared MSCs isolated from MRL/MpJ mice, known to demonstrate enhanced regenerative capacity, to those from C57BL/6 wild-type (WT) mice. Compared with WT-MSCs, MRL-MSCs demonstrated increased proliferation, in vivo engraftment, experimental granulation tissue reconstitution, and tissue vascularity in a murine model of repair stimulation. The MRL-MSCs also reduced infarct size and improved function in a murine myocardial infarct model compared with WT-MSCs. Genomic and functional analysis indicated a down regulation of the canonical Wnt pathway in MRL-MSCs characterized by significant up-regulation of sFRPs. Specific knockdown of sFRP2 by shRNA in MRL-MSCs decreased their proliferation and their engraftment in and the vascular density of MRL-MSC-generated experimental granulation tissue. These results led us to generate WT-MSCs overexpressing sFRP2 (sFRP2-MSCs) by retroviral transduction. sFRP2-MSCs maintained their ability for multilineage differentiation in vitro and, when implanted in vivo, recapitulated the MRL phenotype. Peri-

infarct intramyocardial injection of sFRP2-MSCs resulted in enhanced engraftment, vascular density, reduced infarct size, and increased cardiac function after myocardial injury in mice. These findings implicate sFRP2 as a key molecule for the biogenesis of a superior regenerative phenotype in MSCs.

MRL/MpJ "Superhealer" Mouse

To better understand the role of stem cells in regenerative biology, we studied the "superhealer" MRL/MpJ mouse, generated by interbreeding 4 different strains [77]. This strain was found to be capable of completely closing 2 mm surgical ear holes within 30 days whereas control (Bl/6) mice leave residual, open holes [78]. Upon right ventricular cryoinjury, this "superhealer" demonstrated regeneration of the wound with scarless myocardium, whereas the control mice demonstrated acellular scars [79]. Using a BM sex-mismatched transplant model, the authors showed that MRL hearts had 3-fold greater BM-derived cells in the myocardium than uninjured animals or injured WT mice [79]. More recently, the group showed that myocardial regeneration in this model could be recapitulated in WT (C57BL/6) mice after BM engraftment with hematopoietic cells derived from MRL/MpJ fetal liver [80]. This led us to hypothesize that BM-derived cells from the MRL strain may exhibit an enhanced regenerative phenotype. Our findings show enhanced efficacy of BM-derived MRL-MSCs and demonstrate that this phenotype is due to the activity of the Wnt signaling modulator, sFRP2.

Canonical Wnt/β-catenin Signaling

Wnt/β-catenin signaling is necessary for the commitment/differentiation of mesenchymal cells to osteocytes, chondrocytes and adipocytes [81-84]. Consistent with this, the Wnt inhibitor, Dkk1, promotes human MSC self-renewal [85]. sFRP family of proteins bind directly to Wnts to prevent receptor binding and activation of Wnt signaling [86]. Our study shows that sFRP2 directly modulates MSC proliferation and engraftment and that increased sFRP2 expression in MSCs is associated with enhanced therapeutic efficacy of MSC therapy in wound granulation tissue formation and in repair of infarcted myocardium.

Isolation and Characterization of Two Populations of MSCs

Murine MSCs were isolated from both MRL/MpJ (MRL, *n* = 2 independent lines) and Bl/6 (WT) strain (an additional Bl/6 MSC isolate was purchased from Tulane Center for Gene Therapy). The MSCs were characterized by immunofluorescent staining and confirmed to be $CD45^-$, $CD11b^-$ (data not shown). These MSCs were positive for the cell surface antigens $SCA1^+$ and $CD44^+$ as analyzed by flow cytometry (Figure 3A). To confirm MSC phenotype [1, 10], each line was shown to be capable of differentiation along 3 principal lineages: osteoblast, adipocyte, and chondrocyte (Figure 3B and 3C). Studies were performed with at least 2 different MSC lines of each phenotype and the data combined.

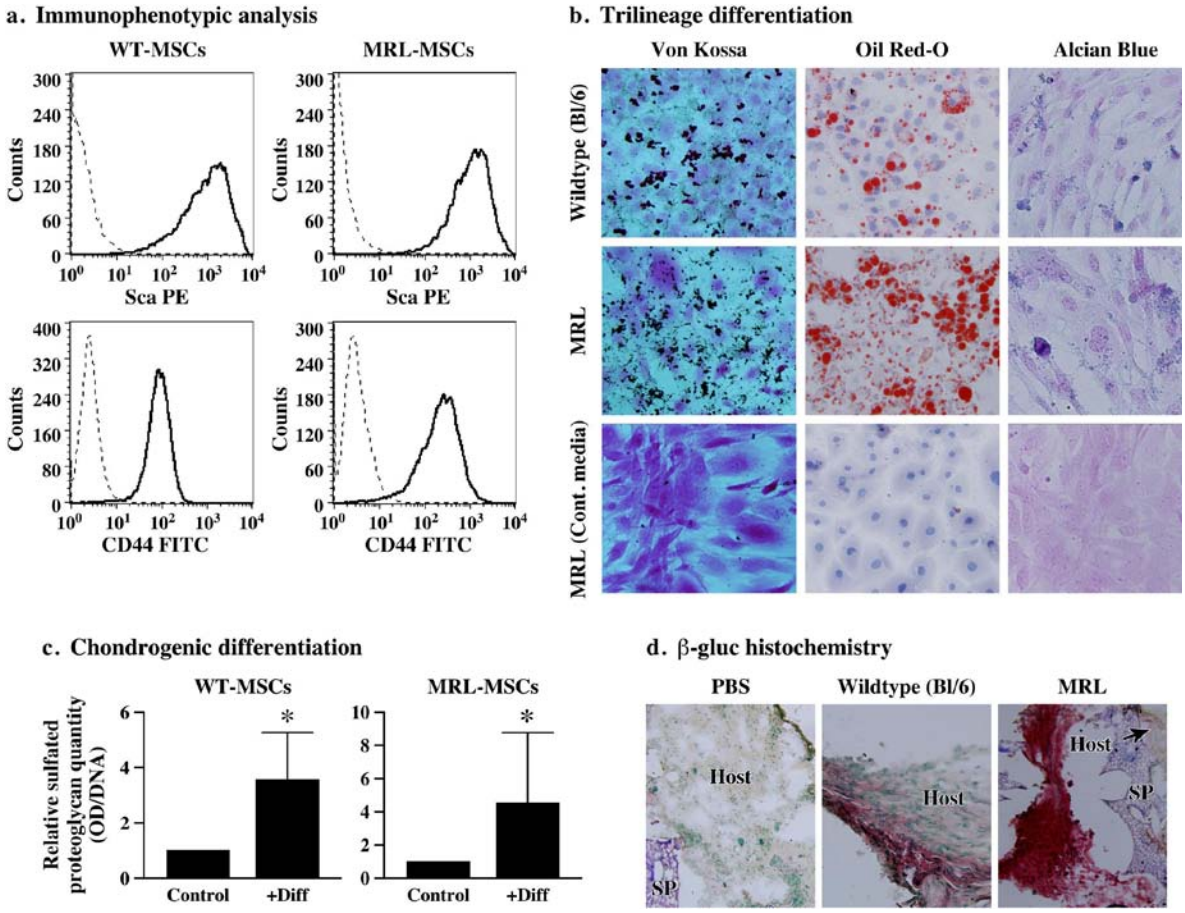

Figure 3. Isolation and Characterization of Two Populations of MSCs

(a) Isolated MSCs were shown to express MSC markers, including CD44 and Sca1 (dark line), by FACS. Cells stained with isotype antibodies are shown in dotted gray line.
(b) MSC multipotency was confirmed by positive differentiation into adipocytes, osteocytes and chondrocytes. MSCs maintained in control media where differentiation was not induced also are shown.
(c) Graphical representation of quantified sulfated proteoglycans in differentiated cells. Fold change over non-differentiated MSCs, normalized to DNA content.
(d) Photomicrograph of β-gluc histochemical analysis of PBS, WT- and MRL-MSC-loaded sponge cryosection showing abundant engraftment of MSCs within granulation tissue (β-gluc positive, red) and adjacent β-gluc negative host tissue. SP, sponge matrix.

MRL-MSCs Engrafted Extensively and Induced Vigorous, Well-Vascularized Granulation Tissue

To compare the effect of the different MSCs in promoting both the quantity and quality of granulation tissue deposition, we used the polyvinyl alcohol (PVA) sponge model of repair stimulation. This model is widely used to study granulation tissue deposition resembling healing by secondary intention [87, 88]. MSC engraftment (persistence in tissue), vascularity, and organization of the resultant granulation tissue were compared among sponges implanted into the same animal and across multiple animals. When implanted into mice genetically deficient for β-glucuronidase (β-gluc), both WT- and MRL-loaded sponges gave rise to abundant granulation tissue compared with sponges loaded with vehicle (PBS) (Figure 4A–C). This enabled us to distinguish β-gluc-positive MSC-derived tissue (i.e., assess engraftment) from β-gluc-negative host tissue. Sponges injected with MRL-MSCs had significantly greater amount of granulation tissue over a given cross-sectional area than those loaded with WT-MSCs (Figure 4A-C). Granulation tissues observed in sponges treated with MRL-MSCs (Figure 4C and 4F) and WT-MSCs (Figure 4B and 4E) appeared highly organized with abundant collagen deposition. By contrast, sponges treated with PBS (Figure 4D) demonstrated loose, disorganized tissue architecture with markedly reduced collagen deposition. The majority of the granulation tissue in MSC-loaded sponges (Figure 3D) showed substantial engraftment with implanted MSCs as evidenced by the extensive, red (β-gluc-positive) histochemical staining whereas the PBS-loaded sponges (negative control) contained only β-gluc-negative host cells.

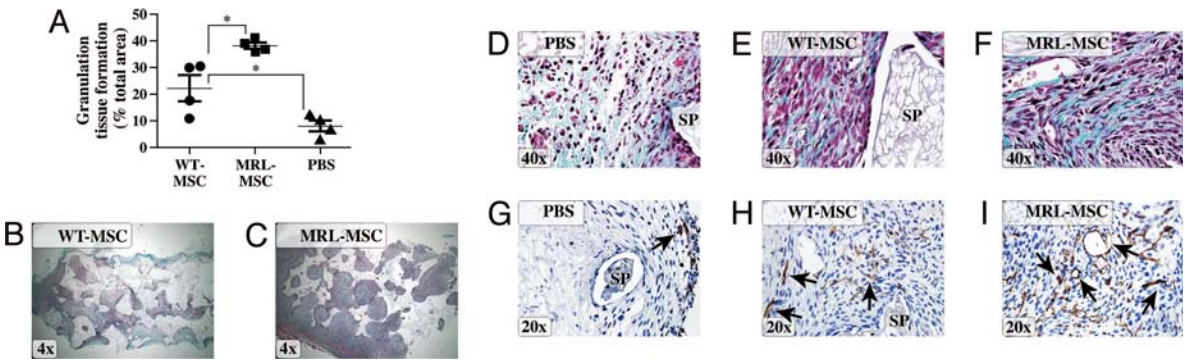

Figure 4. MRL-MSCs Generated More Advanced Wound Granulation Tissue

*(*A) Graph of granulation tissue area in representative histological sponge sections as a percentage of total sponge area. One-way ANOVA with Bonferroni correction was used to compare data between WT vs. MRL or PBS, $n = 4$ in each group.

Representative low power Trichrome images show decreased granulation tissue in WT- (*B*) vs. MRL- (*C*) MSC-loaded sponges.

(*D*–*F*) High power Trichrome images show that MSC-loaded sponges (*E* and *F*) were more organized, highly cellular and with abundant type I collagen (blue) as compared with PBS control (*D*).

(*G*–*I*) Representative immunostained sections using anti-PECAM-1 to designate vascular density from PBS-loaded (*G*), WT (*H*), or MRL (*I*) MSC-derived sponge granulation tissue. SP, sponge matrix, arrows point at positive stain, *, $P < 0.05$.

Biochemical measurement for β-gluc enzyme activity (a quantitative measure of MSC engraftment) showed greater than 3-fold increased engraftment of MRL-MSCs compared with WT-MSCs (Figure 5A). Furthermore, the granulation tissue derived from MRL-MSCs was comparatively more vascularized than that from WT-MSCs as determined by greater density of PECAM-1 immunopositive vascular structures (Figure 4H, 4I and 5B). The observed increased engraftment with MRL-MSCs is consistent (in part) with greater than 2-fold increased in vitro proliferation of MRL-MSCs over WT-MSCs (Figure 5C). However, the number of cells (affected by proliferation rate) does not correlate directly with engraftment, suggesting that these are distinct mechanisms [89].

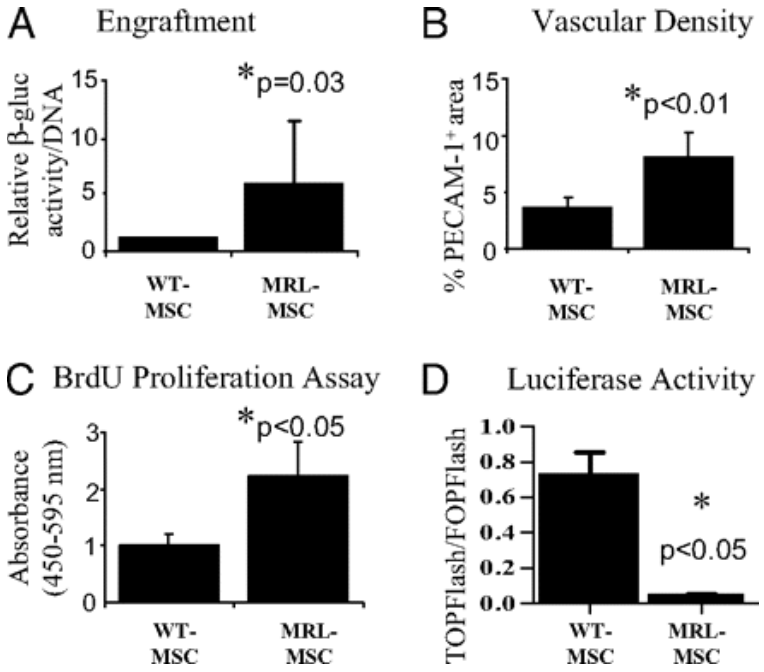

Figure 5. MRL-MSCs Showed Higher Engraftment and Vascularity

(*A*) β-gluc-specific activity (MSC marker) normalized to total cellular DNA content of paired WT- and MRL-MSC sponge granulation tissue samples were calculated and the average of the fold change for *n* = 7 animals were graphed to represent engrafted MSCs.
(*B*) Vascular density graphed as percentage of immunopositive PECAM-1 area/total tissue area in histological sections from granulation tissue. Data represents averages of multiple 40X fields from unpaired samples (*n* = 6).
(*C*) In vitro proliferation of WT- and MRL-MSCs using BrdU ELISA; *n* = 5 experiments performed in triplicate.
(*D*) Basal normalized luciferase activity; *n* = 2 experiments performed in duplicate. Unpaired Student's *t* test was used.

MRL-MSCs Displayed a Down-Regulation of Wnt Target Genes and Increased Expression of sFRPs

To determine the molecular basis for the enhanced repair properties of MRL-MSCs, we compared their gene expression to WT-MSCs. Several inhibitors of the β-catenin/Wnt (canonical) signaling pathway belonging to the sFRP family were significantly enriched in MRL-MSCs (Figure 6A).

An evaluation of target genes that are known to be transcriptionally up-regulated by the canonical Wnt pathway (and hence should be decreased in MRL-MSCs) uncovered 3 genes, Cyclin D1 [90], Sox2 [91] and Axin2 [92], that had >4-fold reduced expression in MRL-MSCs (Figure 6A and Table 3).

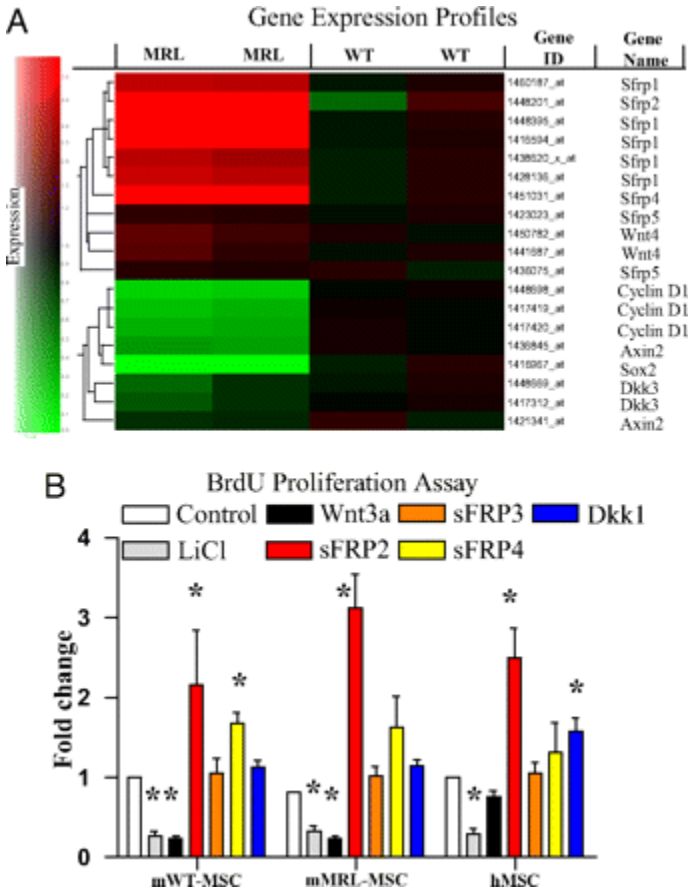

Figure 6. MRL-MSCs Demonstrated a Down-regulation of Canonical Wnt Pathway by Up-regulation of sFRPs

(*A*) Expression of known Wnt pathway genes (rows) in MSCs isolated from WT and MRL mice in duplicate experiments, from low (green) to high (red). Gene tree (to the left of the rows) corresponds to the degree of similarity of the pattern of expression for genes.
(*B*) In vitro proliferation of murine and human MSCs relative to basal levels (e.g., media alone) in the presence of LiCl (10 mM) or various recombinant Wnt pathway factors: 50 ng/ml Wnt3a, 100 ng/ml sFRP2, 100 ng/ml sFRP3, 2 µg/ml sFRP4, or 100 ng/ml Dkk1. The data shown are the fold change relative to media alone within each given cell type. Data are from at least 3 experiments performed in triplicate. Unpaired Student's *t* test with Bonferroni's correction was used. *, $P < 0.05$.

Interestingly, the microarray data showed increased Wnt4 transcripts in MRL-MSCs. Wnt4 is involved in regulating mesenchymal to epithelial transformation in the kidney and whose activity is thought to be regulated by sFRP2; in other reports Wnt4 induces sFRP2 expression [93]. Quantitative real-time RT-PCR confirmed the gene expression differences for a subset of these genes (Table 3). sFRP2 and sFRP4 transcripts were up-regulated in MRL-MSCs by >250- and 30-fold, respectively. The aforementioned canonical target genes were significantly down-regulated in MRL-MSCs between 5- and 12-fold, consistent with the genomic profile (Table 3).

Table 3. Wnt Pathway Inhibitors are Up-regulated and Wnt Downstream Targets are Down-regulated in MRL-MSCs

Gene Name	Fold Change	p	n
Wnt Pathway Inhibitors			
Secreted frizzled-related sequence protein 2 (Sfrp2)	251.8 ± 346	≤ 0.05	9
Secreted frizzled-related sequence protein 4 (Sfrp4)	31.61 ± 34.97	≤ 0.05	6
Dickkopf homolog 1 (Dkk1)	None Detected		N/A
Wnt Pathway Activators			
Axin 2	0.1998 ± 0.1364	< 0.01	7
High mobility group box protein (Sox2)	0.0785 ± 0.0410	< 0.01	6
Cyclin D1	0.2119 ± 0.1316	< 0.01	8

This gene expression signature would predict a reduction in canonical Wnt signaling in MRL-MSCs. An optimized version of the TOPFlash reporter was used to compare constitutive β-catenin-mediated transcriptional activation in MRL- and WT-MSCs [94] (Figure 5D). Consistent with our prediction, MRL-MSCs exhibited a significant reduction in TOPFlash/FOPFlash ratio under basal conditions. We next assessed if murine and human MSC proliferation was modulated by Wnt signaling (Figure 6B). Wnt pathway activation through either addition of LiCl or recombinant murine Wnt3a decreased proliferation for both murine (WT and MRL) and human MSCs; the small decrease of human MSC proliferation with Wnt3a treatment was not statistically significant, possibly reflecting species-specific differences in Wnt/Frizzled receptors. Dkk1, surprisingly, did not affect murine MSCs but showed a statistically significant increase with human MSC proliferation in vitro, consistent with previous studies [85, 95]. Although sFRP4 increased WT-MSC proliferation, only sFRP2 mediated a consistent and notable increase in proliferation in both murine and human MSC lines. To underscore the significance of the Wnt pathway in engraftment of MRL-MSCs in vivo, we injected LiCl every other day directly into WT- or MRL-MSC preloaded sponges. As anticipated, LiCl-mediated activation of canonical Wnt signaling significantly reduced MRL-MSC engraftment to levels comparable with WT-MSCs (Figure 7A and 7B).

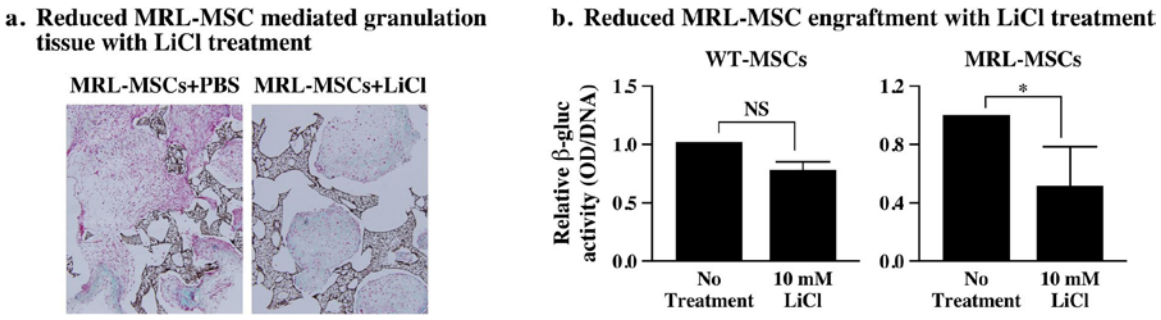

Figure 7. Effects of Wnt Signaling Activation on MSCs - *in vivo* LiCl Treatment

(*a*) Representative low power Trichrome images show decreased granulation tissue in MRL-MSC-loaded sponges treated with Lithium Chloride (LiCl) vs. PBS control. Note that LiCl (Wnt activation) promoted in vivo differentiation of MSCs into cartilage.
(*b*) Graphical representation of β-glucuronidase activity as a marker of MSC engraftment in the presence or absence of LiCl treatment. Two-tailed, unpaired student's *t* test was performed to compare the effects of LiCl on the levels of engraftment. Asterisk designates statistical significance of $P < 0.05$. NS, no statistical difference.

MSCs Differentially Expressed Wnt Constituents

To investigate the contribution of secreted Wnt pathway members on the regulation of β-catenin in MSCs in vivo, we generated stably-transduced WT-MSC lines overexpressing Wnt3a, Dkk1 or sFRP2. Co-expression of GFP with each cDNA enabled FACS enrichment of vector-transduced MSCs (>90%; data not shown; Table 4).

Table 4. Transduction Characterizations

Transduct	No. of Transductions	Average Transduction Efficiency, %	Standard Deviation, %
GFP	4	50.64	± 24.03
Dkk1	2	85.5	±14.14
sFRP2	4	48.12	± 9.61
Wnt3a	6	26.15	± 8.95

Control transducts were generated that expressed GFP alone (GFP-MSC). Fold increase of sFRP2 protein expression in transduced WT cells (sFRP2-MSCs) assessed by immunoblot was comparable to the fold increase observed between GFP-MSCs and MRL-MSCs (Figure 8A). Wnt3a expression was verified by immunofluorescent staining of sorted (GFP-positive) cells as it was difficult to obtain sufficient numbers of cells for an immunoblot (Figure 9A); overexpression of Wnt3a in MSCs (Wnt3a-MSCs) abrogated their proliferation in culture (Figure 8B).

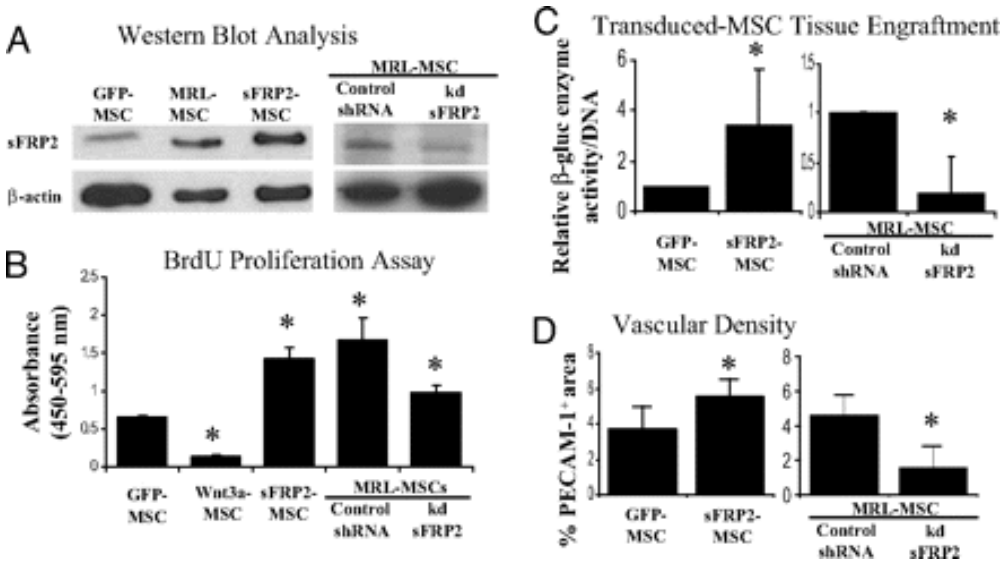

Figure 8. sFRP2 Promotes MSC Proliferation, Engraftment and Vascular Density of Stem Cell Generated Granulation Tissue

(*A*) sFRP2-MSCs were sorted for GFP expression and analyzed by immunoblot for specific protein expression. WT-MSCs transduced with vector containing GFP alone (GFP-MSC) were also sorted in parallel. MRL-MSCs transduced with lentiviral control construct (Control shRNA) and MRL-MSCs with shRNA knockdown of sFRP2 (MRL-kd-sFRP2, clone 75B) were selected by puromycin resistance and analyzed by immunoblot for specific protein expression.
(*B*) Cell proliferation assay of GFP-MSCs, MSCs expressing specific Wnt pathway components, Control shRNA, and MRL-kd-sFRP2 (clone 75B) $n \geq 3$ independent experiments.
(*C*) β-gluc specific activity normalized to total cellular DNA content of paired GFP-MSCs and sFRP2-MSC loaded granulation tissue and MRL-kd-sFRP2 paired to Control shRNA loaded sponges. $n = 5$ sponges of each condition.
(*D*) Vascular density of granulation tissue derived from sFRP2-MSCs compared with control MSCs and MRL-kd-sFRP2 MSCs compared with Control shRNA graphed as percentage of immunopositive PECAM-1 area/total tissue area in 40× fields. One-way ANOVA with Bonferroni correction was used to compare the proliferation data. Paired Student's *t* test was used for comparisons of engraftment and vascularity data. *, $P \leq 0.05$.

MSC transducts expressing Dkk1 (Dkk1-MSCs), sFRP2 or GFP retained the capacity for tril-ineage differentiation (Figure 9B and 9C) and express CD44 and SCA1 by FACS (data not shown). Regulation of canonical Wnt signaling activity of conditioned media from each MSC transduct line was assessed in HEK 293 cells stably transfected with TOPFlash Wnt reporter system. Recombinant protein was used as a positive control. As expected, conditioned media from Wnt3a-MSC resulted in increased luciferase activity over conditioned media from vector-transfected MSCs (GFP-MSC), whereas conditioned media from Dkk1- or sFRP2-MSCs resulted in comparatively reduced β-catenin-mediated transcriptional activity (Figure 9D).

Wnt signaling in sFRP2-MSCs was decreased compared with GFP-MSCs as assessed by luciferase activity after transfection with TOP/FOPFlash reporter constructs (Figure 9E).

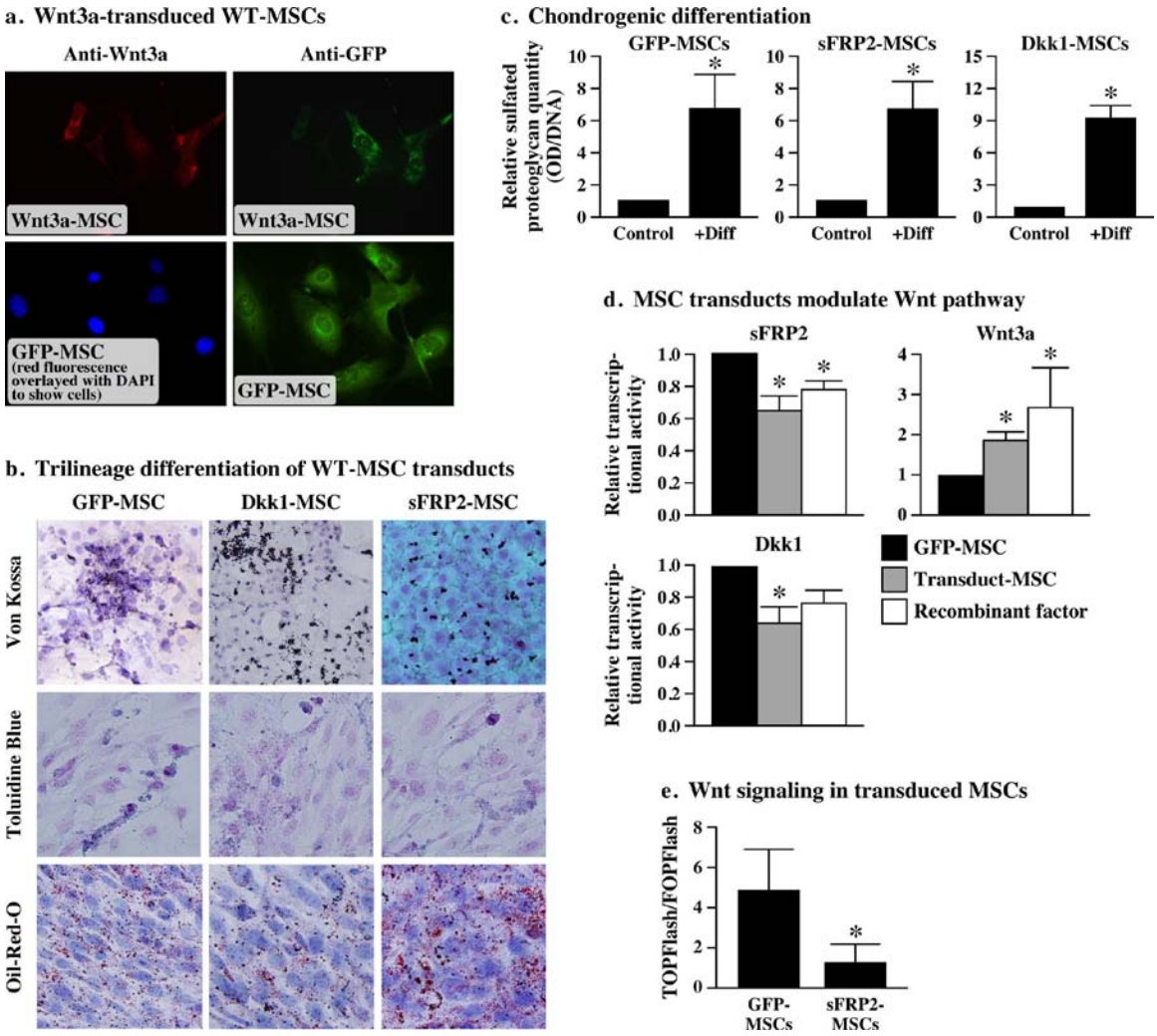

Figure 9. Characterization of MSCs Transduced With Wnt Constituents

(*a*) GFP-sorted WT (Bl/6)-derived MSCs transduced with Wnt3a IRES GFP (Wnt3a-MSCs) and vector control (GFP-MSCs), were assessed by immunofluorescence to confirm GFP/Wnt3a co-expression.
(*b*) Multipotency of MSC transducts was confirmed by positive differentiation into adipocytes, osteocytes and chondrocytes.
(*c*) Graphical representation of sulfated glycosaminoglycans as measurement of chondrogenic differentiation. Fold change over non-differentiated transduced MSCs, normalized to DNA content.
(*d*) Luciferase activity in HEK cells stably transfected with TOPFlash reporter after treatment with conditioned media from designated MSC transducts or GFP-MSC, as baseline. 50ng/ml Wnt3a, 100 ng/ml Dkk1, or sFRP2 recombinant proteins were used as positive controls. The results were the average of the fold change from 3 independent experiments performed in duplicate.
(*e*) Basal normalized luciferase activity as a measurement of canonical Wnt signaling in transduced MSCs. The effect of sFRP2 was assessed by transfecting sFRP2-MSCs and GFP-MSCs with TOP/FOPFlash reporter constructs.

sFRP2 Enhanced MSC-Mediated Wound Repair

As discussed, Wnt3a expression abolished MSC proliferation and these cells died after 4–6 weeks in culture. By contrast, overexpression of sFRP2 resulted in >3-fold increase in proliferation as compared with GFP-MSC (Figure 8B). Overexpression of Dkk1 did not alter the proliferation rate over GFP-MSCs (Figure 10A and 10B). These effects are consistent with our observation using recombinant proteins (Figure 6B).

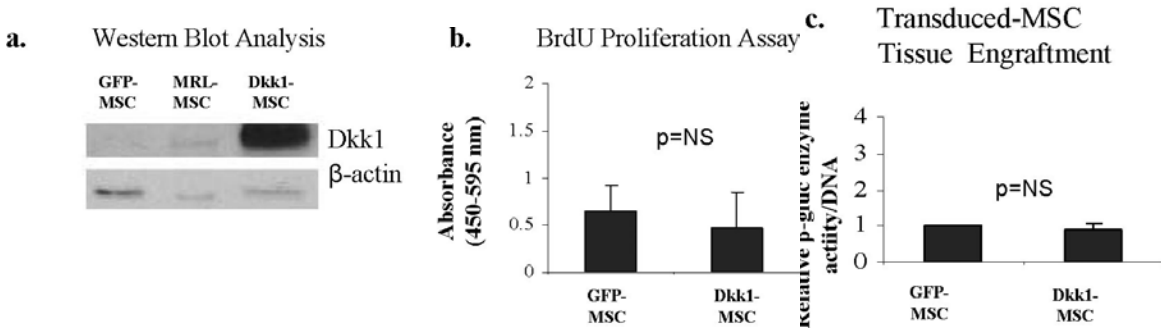

Figure 10. Wnt Inhibition of Murine MSCs through Dkk1 Does Not Promote MSC Proliferation and Engraftment

(*a*) WT-MSCs were retrovirally transduced to express Dkk1 linked to an IRES GFP (Dkk1-MSCs). Transduced cells were sorted for GFP expression and analyzed by immunoblot for specific protein expression. Dkk-1 levels in conditioned media from transduced cells were 1.29±0.11µg/ml and undetectable in GFP-MSCs. WT-MSCs transduced with vector containing GFP alone (GFP-MSC) were also sorted in parallel.
(*b*) Cell proliferation assay.
(*c*) β-gluc specific activity normalized to total cellular DNA content of paired GFP-MSC or Dkk1-MSC-loaded granulation tissue. One way ANOVA with Bonferroni correction was used to compare data between GFP-MSC and Dkk1-MSC.

Moreover, further testing of Dkk1-MSC transducts failed to show changes in murine MSC engraftment or MSC-derived sponge granulation tissue (Figure 10C) over GFP-MSCs, suggesting that murine MSCs, unlike human MSCs, failed to respond to Dkk1-mediated Wnt inhibition.

To assess the role of the Wnt inhibitor sFRP2 in promoting both the quantity and quality of MSC-generated granulation tissue, we loaded PVA sponges with sFRP2- or GFP-MSCs before implantation into β-gluc-deficient mice. β-gluc enzyme activity in granulation tissue was significantly increased (>3-fold) in sFRP2-MSC-loaded sponges compared with GFP-MSC-loaded controls (Figure 8C). Furthermore, examination of vascular density using PECAM-1 immunostaining showed that granulation tissue generated from sFRP2-MSCs was more densely vascularized than GFP-MSCs (Figure 8D). To examine if sFRP2-MSCs directly contributed to the microvasculature of granulation tissue, we performed co-localization by confocal microscopy using anti-GFP (to identify MSCs) and anti-PECAM-1. MSC-derived vascular structures were evident within the MSC-derived granulation tissue (Figure 11A) suggesting that MSCs underwent trans-differentiaion into the endothelial lineage to contribute to repair tissue vasculature.

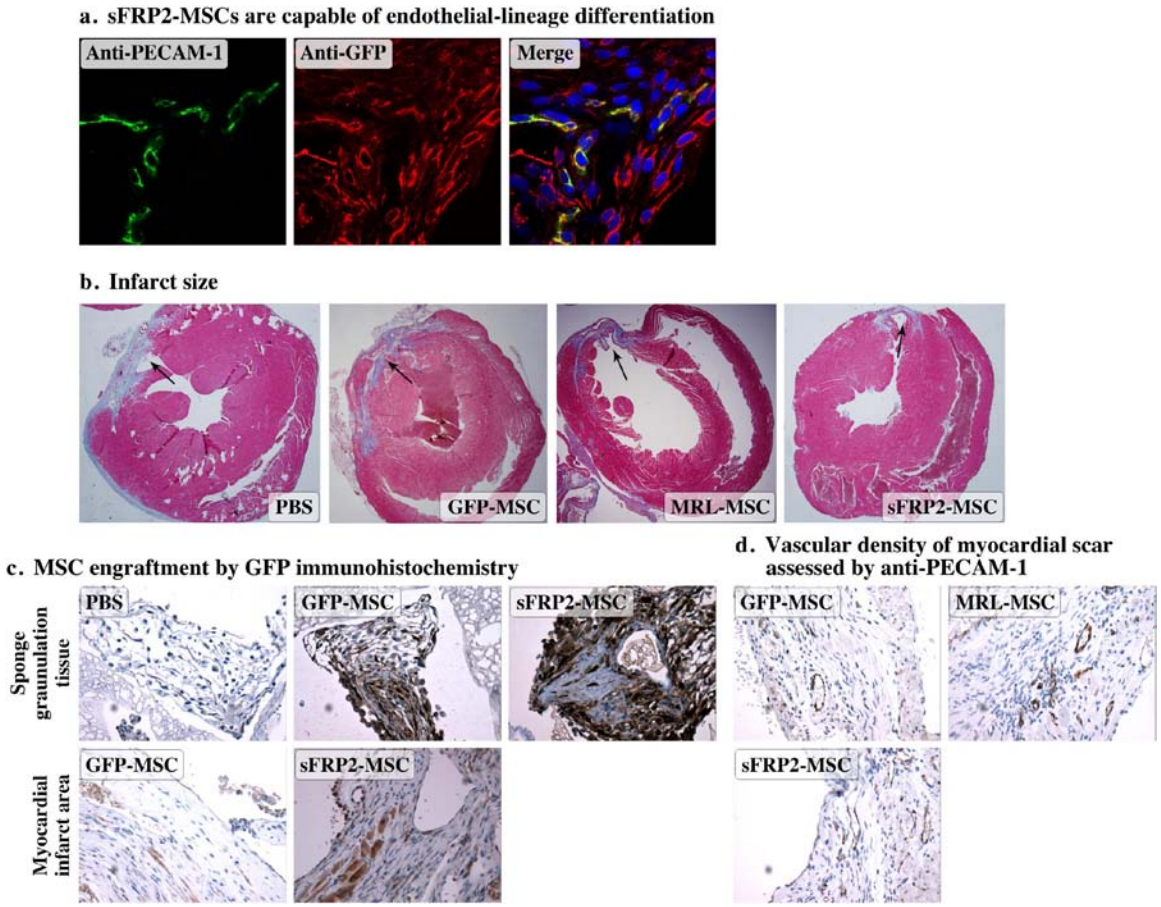

Figure 11. MSC-Mediated Cardiac Therapy

(*a*) Representative Z plane shows high degree of co-localization of microvascular endothelial cells (anti-PECAM, green) and the sFRP2-MSC marker, GFP (red). Fluorescent images were acquired by confocal fluorescent microscopy with 60x lens. DAPI staining of the same slide shows the location of the nuclei.
(*b*) Representative Masson trichrome-stained sections of hearts from mice 30 days after receiving PBS, GFP-MSC, MRL-MSC or sFRP2-MSC after coronary vessel ligation. MRL and sFRP2-MSC treated hearts had smaller infarcts with less collagen deposition (blue staining in trichrome) and more muscle (increased red staining).
(*c*) Engraftment of sFRP2- and GFP-MSCs was assessed by immunostaining with anti-GFP (brown). sFRP2-MSC showed increased engraftment in both models, however, there was significantly higher engraftment within sponge granulation tissues than in healed myocardial scar.
(*d*) Representative immunostained sections of myocardial scar using anti-PECAM-1 to designate vascular density among experimental cohorts.

Proliferation and Enhanced Engraftment of MRL-MSCs Are Mediated by sFRP2.

We sought to determine is sFRP2 inhibition could abrogate the MRL-MSC phenotype. Knockdown of sFRP2 mRNA transcripts with 3 independent shRNAs were assessed by real-time RT-PCR (Table 5). MRL-kd-MSCs (derived using shRNA clone 75B) were expanded and further tested by immunoblot and showed a ≈70% reduction in sFRP2 protein as compared with MRL -MSCs stably transduced with control shRNA (Figure 8A). Specific sFRP2 knockdown also decreased proliferation by 2-fold over control shRNA-MSCs (Figure 8B). Furthermore, MRL-kd-MSCs showed >5-fold decrease in MSC engraftment in experimental granulation tissue (Figure 8C). Importantly, the experimental granulation tissue generated by MRL-kd-sFRP2 were also 3-fold less densely vascularized, as assessed by PECAM-1 staining, when compared with control shRNA MRL-MSCs-loaded sponges (Figure 8D).

Table 5. MRL-kd-MSCs Transduction Characterizations

Clone	Fold Change	p
Control A	1	N/A
Control B	1	N/A
75B	0.08 ± 0.03	= 0.048
76B	0.57 ± 0.20	= 0.117
77C	0.035 ± 0.02	= 0.059

sFRP2 Facilitated MSC Engraftment and Cardiac Remodeling/Repair

We then assessed whether sFRP2 overexpression could improve MSC-mediated myocardial regeneration by injecting sFRP2-MSCs, GFP-MSCs, MRL-MSCs, or vehicle PBS into the peri-infarct area of the left ventricle after coronary artery ligation. Ventricular remodeling and cardiac function were analyzed by echocardiography at 7 and 30 days post MI (Table 6). The top four rows in Table 6 represent the mean and standard error mean (± SEM) values for each treatment at day 7 and day 30. The mean ± SEM percentage difference (Δ%) values are in the bottom three rows. One-way ANOVA with Newman–Keuls multiple comparison test was used to compare the Δ% values for each echocardiographic parameter. [*, $P < 0.05$ PBS vs. sFRP2-MSC; †, $P < 0.05$ GFP-MSC vs. sFRP2-MSC; ‡, $P < 0.05$ GFP-MSC vs. MRL-MSC; §, $P < 0.05$ PBS vs. MRL-MSC. PBS $n = 7$, GFP-MSC $n = 6$, MRL-MSC $n = 5$, sFRP2-MSC $n = 7$.]

Table 6. sFRP2 Aids in Remodeling and Improves Function of Injured Hearts

	PBS		GFP-MSCs		MRL-MSCs		sFRP2-MSCs	
	d7	d30	d7	d30	d7	d30	d7	d30
LVIDD (cm)	0.31±0.05	0.36±0.06	0.34±0.07	0.37±0.08	0.28±0.02	0.26±0.03	0.32±0.03	0.34±0.04
LVIDS (cm)	0.19±0.04	0.21±0.04	0.20±0.08	0.25±0.08	0.16±0.01	0.13±0.03	0.18±0.04	0.17±0.03
FS	39.7±5.68	34.3±7.70	36.7±8.8	32.7±10.1	43.92±5.21	45.74±7.27	43.5±7.41	48.6±4.50
EF	0.77±0.05	0.69±0.10	0.72±0.12	0.67±0.13	0.81±0.06	0.83±0.07	0.80±0.08	0.85±0.04
ΔLVIDS, %	19.98±28.38		30.36±30.13‡†		-18.28±19.80‡		-5.07±14.53†	
ΔFS, %	-13.17±15.71*		-10.28±16.33†		3.81±6.79		13.82±16.17*†	
ΔEF, %	-9.89±12.39*		-7.28±10.68†		2.17±2.21		6.24±7.33*†	

Left ventricle (LV) internal dimension diastolic (LVIDD) and LV internal dimension systolic (LVIDS) reflect remodeling of the infarcted ventricle. At 30 days post MI, both dimensional parameters were smaller in the MRL-MSC and sFRP2-MSC recipients, suggesting a role for sFRP2 in chamber remodeling. The percentage difference in LVIDS between day 7 and day 30 was significantly reduced in animals receiving sFRP2-MSCs (Figure 12A). When compared with the GFP-MSC, recipients of both the MRL-MSC and sFRP2-MSC showed improved ventricular remodeling. To determine whether sFRP2 improved cardiac function, the percentage differences in ejection fraction (EF) and fractional shortening (FS) (Figure 12B) between 7 and 30 days after treatment were analyzed (Table 6). The MRL recipients showed an increase in both ΔEF (2.17%) and ΔFS (3.18%) when compared with WT-MSC ‒7.28% and −10.28%,

respectively) and PBS-injected (−9.89% and −13.17%, respectively) controls. In contrast, sFRP2-MSC cohorts exhibited significant functional improvement 30 days post infarct (ΔEF 6.24% and ΔFS 13.82%). These results together indicate sFRP2 overexpression has a significant positive effect on cardiac function.

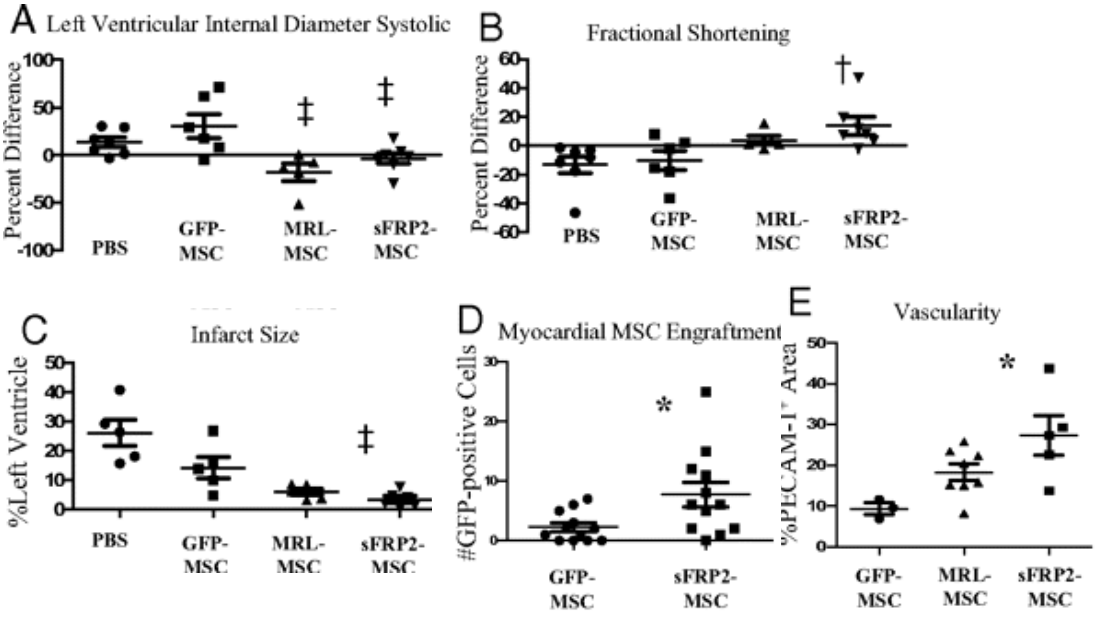

Figure 12. sFRP2 Aids in Remodeling and Improves Function of Injured Hearts

Fractional shortening (*A*) and LVIDS (*B*) determined by echocardiography are plotted as percentage difference (Δ%) values (mean +/- SEM) between 7 and 30 days after infarct to reflect therapy-mediated impact on remodeling or function. Increased Δ% in FS measured in sFRP2-MSC-treated hearts compared with GFP-MSC-treated hearts demonstrates enhanced cardiac function.
(*C*) Infarct size was significantly attenuated in hearts injected with sFRP2-MSCs compared with control GFP-MSCs. One-way ANOVA and Newman–Keuls multiple comparison test: $^{\dagger}P < 0.05$ vs. PBS and GFP-MSC; $^{\ddagger}P < 0.05$ vs. GFP-MSC.
(*D*) Engraftment of transplanted MSCs within myocardial sections 30 days after MI, immunohistochemistry for GFP.
(*E*) PECAM-1-positive structures reflecting microvessel density within scar tissue were quantified. *, $P < 0.05$ using One-way ANOVA with Newman–Keuls post test. (Representative photomicrographs of infarct histology are shown in Figure 11)

Mean percentage of LV area infarcted in PBS-treated control animals was 26 ± 10% (Figure 12C and 11B). Injection of GFP-MSCs had a modest protective effect, limiting the extent of the infarction to 14% of LV (p = NS) (Figure 12C). In contrast, injection of MRL-MSCs significantly limited infarct size to 6.0% of the LV ($P < 0.05$ vs. PBS). Notably, injection of sFRP2-MSCs limited infarct size even more dramatically to 3.4% ($P < 0.05$ vs. PBS and the GFP-MSC group). Compared with the PBS group, we observed a relative reduction in infarct size of 12% in the GFP-MSC group and 23% in the sFRP2-MSC group.

Myocardial engraftment of MSCs was assessed by counting GFP-positive cells. Whereas significant engraftment was evident grossly within granulation tissue of sponge implants (Figure 4G and 11C), the numbers of MSCs within the myocardium 30 days after injection were comparatively fewer (Figure 11C). However, the sFRP2-MSCs resulted in a significant increase in the number of engrafted MSCs compared with controls (Figure 12D). We examined the myocardial scar region for co-localization of GFP-MSCs with endothelial (anti-PECAM-1) or cardiomyocyte (anti-α-actinin) specific marker and did not observe any (data not shown). Vascular density of the scarred region was assessed by immunohistochemistry for PECAM-1 and showed a statistically significant increase with sFRP2-MSCs compared with GFP-MSCs (Figure 12E and 11D).

Discussion

Although MSCs are a promising source of cell therapy for heart and wound regeneration, little is known about the molecular pathways that modulate MSC-mediated regeneration and repair [89, 96]. Furthermore, the extent to which repair and regeneration mediated by MSCs relies on their engraftment and direct contribution versus serving as effectors to alter the stem cell microenvironment is not understood [96]. The distinct soft tissue repair models used in this study provided different in vivo contexts to study MSC-driven therapy. The sponge soft tissue repair model also permitted clear demarcation and evaluation of angiogenesis, organization, and contribution of MSC-derived granulation tissue. The isolation and characterization of 2 strain specific populations of MSCs with differing in vivo regenerative properties led us to identify sFRP2 as a key molecule that mediates self-propagation of both human and mouse MSCs in vitro and whose overexpression enhanced MSC-mediated angiogenesis and therapeutic potency.

A role for Wnt signaling in modulating MSC biology was suggested by molecular profiling of the MSC populations isolated from the regenerative MRL/MpJ mice, as compared with the MSCs isolated from WT (Bl/6) strain. Together, our data suggest that Wnt signaling inhibition correlated with the superior properties exhibited by MRL-MSCs; these included enhanced proliferation and the ability to mediate more abundant, better organized and vascularized granulation tissue in implanted PVA sponges. Consistent with our findings, several lines of evidence from published reports [81-83] support a role

for Wnt inhibition in regulating mesenchymal stem cell self-renewal and expansion. Importantly, Wnt/β-catenin activation has been shown to be necessary for the commitment/differentiation of mesenchymal cells to osteocytes, chondrocytes, myoblasts, and adipocytes [81-83]. Additionally, Dkk1, an inhibitor of the canonical Wnt pathway, increased human MSC proliferation and promoted entry into the cell cycle in vitro [85]. Consistent with these studies, our findings support a role for canonical Wnt activation in MSC lineage commitment and, conversely, Wnt inhibition in self-renewal.

Recently, Liu *et al.* [97] reported that accelerated aging and associated depletion and dysfunction in stem cells in various tissues and organs is associated with increased Wnt activity. Expression of klotho, a secreted protein that binds and sequesters Wnt and leads to suppression of Wnt activity, and its absence in mice leads to early onset age-related changes [97]. Another study found that activation of Wnt signaling promoted tissue specific stem cell aging and increased tissue fibrosis [98]. Both studies mentioned above broadly support our hypothesis and link Wnt inhibition to stem cell maintenance and function.

We identified an effect of sFRP2, an inhibitor of Wnt signaling, on MSC self-propagation by comparing MSCs from mouse strains with markedly different healing properties. Whereas canonical Wnt activation, either through addition of exogenous activators or by induced overexpression of Wnt3a, dramatically inhibited baseline MSC proliferation, addition of sFRP2 resulted in significantly increased proliferation of both mouse and human MSCs. This increase was much greater than that seen with other sFRPs tested and recombinant Dkk1,

which caused a statistically significant increase in human MSC proliferation. Dkk1 inhibits Wnt signaling by binding to LRP5 and LRP6 and blocking their interaction with Wnt and Frizzled [99]. Kremen 1 and 2 are transmembrane Dkk1 receptors that synergize with Dkk1 to inhibit Wnt signaling [99]. Kremen transcripts were undetected in murine MSCs through microarray analysis (data not shown). This observation may explain the lack of response of murine, but not human, MSCs to Dkk1. Interestingly, despite the very high level of endogenous sFRP2 in MRL-MSCs, addition of increasing amounts of recombinant sFRP2 continued to increase proliferation, suggesting significant residual Wnt activity and/or non-canonical roles of sFRP2. Moreover, specific knockdown of sFRP2 in MRL-MSCs resulted in abrogation of the comparatively enhanced wound tissue reconstitution phenotype observed in MRL-MSCs.

MSCs genetically modified to overexpress sFRP2 or Dkk1 were used to investigate the effect of these factors in MSC-mediated tissue repair. Importantly, increased constitutive expression of either Wnt pathway molecule did not abolish expression of mouse MSC surface markers, such as CD44 or SCA1, or the capacity for multilineage differentiation, albeit our experiments did not address whether these factors affected differentiation kinetics. sFRP2-MSCs replicated the MRL-MSC phenotype of enhanced engraftment in situ, increased angiogenesis, and in the setting of acute myocardial injury, resulted in significantly reduced infarct size. Consistent with the histological data, there was enhanced residual myocardial function and attenuation of adverse cardiac remodeling 30 days post MI. Although the numbers of sFRP2-MSCs remaining

30 days post infarction (engraftment) were greater than GFP-MSCs, the overall number of implanted MSCs remaining in the myocardium was considerably lower than those comprising the granulation tissue formed in the sponge model (Figure 11). This finding would suggest that type of injury and the stem cell microenvironment may influence the underlying mechanisms of repair, i.e., direct contribution vs. paracrine effects. The data also suggest that the injury environment may dramatically affect implanted stem cell survival and persistence in vivo. The molecular signals that impact the degree of MSC engraftment are not known.

sFRP2 was first isolated from a BM-derived stromal cell line and was proposed to serve as an inhibitor of Wnt signaling by binding and sequestering the *Drosophila* Wnt homologue, Wingless [100]. Subsequent studies have shown inhibition of Wnt signaling by direct binding to and sequestering of Wnt3a [101]. sFRP2 has been shown to protect against UV- or TNF-induced apoptosis in a canine cancer cell line [86]. Recently sFRP2 was found to be a key factor secreted by genetically engineered MSCs overexpressing Akt [71]. This last study showed that much of the MSC-mediated improvement in myocardial function resulting from Akt-MSC therapy could be attributed to a downstream increase in sFRP2. Moreover, sFRP2 was shown to directly prevent cardiomyocyte death, and thereby, serve as a stem cell-derived paracrine factor to influence cardiomyocyte survival and repair [71]. The enhanced myocardial repair observed in our study can be attributed, at least in part, to this mechanism. Our study also demonstrated that sFRP2 caused a robust increase in MSC

therapy-induced angiogenesis. sFRP1 and 4 overexpression in endothelium have recently been shown to increase neovascularization in hind limb ischemia by regulation of Wnt and Rac1 signaling [102]. We do not know, however, whether sFRP2 works in a similar manner via direct paracrine effects on endothelial cells, indirectly via up-regulation of other angiogenic factors, or via MSC propagation. Notably, a variety of key pro-angiogenic genes are up-regulated in sFRP2-MSCs compared with GFP-MSCs as determined by gene expression profiling (Table 7). Finally, our findings also demonstrate that, in addition to potential paracrine function on target tissues, sFRP2 serves an autocrine and/or cell-intrinsic role in MSCs to mediate self-propagation and engraftment. MSCs appear to be multipotential effector cells whose own preservation and growth in vivo, such as those mediated by sFRP2, may lead to enhanced regenerative efficacy.

Table 7. sFRP2-MSCs Express Several Angiogenic Factors

Gene ID	Gene Name	Fold Change in sFRP2-MSC
1422516_a_at	Fibp (Fibroblast growth factor intracellular binding protein)	2.2
1433489_s_at	FfgR2 (Fibroblast growth factor receptor 2)	2.1
1419417_at	VegfC (Vascular endothelial growth factor C)	2.3
1418711_at	Pdgfa (Platelet-derived growth factor, alpha)	2.4
1417148_at	Pdgfrb (Platelet derived growth factor receptor, beta polypeptide)	2.6
1421919_a_at	Ccr9 (Chemokine [C-C motif] receptor 9)	11.9
1450652_at	Ctsk (Cathepsin K)	16.7
1450029_s_at	Itga9 (Integrin alpha 9)	2.3
1455158_at	Itga3 (Integrin alpha 3)	2.7
1425039_at	Itgbl1 (Integrin beta-like 1)	5.7
1454966_at	Itga8 (Integrin alpha 8)	4.5
1423268_at	Itga5 (Integrin alpha 5)	3.3
1446180_at	Lamb1-1 (Laminin beta subunit-1)	5.0
1446534_at	Angptl2 (Angiopoietin-like 2)	2.5
1417130_s_at	Angptl4 (Angiopoietin-like 4)	2.2
1419671_a_at	Il17rc (Interleukin 17 receptor C)	2.5
1421670_a_at	Irak4 (Interleukin-1 receptor-associated kinase 4)	2.1
1435040_at	Irak3 (Interleukin-1 receptor-associated kinase 3)	3.6
1448950_at	Il1r1 (Interleukin 1 receptor, type I)	4.4
1443937_at	Il2rb (Interleukin 2 receptor, beta chain)	21.7
1425145_at	Il1rl1 (Interleukin 1 receptor-like 1)	3.2
1416295_a_at	Il2rg (Interleukin 2 receptor, gamma chain)	5.2
1425560_a_at	S100a16 (S100 calcium binding protein A16)	2.3
1448367_at	Sdf4 (Stromal derived factor 4)	3.9

Conclusion

The mechanism by which sFRP2 modulates MSC proliferation and tissue engraftment will be assessed in the following chapter. sFRP2, but not other sFRPs tested, uniquely enhanced robust proliferation. Understanding the molecular regulation of MSCs by sFRP2 would have important implications for improving cell-based therapies using MSCs for wound and myocardial repair.

CHAPTER III

SFRP2 SUPPRESSION OF BMP AND WNT SIGNALING MEDIATES MSC SELF-RENEWAL PROMOTING ENGRAFTMENT AND MYOCARDIAL REPAIR

Introduction

Transplantation of MSCs is a promising therapy for ischemic injury; however, inadequate survival of implanted cells in host tissue is a substantial impediment in the progress of cellular therapy. sFRP2 has recently been highlighted as a key mediator of MSC-driven myocardial and wound repair. Notably, sFRP2 mediates significant enhancement of MSC engraftment *in vivo*. We hypothesized that sFRP2 improves MSC engraftment by modulating self-renewal through increasing stem cell survival and by inhibiting differentiation. In previous studies, delineated in the previous chapter, we demonstrated that sFRP2-expressing MSCs exhibited an increased proliferation rate. In the current chapter, we show that sFRP2 also decreased MSC apoptosis and inhibited both osteogenic and chondrogenic lineage commitment. sFRP2 activity occurred through the inhibition of both Wnt and BMP signaling pathways. sFRP2-mediated inhibition of BMP signaling, as assessed by levels of phosphorylated SMADS 1, 5 and 8 (pSMAD 1/5/8), was independent of its effects on the Wnt pathway. We further hypothesized that sFRP2 inhibition of MSC lineage commitment may reduce heterotopic osteogenic differentiation within the injured myocardium, a reported adverse side effect. Indeed, we found that sFRP2-MSC-treated hearts and wound tissue had less ectopic calcification. This work provides important

new insight into the mechanisms by which sFRP2 increases MSC self-renewal leading to superior tissue engraftment and enhanced wound healing.

Self-renewal Capacity of MSCs

Self-renewal is an intrinsic property of stem cells that allows them to give rise to non-differentiated daughter cells by proliferating, preventing apoptosis, and avoid lineage commitment [56, 103]. This process is important for the maintenance of a stem cell pool that, in the case of MSCs, can exert a more robust effect within the context of a wound. Although several cytokines, growth factors, adhesion molecules, and extracellular matrix components have been identified as cues that signal MSCs to differentiate, the molecular signals that modulate MSC self-renewal remain unknown[56]. Data from the hematopoietic stem cell (HSC) field have documented the involvement of Wnt, Notch and BMP signaling cascades in self-renewal; these pathways are implicated in the expansion of undifferentiated HSCs that upon transplantation into lethally irradiated mice successfully reconstitute the cleared bone marrow[104-106]. Although no data are available to demonstrate the role of these pathways in MSC self-renewal, the Wnt and BMP cascades are involved in MSC lineage commitment. Canonical Wnt signaling directs osteogenic differentiation of MSCs by stimulating the expression of osteocalcin[107], this pathway is also involved in early chondrogenesis[108]. The BMP pathway also modulates osteogenic differentiation of MSCs by controlling osteocalcin[109], and BMP2 induces chondrocyte fate determination[110]. The Wnt cascade is involved in other

cellular processes besides differentiation; canonical Wnt signaling inhibition, through the activity of Dkk-1, increases human MSC proliferation without overt differentiation[111]. The mechanisms by which MSCs modulate these signaling events during growth and/or lineage commitment remain unknown. The data herein, describes the ability of sFRP2 to promote MSC self-renewal by inhibition of both the Wnt and BMP pathways.

sFRP2 has recently been implicated by our group and others as a mediator of MSC-driven myocardial and wound repair; however, the mechanisms are unclear. sFRP2-mediated regeneration can be attributed, at least in part, to its paracrine role in mediating myocardial survival by inhibiting apoptosis[71]. However, there are compelling data that sFRP2 has direct effects on MSCs themselves. Overexpression of sFRP2 by MSCs results in increased MSC proliferation and long-term engraftment *in vivo*[75].

Documented and Suspected Roles of sFRP2

The members of the secreted frizzled-related protein (sFRPs) family contain a region with high homology to the cysteine-rich domain (CRD) of the Wnt-pathway frizzled receptors[100]. sFRPs bind Wnt glycoproteins through the CRD, preventing them from reaching their cognate receptors[112]. The five mammalian members, sFRP1-5, have been associated with several developmental and disease processes [113, 114]. Their documented effect thus far has been that of Wnt inhibition [112].

Here, we demonstrate that sFRP2 plays dual and important roles in increasing MSC self-renewal by inhibiting both the Wnt and BMP pathways. We show that sFRP2 confers apoptotic resistance to MSCs in parallel to Wnt pathway inhibition. sFRP2 affects the rate of MSC multilineage differentiation; processes directed by Wnt and BMP signaling. This article is the first to demonstrate that sFRP2 directly inhibits BMP signaling in MSCs. The data contained within describes the mechanisms by which sFRP2 enhances MSC self-renewal to promote MSC-mediated wound healing.

sFRP2 Increases MSC Engraftment and Inhibits Canonical Wnt Signaling to Protect MSCs from Undergoing Apoptosis

sFRP2 has been identified as a key factor responsible for the biogenesis of a superior MSC phenotype[71, 75]. We traced the ability of MSCs to remain within PVA sponges two weeks following implantation in the ventral subcutaneous space of β-gluc$^{-/-}$ mice. The activity of β-glucuronidase within the extracted sponges served as a surrogate marker for the MSCs. As seen in Figure 13A, sFRP2-overexpressing MSCs have statistically significant increased engraftment within granulation tissue. In this figure, each mouse corresponds to one line, a clear trend in the increase of enzyme activity in the sFRP2-MSC-loaded sponges is observed. Overall, sFRP2-overexpression resulted in an approximate 2-fold increase in engraftment. In a previous study, we showed a similar (2- to 3-fold) increase in engraftment in an *in vivo* model of myocardial infarction and wound repair[75]. To understand the cellular basis of the enhanced engraftment, we assessed if this effect was due, in part, to decreased apoptosis.

We determined basal levels of activated Caspase 3 by indirect immunofluorescence (IF) of MSCs stably overexpressing sFRP2 (sFRP2-MSCs) vs. those stably transduced with empty vector (GFP-MSCs). Approximately 47 $\pm$ 18 percent of GFP-MSCs were undergoing apoptosis under high-confluency *in vitro* conditions, whereas only 8.5 $\pm$ 4.3 ($p=0.002$) percent of sFRP2-MSCs were positive for this effector caspase (Figure 13B).

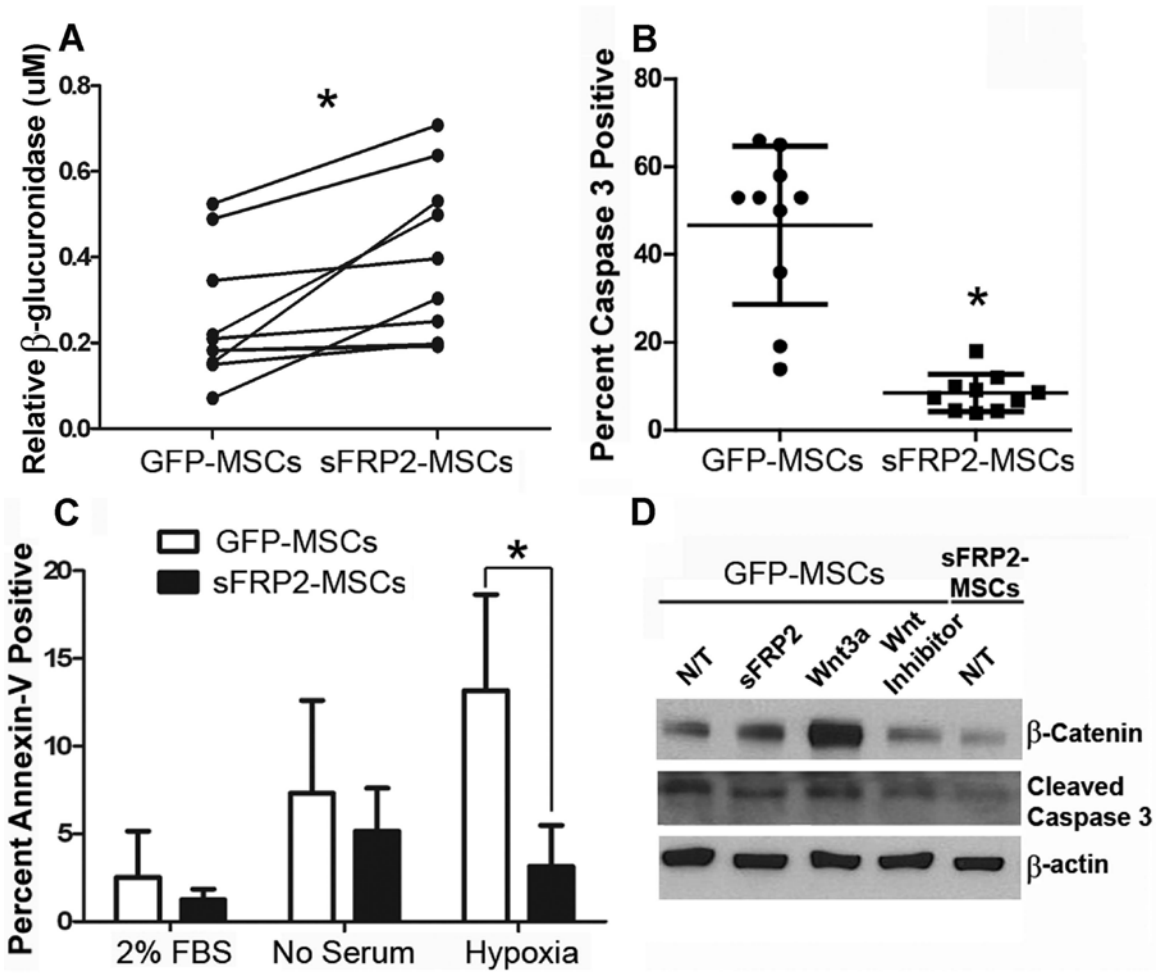

Figure 13. sFRP2 Enhances Engraftment and Protects MSCs from Undergoing Apoptosis by Inhibiting Canonical Wnt Signaling

(A) Levels of β-gluc enzyme activity, normalized to DNA content, are higher within sFRP2-MSC-loaded PVA sponges. Data show the enzymatic activity within the different sponges implanted in the same mouse. *, p = 0.041, Mann Whitney U-Test, n = 11.
(B) Basal levels of activated caspase 3 positivity in sFRP2-MSCs are reduced as compared with GFP-MSCs, as determined by IF. *, p = 0.002, Mann Whitney U-Test, n = 10.
(C) Quantification of flow cytometry analysis for annexin V in GFP-MSCs and sFRP2-MSCs grown in 2% serum, serum-starved, or hypoxic conditions. n = 9; one-way ANOVA with Bonferroni's multiple comparison test.
(*D)* Representative Western blot analysis of cytoplasmic lysates of GFP-MSCs treated with sFRP2 (100 ng/ml), Wnt3a (50 ng/ml), or pyrvinium (100 nm). *N/T*, no treatment, n = 3. sFRP2 inhibits canonical Wnt signaling and concomitantly reduces apoptosis.

To detect apoptosis by an independent method, we assessed Annexin V levels on MSCs grown under 2% serum, 0% serum, or low oxygen conditions, by flow cytometry. The level of apoptosis was increased to ~7% when MSCs were grown in no serum as compared to low serum (~2.5%). Hypoxia (5% O2) further doubled the level of apoptosis. An overall two-fold decrease in Annexin V positive cells was observed in sFRP2-MSCs regardless of the *in vitro* conditions. Statistical significance was only achieved when the cells were exposed to hypoxia (Figure 13C).

To determine if the ability of sFRP2 to protect MSCs from undergoing apoptosis was, in part, due to its Wnt inhibitory activity, we grew GFP-MSCs and sFRP2-MSCs under hypoxic conditions. GFP-MSCs were treated with recombinant sFRP2, Wnt3a, or the small molecule Wnt inhibitor Pyrvinium. Pyrvinium causes inhibition of Axin degradation and promotes degradation of both β-catenin and Pygopus thereby leading to functional inhibition of the canonical Wnt cascade[115]. Western blot analysis of the cytoplasmic extracts of these cells revealed that sFRP2-MSCs had decreased Wnt activity, as observed by the levels of β-catenin, when compared to GFP-MSCs. As seen in Figure 13D, a decrease in Wnt signaling correlated with a decrease in activated Caspase 3 levels; sFRP2-MSCs had approximately 44% lower levels of the cleaved Caspase 3 fragment.

sFRP2 Inhibits Chondrogenic and Osteogenic Differentiation of MSCs *in-vitro*

Control of the balance between stem cell self-renewal and subsequent differentiation is crucial to the therapeutic efficacy of MSCs. To enhance their engraftment within wounds, MSCs must promote their survival and delay differentiation. We assessed the effect of sFRP2 overexpression on the *in vitro* multilineage commitment by two different methods. First, we performed quantitative real-time PCR (qRT-PCR) analysis of peroxisome proliferator-activated receptor gamma (PPAR-γ), Collagen XI and Osteocalcin as specific markers of the adipogenic, chondrogenic and osteogenic lineages, respectively. The transcript levels were normalized to 18S content. Second, quantification of biochemical markers for adipogenic, chondrogenic and osteogenic differentiation was also carried out: Oil Red-O, dimethyl methylene blue (sulphated glycosamino glycans) and Alizarin Red, respectively. Figure 14A depicts the changes in the transcript levels of the different lineage markers, and the quantification of the stains is seen in Figure 14B. sFRP2-MSCs had no difference in the levels of PPAR-γ or Oil Red-O stain compared to GFP-MSCs. On the other hand, sFRP2 had an inhibitory effect on the chondrogenic and osteogenic differentiation. Decreased chondrogenesis was seen in the lower levels of

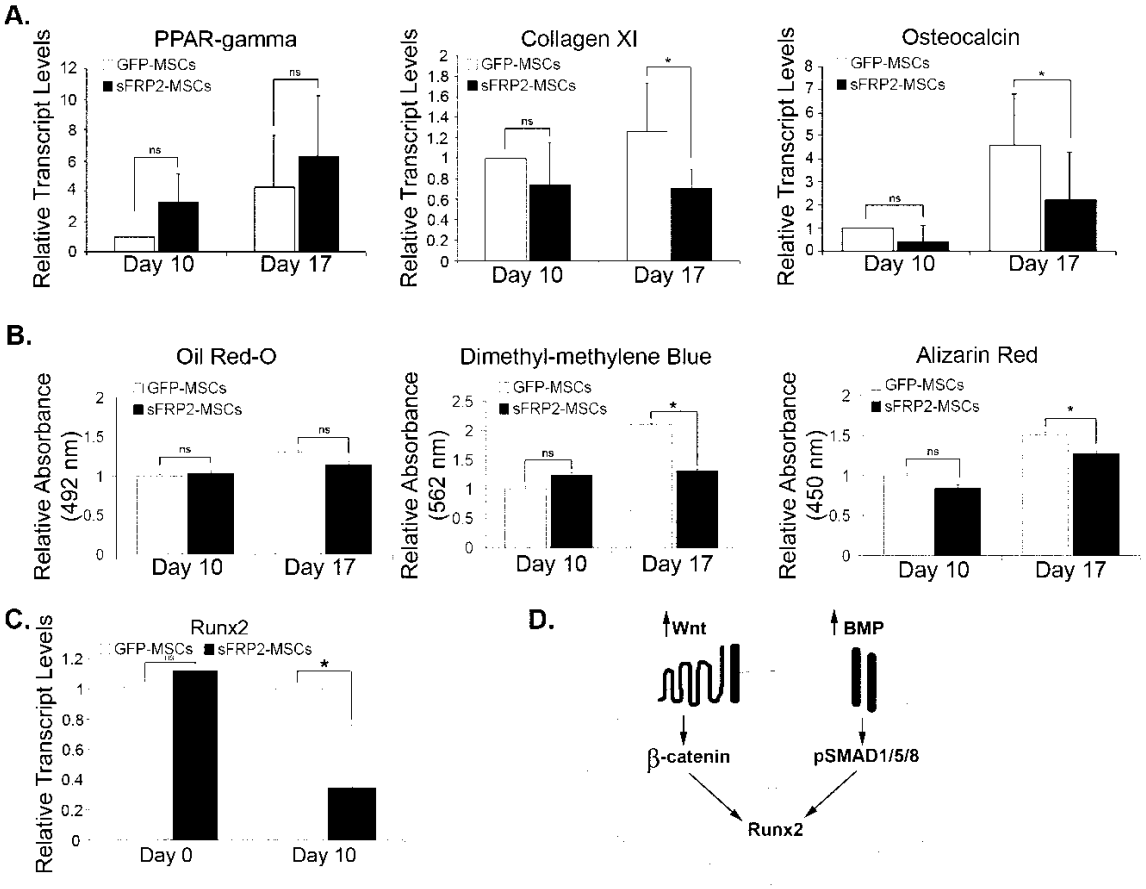

Figure 14. sFRP2 Decreases the Chondrogenic and Osteogenic Differentiation of MSCs, Not on Adipogenesis

(A) Relative transcript levels of PPAR-γ (adipogenic marker, *n* = 3), collagen XI (chondrogenic marker, *n* = 4), and osteocalcin (osteogenic marker, *n* = 5) increase in relation to time in GFP-MSCs and sFRP2-MSCs under differentiating conditions. There is no effect of sFRP2 in the adipogenic potential of the MSCs. There is decreased chondrogenic and osteogenic commitment of sFRP2-MSCs compared with GFP-MSCs as observed by the lower levels of collagen XI and osteocalcin. *ns*, not statistically significant, *, $p \leq 0.05$.
(B) Quantification of Oil Red-O stain demonstrates no difference in the oil droplet formation between GFP-MSCs and sFRP2-MSCs. The amount of sulfated glycosaminoglycans quantified by the use of dimethyl methylene blue dye in sFRP2-MSCs is lower compared with GFP-MSCs. There is decreased extracellular calcification (as quantified by the Alizarin Red stain) in sFRP2-MSCs, compared with GFP-MSCs. *, $p \leq 0.05$, $n = 4$.
(C) Relative transcript levels of Runx2, a transcription factor that controls osteocalcin expression, is not changed in non-differentiated MSCs. During osteogenic differentiation, Runx2 levels are greater in GFP-MSCs. *, $p \leq 0.05$, $n = 4$.
(D) Model figure depicting that canonical Wnt and BMP signaling cascades are involved in the regulation of Runx2 in MSCs.

Collagen XI and sulphated glycosamino glycans observed in sFRP2-MSCs. The decreased osteogenic differentiation of sFRP2-MSCs was observed in the statistical reduction of osteocalcin transcript levels and the amount of calcified matrix (as determined by Alizarin Red staining) compared to GFP-MSCs.

We confirmed the involvement of Wnt and BMP signaling in MSC lineage commitment *in vitro* and *in vivo* (Figure 15A, 15B and 15C). The addition of recombinant Wnt3a or BMP2 was not sufficient to increase the *in vitro* osteogenic or chondrogenic differentiation of sFRP2-MSCs (Figure 15D), thus sFRP2 could decrease differentiation by inhibiting either pathway.

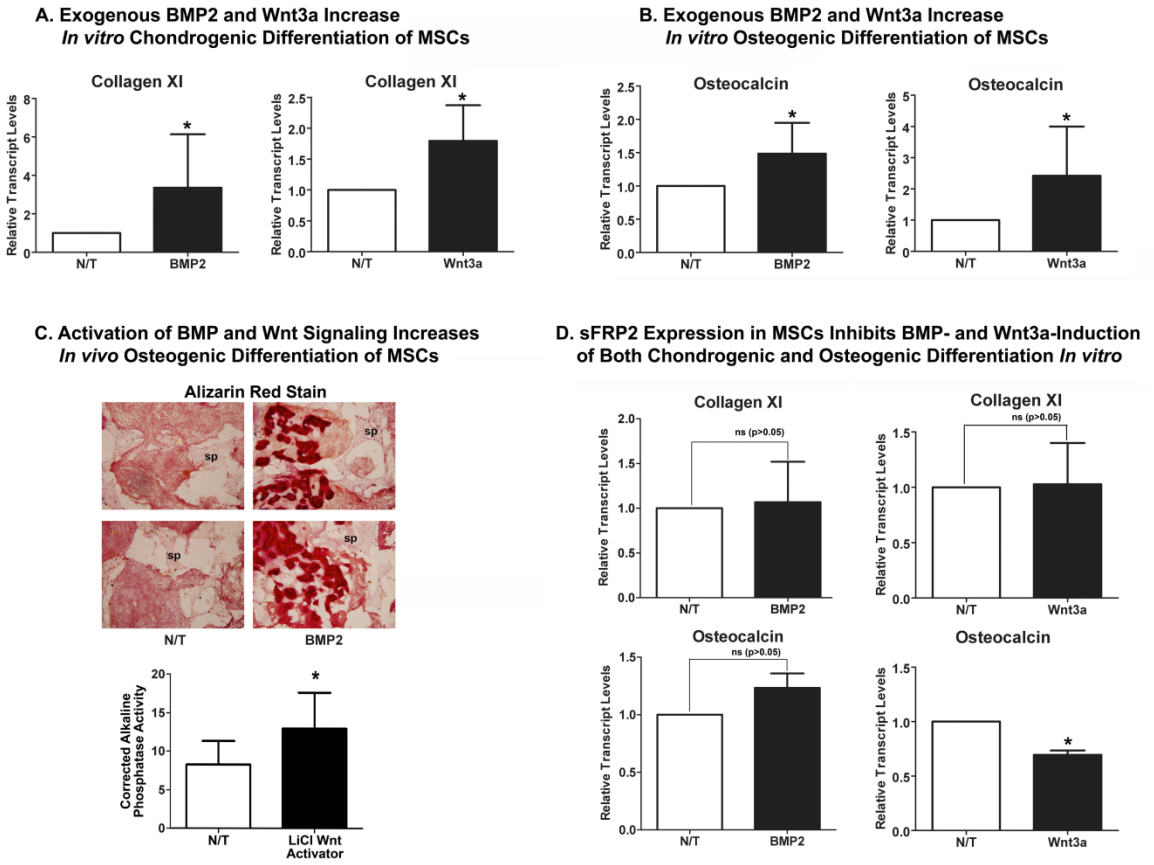

Figure 15. BMP and Wnt Signaling are Involved in MSC Lineage Commitment *in vitro* and *in vivo*; sFRP2 Inhibits this Effect

(A) Exogenous recombinant BMP2 (100 ng/ml) and Wnt3a (50 ng/ml) increase the levels of collagen XI transcripts in MSCs *in vitro*.
(B) Addition of BMP2 (100 ng/ml) and Wnt3a (50 ng/ml) increase the osteocalcin transcript levels of MSCs *in vitro*. n=6 cohorts per treatment group per lineage.
(C) Representative images of Alizarin Red stained PVA sponges that were treated with 30 µg/kg/day of BMP2 admixed with growth factor reduced matrigel or matrigel alone. BMP2 treatment increased extracellular calcification as observed by the bright red nodules. sp=sponge (20X); n=4. Wnt activation by LiCl increases osteogenic differentiation of MSCs within PVA sponges. The levels of alkaline phosphatase activity (normalized to DNA content) in LiCl-treated sponges is higher compared to PBS-treated controls.
(D) The increase in collagen XI and osteocalcin transcript levels is not observed in the sFRP2-MSC cohort after addition of BMP2 (100 ng/ml) or Wnt3a (50 ng/ml) to the differentiating conditions. *$p \leq 0.05$, Two -tailed, paired student's T-test; ns=not significant; n=3; N/T=no treatment.

To further determine the effect of sFRP2 on the decreased osteogenic differentiation of MSCs, we quantified the levels of Runx2 transcription factor by qRT-PCR. This transcription factor is essential for bone formation; its deletion completely oblates ossification[116]. Bone specific activation of the osteocalcin promoter is regulated by Runx2[117]. Wnt signaling, as well as BMP signaling, are involved in osteogenic lineage commitment in part, by regulating the expression of Runx2[107, 118]. Although there was no difference in the baseline levels of Runx2 transcripts in, Runx2 levels were decreased in sFRP2-MSCs undergoing osteogenic differentiation (Figure 14C). We came up with a working model seen in Figure 14D where we hypothesize that sFRP2 could be regulating Runx2 expression by inhibiting either the Wnt or the BMP pathways. This model prompted us to determine if sFRP2 plays a role in BMP signaling.

sFRP2 Inhibits Phosphorylation of Nuclear SMAD 1/5/8 in a Wnt-independent Manner

Data from the chick, *Xenopus* and zebrafish homologues of sFRP2 indicate that this protein could inhibit the BMP pathway [119]. BMPs mediate their signals through phosphorylation of specific receptor-associated Smads, which then complex with other Smads, translocate to the nucleus and affect gene transcription. We explored whether, under basal conditions, sFRP2 overexpression altered the transcript levels of BMP2, known to play a role in both osteogenic and chondrogenic commitment [109, 110]. Baseline relative transcript levels of BMP2 were similar in both groups (Figure 16A). We explored if BMP downstream targets were differentially regulated in sFRP2-MSCs compared to

GFP-MSCs and found a significant decrease in the transcript levels of both ID-2 and ID-3 transcript levels (Figure 16B). To further explore if sFRP2 altered basal BMP signaling we utilized a BMP-responsive luciferase reporter construct driven by the ID-1 gene [120]. GFP-MSCs and sFRP2-MSCs were co-transfected with the ID-1 reporter construct as well as a β-gal expression vector employed to ensure equal transfection efficiency. The addition of recombinant sFRP2 to GFP-MSCs led to a decrease in luciferase production. Moreover, sFRP2-MSCs had significantly reduced levels of luciferase activity (Figure 16C), suggesting a role for sFRP2 in BMP signaling inhibition, an effect that has not been previously documented for this mammalian protein. Recombinant BMP2 treatment increases the luciferase signal in both cell types (data not shown). To assess BMP signaling by an independent method, we quantified the number of nuclei positive for pSMAD1/5/8 by IF. sFRP2-MSCs had a statistically significant, seven-fold decrease in the percentage pSMAD positive nuclei under basal conditions (Figure 16D). Figure 16E shows representative images of a series of IF studies where GFP-MSCs were serum starved prior to treatment with recombinant BMP2 for one hour and subsequent treatment for 30 minutes with either recombinant sFRP2, sFRP3, Pyrvinium, or the BMP inhibitor Dorsomorphin. Dorsomorphin has been shown to selectively inhibit BMP type 1 receptors, and subsequent pSMAD1/5/8 signaling, presumably by blocking the ALK2, ALK3, and ALK6 receptor kinase function[121]. Only Dorsomorphin and sFRP2 statistically decreased the percentage of pSMAD positive nuclei. Wnt inhibition through the activity of either Pyrvinium or sFRP3 did not affect the

nuclear localization of pSMAD1/5/8. The quantification of these experiments is seen in Figure 16F. The capacity of sFRP2 to inhibit nuclear pSMAD1/5/8 was concentration dependent (data not shown). Our data showed that while BMP2 transcript levels were similar in sFRP2-MSCs, BMP signaling was significantly down-regulated relative to GFP-MSCs.

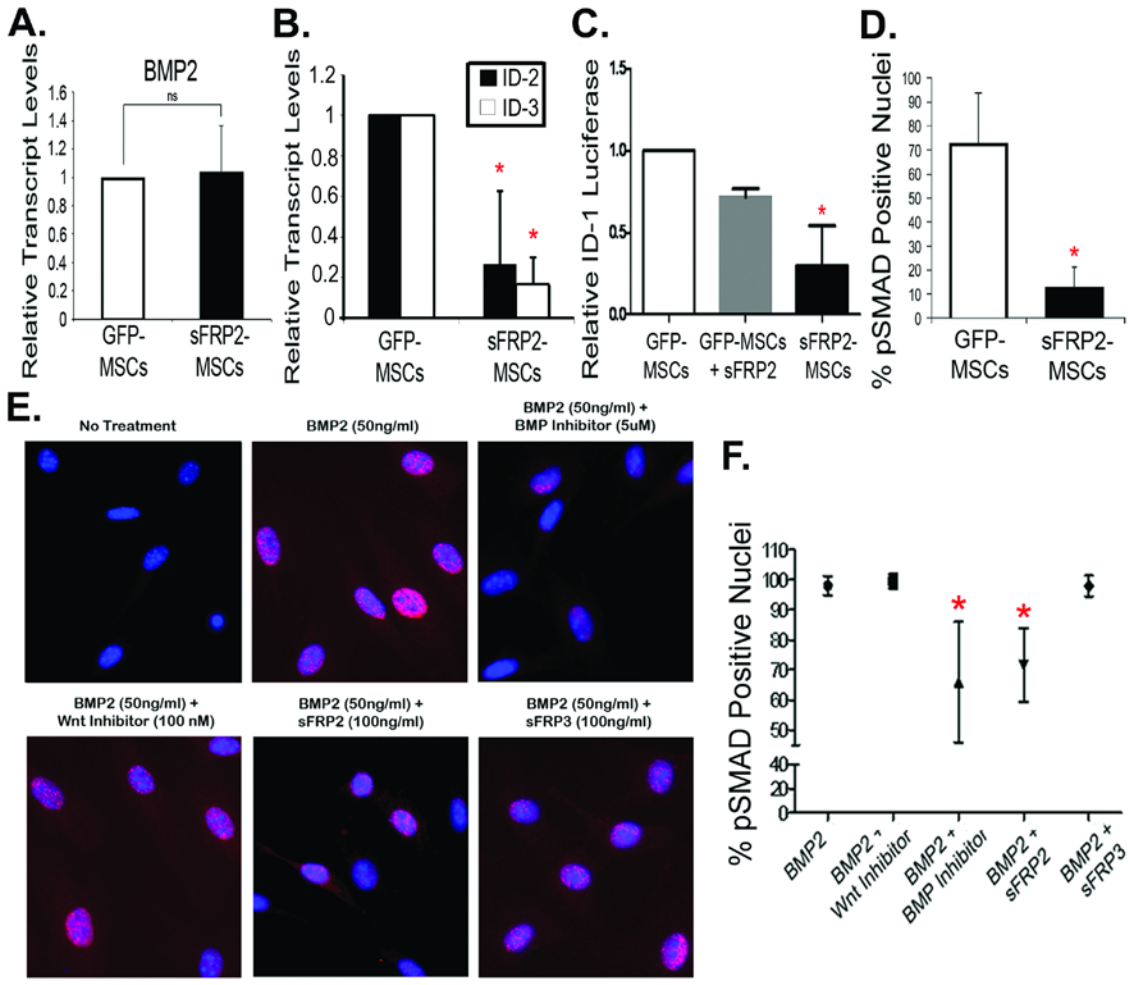

Figure 16. sFRP2 Inhibits Phosphorylation of Nuclear SMAD 1/5/8 in a Wnt-Independent Manner and Causes Functional Inhibition of BMP Signaling

*(*A) No changes in the relative transcript levels of BMP2 in serum-starved GFP-MSCs and sFRP2-MSCs. $n = 4$.
(B) Significant decrease in the relative transcript levels of BMP downstream target genes ID-2 and ID-3 in serum-starved sFRP2-MSCs compared with GFP-MSCs. $n = 3$, *, $p < 0.01$.
(C) Involvement of sFRP2 in BMP signaling demonstrated through transcriptional inhibition of BMP-driven luciferase reporter. sFRP2-MSCs had lower basal BMP activity. Addition of recombinant sFRP2 reduced luciferase activity in GFP-MSCs. $n = 4$, *, $p < 0.0001$.
(*D)* sFRP2-MSCs exhibit decreased basal phosphorylation of nuclear SMAD1/5/8 as determined by indirect immunofluorescent analysis. Average percentage of positive nuclei per high power field is shown, at least 4 fields counted in three independent experiments. *, $p = 0.006$.

Figure 16 -- Continued
(*E)* Representative photomicrographs demonstrating modulation of BMP pathway in MSCs in the presence of BMP2 (50 ng/ml), alone or with combination treatments: pyrvinium (100 nm), dorsomorphin (5 μm), sFRP2 (100 ng/ml), or sFRP3 (100 ng/ml). pSMAD 1/5/8 in *red*, DAPI in *blue.*
(F) data (n = 5 independent experiments) quantifying the average percentage of MSCs containing nuclear pSMAD 1/5/8 were graphed and show that only dorsomorphin and recombinant sFRP2 reduced BMP2-induced activation of nuclear pSMAD in MSCs. Mean ± 95%, confidence interval; *, $p < 0.0001$.

Inhibition of Phosphorylated SMAD 1/5/8 Accumulation is Not a BMP-Wnt Crosstalk Event

Although a novel BMP-inhibitory role of sFRP2 was suggested by the above studies, it was important to determine if it was due to a translational crosstalk between Wnt and BMP. We performed immunoblot analysis to determine the time course of phosphorylation of Smads1/5/8. Serum-starved MSCs were treated with recombinant BMP2 for one hour prior to treatment with either sFRP2 or sFRP3. The addition of sFRP2, but not sFRP3, decreased pSMAD1/5/8 levels by 43 ± 17% within 30 minutes of treatment (Figure 17A). sFRP2-mediated BMP pathway inhibition did not require new protein synthesis as addition of protein synthesis inhibitor, cycloheximide, did not abrogate sFRP2's effects. We examined whether Pyrvinium could affect the levels of pSMAD1/5/8; whereas Dorsomorphin significantly reduced BMP2-induced phosphorylation of Smads1/5/8 by 62 ± 14%, there was no significant diminution by Pyrvinium (Figure 17B). The ability of sFRP2 to inhibit pSMAD accumulation was not affected in the presence of Pyrvinium (Figure 18). Together, these data

support a concept that sFRP2 directly modulates the BMP signaling pathway independent of its effect on the Wnt pathway.

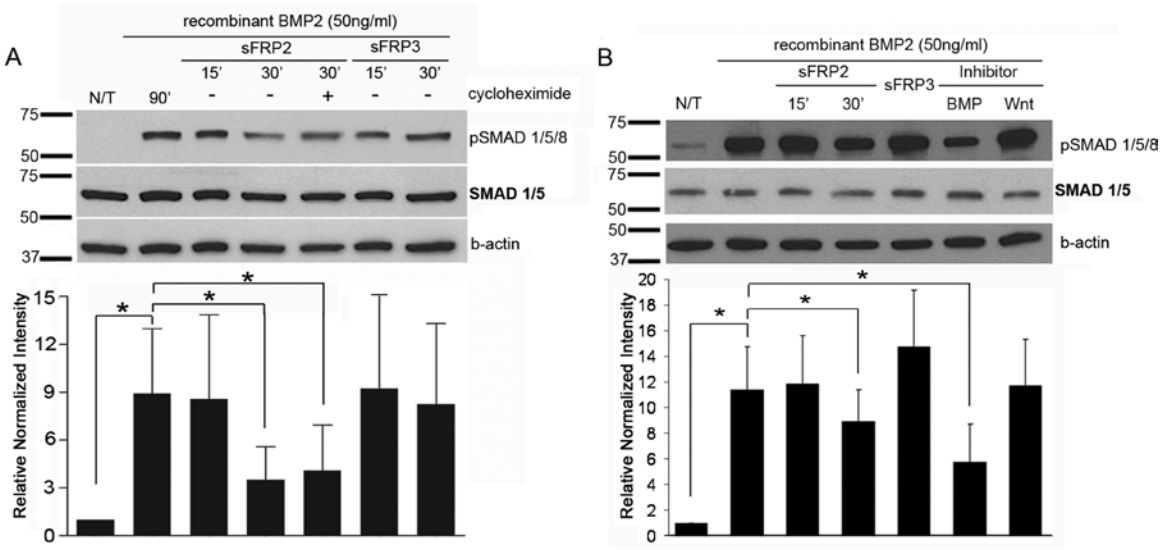

Figure 17. Wnt Independent Inhibition of Phosphorylated SMAD 1/5/8 Accumulation

(A) Time course of sFRP2-induced SMAD1/5/8 phosphorylation in mouse MSCs. MSCs were serum-starved for 24 h and stimulated with recombinant BMP2 (50 ng/ml) for 1 h prior to addition of recombinant sFRP2 (100 ng/ml) or sFRP3 (100 ng/ml) for 15 or 30 min. sFRP2-mediated BMP-signaling inhibition was unaltered by the addition of protein synthesis inhibitor, cycloheximide (10 μm). Representative Western blot analysis and the quantification of the relative pSMAD1/5/8 protein abundance in cell lysates normalized to β-actin; $n = 3$.
(*B)* Serum-starved MSCs were pretreated with BMP2 (50 ng/ml) for 1 h before addition of designated treatments: sFRP2 (100 ng/ml), sFRP3 (100 ng/ml), pyrvinium (100 nm), or dorsomorphin (5 μm). Only sFRP2 and dorsomorphin decreased BMP-induced pSMAD levels. sFRP3 and a Wnt inhibitor did not alter BMP signaling. Representative Western blot analysis and the quantification of the relative pSMAD1/5/8 protein abundance in total cell lysates normalized to β-actin; $n = 3$.

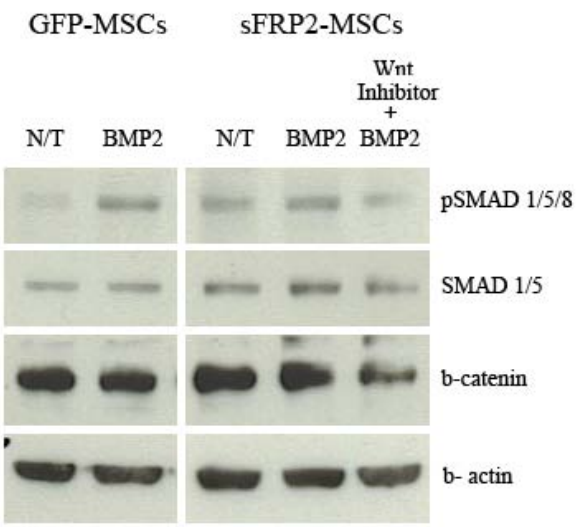

Figure 18. BMP Signaling is Decreased by sFRP2 Even in the Presence of a Wnt Inhibitor

BMP2 treatment (50 ng/ml) increases pSMAD 1/5/8 levels dramatically in GFPMSCs. This increase is not as dramatic in sFRP2-MSCs and is not rescued by the Wnt inhibitor, pyrvinium. N/T=no treatment.

sFRP2-MSCs Demonstrate Decreased Osteogenic Differentiation *in vivo*

We have demonstrated that sFRP2-MSCs have a significant (2- to 3-fold) increase in engraftment compared to GFP-MSCs in two separate *in vivo* models of wound repair[75]. Using the PVA sponge model of granulation tissue formation, we examined whether the increase in engraftment correlated with a decrease in differentiated progeny by visualizing matrix calcification within MSC-loaded sponges. Figure 19A shows representative images of sections of GFP- and sFRP2-MSC-loaded PVA sponges stained for Von Kossa (as an indicator of calcified matrix) and clearly demonstrate the decreased osteogenic differentiation of sFRP2-MSCs. Von-Kossa positive areas were quantified with morphometric analysis and the data are shown in Figure 19B. The inhibition of osteogenic

differentiation observed *in vitro* translates to an *in vivo* setting. These data indicate that increased engraftment was due to the maintenance of un-differentiated MSCs, further demonstrating the effects of sFRP2 on self-renewal.

sFRP2 Expression Reduces Ectopic Calcification of MSC Treated Hearts

A serious reported complication of MSC-mediated myocardial therapy following injury is ectopic calcification and/or ossification[122]. Based on our data which showed that sFRP2 decreases osteogenic differentiation *in vitro* as well as *in vivo* within PVA sponges, we predicted that sFRP2 may ameliorate this complication of MSC therapy. In a previous study we demonstrated that in the setting of myocardial infarcts induced through coronary artery ligation, sFRP2-MSCs reduced infarct size, prevented adverse remodeling and improved cardiovascular function. sFRP2-MSC treated hearts contained a higher density of blood vessels and greater numbers of MSCs at 30 days post infarct and cell therapy[75]. We examined histological sections stained with Von Kossa to detect calcifications within both GFP- and sFRP2-MSC treated hearts (Figure 19C). Von Kossa-positive calcified matrix within the left-ventricular scar tissue was found in almost 70% of GFP-MSC treated (4/6) hearts but only in 14% of sFRP2-MSC treated hearts (1/7) (Figure 19D). These data suggest that sFRP2 not only drives more effective MSC-mediated repair but may reduce the frequency by which MSC-mediated therapy may induce ectopic myocardial calcifications.

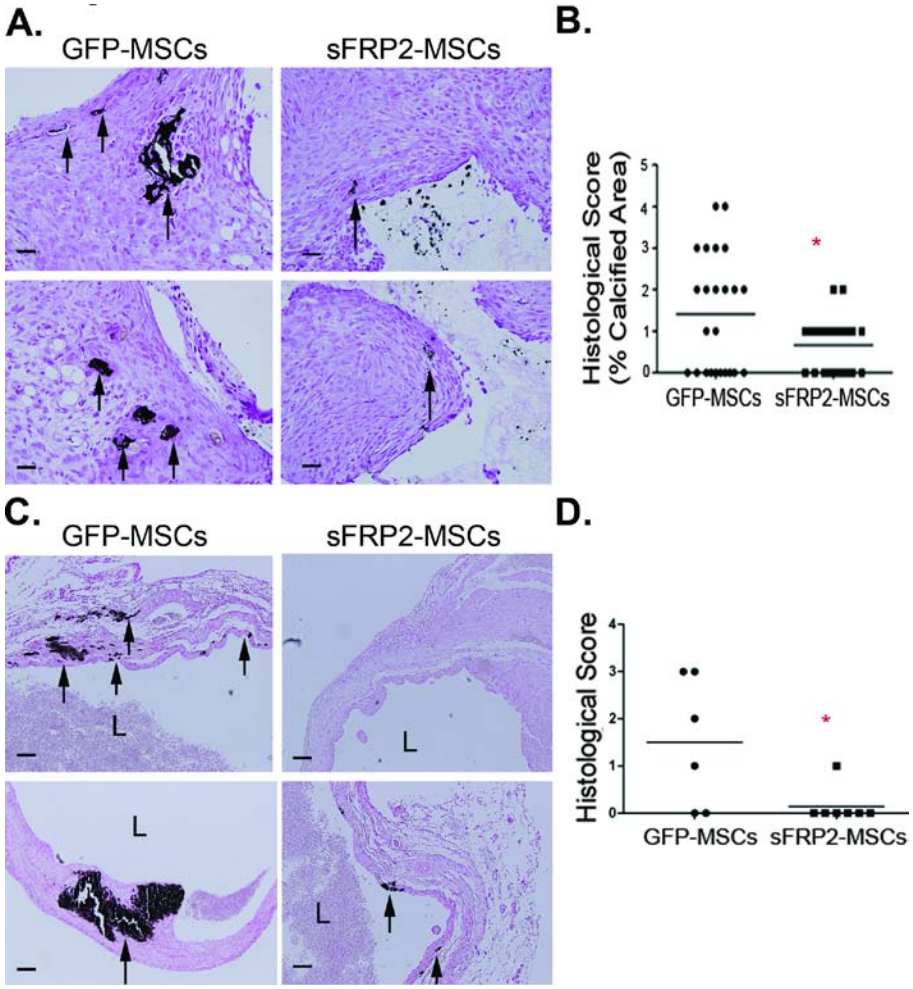

Figure 19. Overexpression of sFRP2 Causes Decreased Ectopic Calcification within Infarcted Myocardium

(A) sFRP2-MSCs, which have higher levels of engraftment within PVA-sponges, have decreased osteogenic differentiation *in vivo*. Representative images of calcified matrix within granulation tissue of MSC-loaded PVA sponges. *Black arrows* point to Von Kossa-positive areas (40X).
(*B)* Quantification of the total percentage Von Kossa-positive areas within the granulation tissue in PVA sponges shows a decrease in the amount of calcified matrix within the sFRP2-loaded sponges. Wilcoxon sum ranks test; *, $p = 0.0012$, GFP-MSC $n = 6$, sFRP2-MSC $n = 7$.
(*C)* Representative images of GFP- and sFRP2-MSC-treated hearts of NOD/SCID mice stained for Von Kossa to visualize ectopic calcification. *Black arrows* point to calcified matrix. *L*, lumen (10X).
(*D)* Histological score of the amount and the quality of Von Kossa-positive staining within MSC-treated hearts. sFRP2-MSC-treated hearts, which demonstrated statistically improved cardiac function, have statistically decreased ectopic calcification within the infarcted myocardium. Mann-Whitney U-Test, GFP-MSC $n = 6$, sFRP2-MSC $n = 7$.

Discussion

MSCs are utilized in a variety of preclinical models to ameliorate wound healing. Enhanced cardiac tissue repair mediated by MSCs, in concert with clinical studies suggesting that their clinical use is feasible and safe, have spurred a number of clinical trials using bone marrow-derived MSCs as regenerative cell therapy. At least 14 trials are currently ongoing using MSCs to treat myocardial disease (clinicaltrials.gov)[31]. However, our understanding on how MSCs mediate cardiac and soft tissue repair, including aspects that regulate MSC self renewal, remains incomplete.

sFRP2 has been identified as a factor mediating myocardial repair and wound granulation tissue formation by MSCs[71, 75]. Although sFRP2 has been postulated to function as a paracrine modulator of cardiomyocyte apoptosis[123], we have provided compelling data that sFRP2 is an important autocrine factor for MSCs themselves. sFRP2 overexpression directly up-regulated MSC proliferation *in vitro* and enhanced their long-term engraftment in mouse models of myocardial injury and wound granulation tissue. In these studies we sought to better clarify how sFRP2 was coordinating repair by MSCs at the cellular level. Our studies showed that sFRP2 is an important modulator of MSC self-renewal. In addition to its published role to enhance proliferation[75], we report that it also inhibits both MSC apoptosis and their differentiation along osteogenic and chondrogenic lineages.

Our previous study showed that sFRP2 resulted in a dose-dependent increase in human and murine MSC proliferation *in vitro*. Conversely, addition of

recombinant Wnt3a (or its overexpression in MSCs) resulted in a decreased proliferation rate. Dkk1, an inhibitor of canonical Wnt signaling, has been demonstrated to increase human MSC proliferation and entry into the cell cycle *in vitro[111]*. Taken together with our findings that sFRP2 was able to decrease functional canonical Wnt signaling in MSCs[75], these data suggested that sFRP2 increased proliferation through inhibition of canonical Wnt signaling.

The sFRP family has also been termed the secreted apoptosis-related proteins, or SARPs, and as their name suggests has been documented to play important roles in the cytoprotection of distinct cells[124]. Herein we demonstrated that sFRP2 served to protect MSCs from apoptosis under basal and hypoxic conditions. This pro-survival effect was likely to be mediated by sFRP2 inhibition of canonical Wnt signaling as sFRP2 decreased both β-catenin and cleaved Caspase 3 levels. The anti-apoptotic action of sFRP2 in MSCs closely mirrors its recently reported paracrine anti-apoptotic effects on cardiomyocytes through direct binding of Wnt3a and inhibition of Wnt3a induced activation of Caspase activities[123].

MSCs are capable of differentiating into multiple connective tissue lineages, in particular bone, cartilage and fat. Differentiation of MSCs along these lineages occurs at very low levels spontaneously but is accelerated by specific differentiation-inducing culture conditions. By testing for biochemical and genetic markers characteristic of adipose, cartilage and osteogenic lineages, we showed that sFRP2 inhibited differentiation of MSCs along both cartilage and osteogenic lineages *in vitro*. We further demonstrated a sFRP2-dependent decrease in

transcript levels of Runx2, a transcription factor necessary for osteogenic commitment. Wnt and BMP pathways regulate Runx2 transcript levels, and BMP is a known critical regulator of both osteogenic and chondrogenic differentiation of MSCs, we evaluated the effect of sFRP2 on the BMP pathway. Our data provided evidence that sFRP2 inhibited BMP signaling: sFRP2 inhibited nuclear levels of BMP effectors, pSMAD1/5/8, as well as BMP-signaling-dependent Id-1 driven reporter gene. Inhibition of pSMAD1/5/8 occurred within 30 minutes, independently of protein synthesis, and was not affected by the addition of the Wnt inhibitor, Pyrvinium. These data suggested that sFRP2 inhibition of BMP signaling did not result from crosstalk between the Wnt/BMP pathways and occurred independently of its effect on Wnt inhibition. Moreover, BMP signaling inhibition occurred both with the addition of recombinant sFRP2 as well as in cells overexpressing sFRP2, suggesting that sFRP2 inhibited BMP in a non-self autonomous manner.

The mechanism by which sFRP2 directly inhibits BMP signaling in mammalian cells is not known and, until this report, only clues as to its involvement in BMP signaling were available. For example, the non-mammalian homologue of sFRPs, Sizzled (Szl), establishes dorsal-ventral patterning in the *Drosophila melanogaster*, *Xenopus*, and zebrafish by regulating gradients of BMPs in the developing embryos [119]. The vertebrate dorsal center secretes BMP antagonists, among which Chordin is known to sequester BMP ligands to prevent receptor binding [125]. Szl inhibits BMP signaling by inhibiting the activity of Xolloid-related (Xlr), the metalloproteinase that degrades Chordin. In this

developmental process the effect of Szl on Xlr allows sequestration of BMPs by Chordin[126] and ultimately BMP pathway inhibition. In a cell-free *in vitro* system, mouse sFRP2 interacted with *Xenopus* Xlr to prevent the degradation of *Xenopus* Chordin[127]. Another recent report suggests sFRP2 may play a role in BMP inhibition in the developing embryo; unilateral electroporation of murine BMP and sFRP2 into the chick neural tube blocked the induction of BMP downstream targets[128]. This study did not address whether the observed BMP inhibition was an indirect or a direct effect of sFRP2.

In this paper we show direct, Wnt-independent inhibition of BMP signaling molecules, accomplished not only by overexpression of sFRP2 by MSCs, but by the addition of recombinant mouse sFRP2 to the extracellular space. This biochemical inhibition led to functional inhibition of BMP signaling observed by a decrease in both chondrogenic and osteogenic lineage commitment of MSCs. Compiling our data with the information available about sFRP2 and its non-mammalian homologues, we speculate that the effects of sFRP2 as a BMP inhibitor are carried out in the extracellular space. Our results support the following model (Figure 20): Increased expression of sFRP2 in MSCs inhibits both canonical Wnt and BMP signaling. The resulting cellular effects of sFRP2 on proliferation, apoptosis and differentiation impact MSC self renewal and ultimately engraftment within the wound.

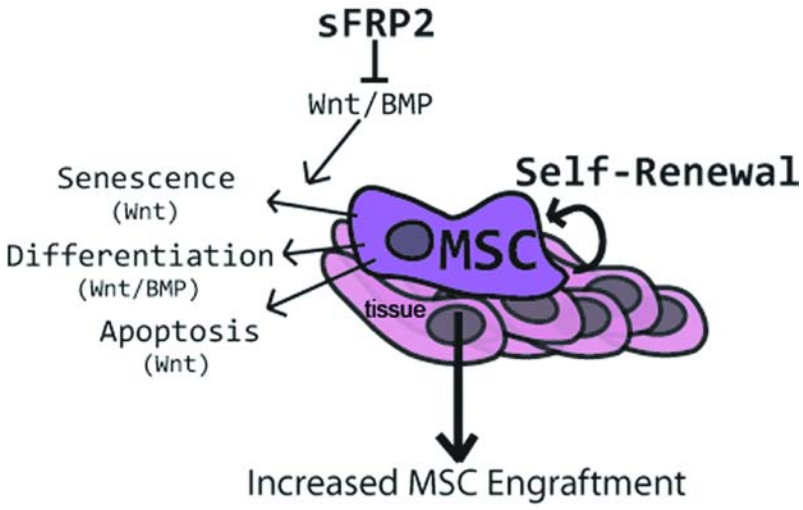

Figure 20. Model of the Proposed Mechanism of Action of sFRP2 in MSC Biology

In the context of a wound, sFRP2 expression by MSCs inhibits Wnt and BMP signaling leading to a decreased senescence (increased proliferation), differentiation, and apoptosis. Inhibition of Wnt and BMP signaling by sFRP2 thereby increases MSC self-renewal and increases their tissue engraftment.

Recent reports have highlighted the potential complication of spontaneous *in situ* osteogenic differentiation of MSCs following cardiac cell therapy. We assessed heterotopic calcification in two, independent *in vivo* models following MSC cell therapy. Our data showed that in the setting of myocardial infarction and within experimental granulation tissue generated in PVA sponges, sFRP2-expressing MSCs demonstrated significantly fewer foci of ectopic calcification than GFP-MSCs. These data suggest that sFRP2-mediated inhibition of differentiation may reduce the risk of heterotopic cartilage and/or bone tissues observed with MSC therapy.

Despite direct injection of large numbers of cells into tissues, preclinical studies show poor engraftment with only small numbers or no MSCs remaining

after 30 days. Hence, a better understanding of the molecular players, such as sFRP2, that favorably modulate MSC self-propagation, engraftment, and differentiation may alter the overall efficacy of MSC cardiac and wound therapy.

CHAPTER IV

CONNECTIVE TISSUE GROWTH FACTOR HAS A PHYSIOLOGIC ROLE IN EARLY WOUND REPAIR

Introduction

Mesenchymal stem cells (MSCs) produce factors that regulate their growth and differentiation, and also have a positive paracrine effect on their local microenvironment. The molecules within the MSC secretome may suppress the local immune system, enhance angiogenesis, inhibit apoptosis or decrease scar formation. Understanding the key paracrine factors secreted by MSCs would give us insight into molecular regulators of repair. Work by our group and others have found that secreted Frizzled-Related Protein 2 (sFRP2) is a key mediator of MSC-directed wound repair. Expression of sFRP2 by MSCs (sFRP2-MSCs) induces an enhanced reparative phenotype compared to vector control-expressing MSCs (GFP-MSCs). We hypothesized that sFRP2 increased MSC-directed wound repair by regulating their secretome. In this work, we performed proteomic analysis on the conditioned media (CM) from sFRP2-MSCs and GFP-MSCs through liquid chromatography tandem mass spectrometry (LC-MS/MS). Raw peptides were transformed into confident protein identifications with the use of IDPicker software. Gene ontologies revealed an increase in several stem cell regulatory groups in the sFRP2-MSC CM. Connective tissue growth factor

(CTGF) was identified and confirmed to be up-regulated in the sFRP2-MSC cohort.

The polyvinyl alcohol (PVA) sponge model of granulation tissue formation became a tool that allowed us to assess the effects of CTGF in wound repair. The temporal regulation of CTGF post sponge implantation demonstrated a role for this molecule in early tissue repair. Significantly decreased collagen transcript levels were observed when recombinant CTGF was administered to empty sponges for six days following sponge implantation. The granulation tissue deposited in the sponges with prolonged CTGF addition was statistically more proliferative and collagenous. These results not only provide direct evidence of a non-pathological role for CTGF in wound repair, but also demonstrate CTGF is an enhancer of early wound tissue. Ultimately, these data shed light into the paracrine effect of MSCs.

MSC Paracrine Effects

MSCs produce a wide array of cytokines, chemokines, adhesion molecules and other bioactive factors that help regulate their growth and differentiation. These factors also have a paracrine effect on the microenvironment by suppressing the local immune system, enhancing angiogenesis, inhibiting apoptosis, and decreasing scar formation[129, 130].

Our group has demonstrated that sFRP2-MSCs deposit better granulation tissue in the PVA sponge model, compared to GFP-MSCs[75]. Treatment of sFRP2-MSCs increased functional parameters and decreased pathological

cardiac remodeling in a murine model of myocardial infarction[75]. Other groups have demonstrated that sFRP2 by itself can reduce fibrosis and improve cardiac function[131]. However, we wanted to determine what other secreted factors were playing a positive role in MSC-directed wound repair.

Proteomic profiling is a tool used to identify key factors not only involved in MSC biology, but also in the repair process[132-134]. Tandem mass spectroscopy (MS/MS) allows for the interrogation of a large pool of unknown peptides and liquid chromatography (LC) is utilized to separate them prior to MS analysis[135, 136]. IDPicker is a bioinformatics software which not just employs decoy database searches to compute the false discovery rate of raw identifications but combines multiple scores to increases confident identifications of proteins from the tryptic peptides. Thus it does not require any statistical distribution inference or machine learning[137].

Connective Tissue Growth Factor

CTGF is a secreted protein belonging to the CCN family of immediate-early genes[138]. This family is rich in cysteine residues and its members are characterized by containing four domains involved in growth factor binding, dimerization, heparin and proteoglycan binding and integrin recognition[139]. Although these domains hint at the biological function of CTGF, its role in wound repair is mostly unknown. Because CTGF is present in a wide variety of fibrotic conditions of the skin, kidney, liver, lung and others[140-142], it is thought to be a

pro-fibrotic molecule. The results presented herein demonstrate a non-pathological role for CTGF in early wound healing.

Results

Proteomic Analysis of MSC Conditioned Media Reveals Important Gene Ontology Changes

Many groups have speculated that the positive effects of MSCs on wound repair rely on their ability to produce soluble factors that enhance the repair process (reviewed in [129]). Previous work from our lab employed two MSC populations to assess *in vivo* repair. MSCs were transduced with an empty retroviral vector (GFP-MSCs) or with the same vector containing sFRP2 (sFRP2-MSCs). sFRP2-MSCs had increased reparative ability in both wound repair models[75, 76]. To determine which secreted proteins would enhance the reparative ability of the sFRP2-MSCs the conditioned media (CM) of three independent GFP-MSC and sFRP2-MSC isolates were obtained after growth in serum-free media for 48 hours. TCA precipitated protein pellets from the CM were trypsin digested. Strong cation exchange chromatography was used to separate the peptide mixture into fractions, which were then individually analyzed by reverse phase LC-MS-MS, the large data sets were handled with IDPicker. The cellular compartment localization of the positively identified proteins was retrieved using uniProtKB (http://www.uniprot.org/) and used as a filter for further analysis; only proteins found in the extracellular space were retained. The gene ontology (GO) information of the over-represented proteins in the sFRP2-MSC

CM revealed an interesting trend towards cellular growth (7%), differentiation (15%), protein homeostasis (22%), growth factors/signaling (24%) and adhesion (32%) as seen in Figure 21A. The complete list of sFRP2-MSC over-represented secreted proteins and their GO information can be found in the Table 8.

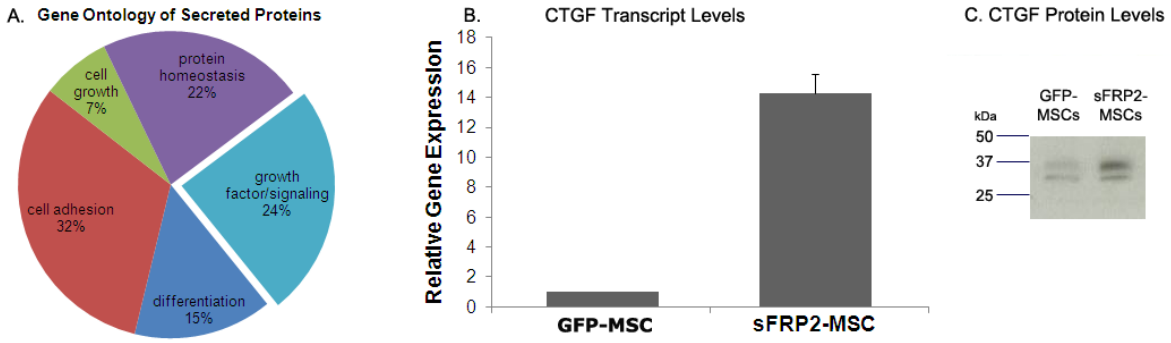

Figure 21. Proteomic Analysis Reveals CTGF Up-Regulation in sFRP2-MSCs

A. Gene ontology (GO) classification of IDPicker positively identified secreted proteins. UniProtKB was used to search for GO and cellular compartment information.
B. Quantitative real-time PCR analysis revealed a 14.3 ± 1.3 increase in CTGF transcript levels in sFRP2-MSCs compared to GFP-MSCs; normalized to 18S content, n=3.
C. Representative blot demonstrating increased CTGF protein in the TCA-precipitated conditioned media of sFRP2-MSCs. The average intensity increase of the ~37 kDa band is 2.57 ± 0.8 as determined by Image J analysis, n=3.

Table 8. List of sFRP2-MSC Over-represented Secreted Proteins

		Protein ID	Coverage	Total Hits	Fold Change
differentiation	Protein FAM20A precursor	IPI:IPI00229820.1	11	9	2
	Cartilage-associated protein precursor	IPI:IPI00111370.1	14	22	1.75
	Bone morphogenetic protein 1	IPI:IPI00469541.1	41	224	1.093458
	Glia-derived nexin precursor	IPI:IPI00115065.1	53	382	1.134078
	Dystroglycan precursor	IPI:IPI00122273.1	31	59	1.034483
	Olfactomedin-like protein 3 precursor	IPI:IPI00308658.3	36	53	1.038462
cell adhesion / heparin binding	Fibronectin type-III domain-containing protein C4orf31 homolog precursor	IPI:IPI00330474.3	32	31	2.1
	Coiled-coil domain-containing protein 80 precursor	IPI:IPI00473455.1	29	63	1.625
	Mama protein	IPI:IPI00119809.1	42	131	1.183333
	Cystatin-C precursor	IPI:IPI00123744.1	67	205	1.5625
	milk fat globule-EGF factor 8 protein isoform 1	IPI:IPI00788387.1	45	131	1.258621
	Calsyntenin-1 precursor	IPI:IPI00470000.2	26	79	1.257143
	Follistatin-related protein 1 precursor	IPI:IPI00124707.1	63	257	1.089431
	Isoform 1 of SPARC-related modular calcium-binding protein 2 precursor	IPI:IPI00378169.1	19	28	1.333333
	Thrombospondin 1	IPI:IPI00118413.2	48	352	1.095238
	Isoform 1 of Periostin precursor	IPI:IPI00338018.1	71	807	1.152
	Isoform 2 of Tenascin precursor	IPI:IPI00420656.3	32	229	1.081818
	Glypican-1 precursor	IPI:IPI00137336.1	51	83	1.128205
	Mesothelin precursor	IPI:IPI00121279.1	31	82	1.157895
cell growth	Calreticulin precursor	IPI:IPI00123639.1	77	245	1.168142
	Urokinase-type plasminogen activator precursor	IPI:IPI00129102.1	49	59	1.458333
	Metalloproteinase inhibitor 2 precursor	IPI:IPI00113863.1	65	139	1.106061
protein homeostasis	Lysyl oxidase homolog 1 precursor	IPI:IPI00380136.3	37	57	1.28
	Sulfated glycoprotein 1 precursor	IPI:IPI00321190.1	69	687	1.107362
	Isoform 1 of Sulfhydryl oxidase 1 precursor	IPI:IPI00223231.2	49	357	1.087719
	Fructose-bisphosphate aldolase A	IPI:IPI00221402.7	70	196	1.020619
	Isoform 1 of Polypeptide N-acetylgalactosaminyltransferase 2	IPI:IPI00420710.1	24	24	2
	gamma-glutamyl hydrolase	IPI:IPI00828662.1	43	56	1.545455
	Procollagen C-endopeptidase enhancer 1 precursor	IPI:IPI00120176.1	57	567	1.139623
	Isoform 1 of Plasma glutamate carboxypeptidase precursor	IPI:IPI00126050.3	37	58	1.148148
	Glutamate dehydrogenase 1, mitochondrial precursor	IPI:IPI00114209.1	27	25	1.083333
growth factor/ signaling	Inhibin beta A chain precursor	IPI:IPI00112347.1	31	32	2.555556
	Connective tissue growth factor precursor	**IPI:IPI00322594.3**	**19**	**16**	**4.333333**
	Plasminogen activator inhibitor 1 precursor	IPI:IPI00131547.1	55	178	1.311688
	EGF-containing fibulin-like extracellular matrix protein 2 precursor	IPI:IPI00126055.1	37	72	1.4
	Calumenin precursor	IPI:IPI00135186.1	65	147	1.19403
	EGF-containing fibulin-like extracellular matrix protein 1 precursor	IPI:IPI00223457.1	36	55	1.894737
	Annexin A2	IPI:IPI00468203.3	62	181	1.154762
	Isoform Long of Beta-1,4-galactosyltransferase	IPI:IPI00131464.1	43	90	1.045455
	Transcobalamin-2 precursor	IPI:IPI00136556.1	47	106	1.163265
	Isoform Alpha of Stromal cell-derived factor 1 precursor	IPI:IPI00108061.3	40	22	1.444444

Connective Tissue Growth Factor is Upregulated in sFRP2-MSCs

Connective tissue growth factor (CTGF) had the highest presence within the sFRP2-MSC group, compared to the GFP-MSC group; it was identified 4.33 fold higher in the sFRP2-MSC group (Table 8). Although the coverage for this protein was only 19% with 16 total hits, the presence of this protein within the sFRP2-MSC CM was striking. CTGF fell within the growth factor GO classification and proved an interesting candidate to further validate since its presence has been well documented in wounds [143, 144].

The regulation of CTGF was confirmed by quantitative real-time PCR (qRT-PCR) analysis of three different sFRP2-MSC isolates compared to their GFP-MSC counterparts. Δ/Δ CT analysis of the results demonstrated that sFRP2-MSCs have higher transcript levels of CTGF. There was a 14.3 ± 1.3 fold increase of CTGF transcripts in the sFRP2-MSC cohort (Figure 21B). This difference in CTGF mRNA levels was also observed at the protein level. As seen in Figure 21C, immunoblotting TCA-precipitated sFRP2-MSC CM revealed an overall 2.57 ± 0.8 fold increase in CTGF compared to GFP-MSC CM. These differences in regulation could be explained in different ways. First, the protein analysis was performed on the secreted fraction (CM) and therefore the protein contained within the cell (*i.e.* newly synthesized, golgi-bound) was not visualized. Second, because CTGF can bind extracellular matrix proteins it might not be in soluble form within the CM. Regardless, the trend was confirmed and CTGF was up-regulated in sFRP2-MSCs.

CTGF is Involved in the Early Stages of the Wound Repair Process

A sustained increase in CTGF within a wound is usually equated to pathological conditions [140-142]. However, we observed increased CTGF in the sFRP2-MSC cohorts which were deemed to improve wound repair. To assess the role of CTGF in wound repair, we used the poly-vinyl alcohol (PVA) sponge model of granulation tissue formation [75, 87, 88]. Prior to implantation, the PVA sponges were soak-loaded with either GFP-MSCs (n=18), sFRP2-MSCs (n=18) or saline control (n=9). The sponges were implanted subcutaneously into NOD/SCID mice. Three animals were sacrificed seven days post-implantation, three more after 15 days and the last cohort 28 days post-surgery. RNA was isolated from each sample and qRT-PCR analysis was performed to assess the levels of CTGF transcripts. As seen in Figure 22A, CTGF transcript levels were the highest at the earliest time-point examined (day 7). The CTGF transcript levels steadily decreased with time. Interestingly, confocal images of immunofluorescently labeled sponge sections demonstrated a steady increase in CTGF protein levels (red) that spiked at day 15 and quickly diminished by day 28 (Figure 22B). Together, these data suggest CTGF is important in early wound repair processes.

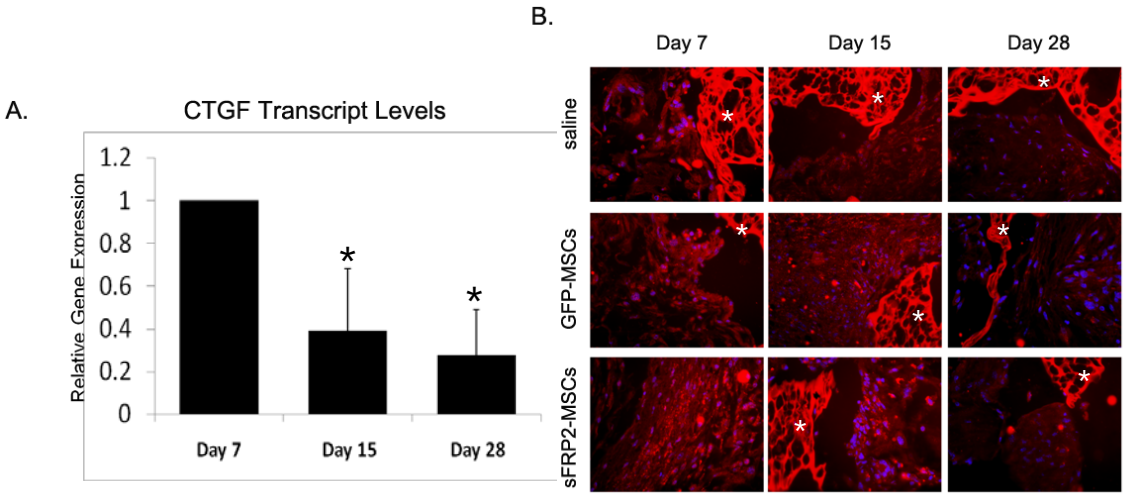

Figure 22. CTGF is Involved in Early Stages of Granulation Tissue Formation

A. The transcript levels of CTGF within GFP-MSC loaded sponges decrease with time as assessed by qRT-PCR; normalized to 18S content, n=6 sponges per time point.
B. Panel of representative confocal images demonstrating CTGF protein levels spike by day 15 and then decrease by day 28 in PVA sponges. Blue = nuclei, red = CTGF, white asterisk = sponge.

Early Exposure to CTGF Prevents Fibrosis, Prolonged CTGF Enhances a Proliferative, Collagenous Granulation Tissue

The previous results suggested that the effects of CTGF could be observed in the absence of the MSCs within the PVA sponges. Therefore we designed an experiment where the levels of CTGF were changed by direct injection of the recombinant protein (rCTGF). To determine the effect of the timing of CTGF availability the cohorts received rCTGF injections (1 µg/day/sponge in 10 µl) every other day for six days, 15 days or 28 days. The saline controls endured the same regimen. For each cohort there were three

animals which totaled six sponges per treatment group, all the animals were sacrificed after 28 days.

The amount of granulation tissue within sponge sections from each cohort was determined. No differences were found in the amount of granulation tissue deposited in the sponges treated with rCTGF for six days (left panel Figure 23A). The sponges which received rCTGF for 28 days had more granulation tissue when compared to the saline control (right panel Figure 23A). Trichrome Blue staining of the sections allowed us to visualize the differences in the quality of the granulation tissue. As expected there was more collagen deposition in the sponges treated with rCTGF for 28 days compared to saline control. However, there seemed to be less collagen deposition in the sponges that were treated with rCTGF for six days.

To determine if indeed the timing of rCTGF administration was affecting fibrosis, we performed qRT-PCR analysis looking at the levels of mouse Collagen 1a2 (Figure 23B). Compared to the saline control, collagen levels decrease if rCTGF was added at the early stages of the wound repair process (blue and red bars, up to day 15). However, if rCTGF administration was prolonged for 28 days (green bars), the collagen levels increased.

To determine if the reason between the disparate amounts of granulation tissue following 28 days of rCTGF was due to more than increased collagen deposition, the sections were stained with Ki67 to assess the proliferation within the tissue. Figure 23C shows that rCTGF for 28 days significantly increased the proliferation of the granulation tissue. Together, these results correlate with the

idea that prolonged exposure to CTGF promotes an activated fibroblast population [145, 146].

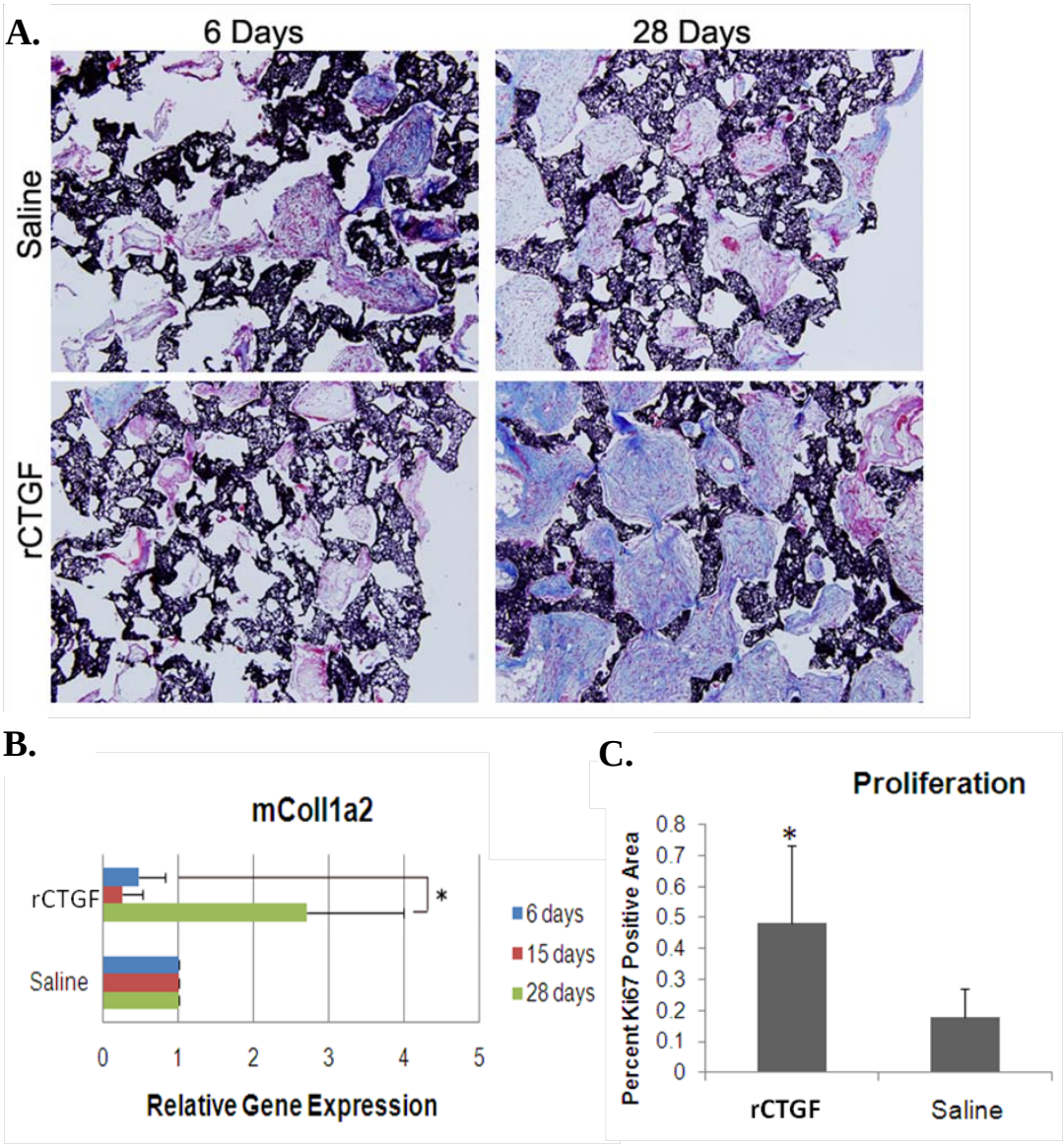

Figure 23. Addition of Recombinant CTGF to PVA Sponges Enhances a Proliferative, Collagenous Granulation Tissue

A. Representative 40X images of Trichrome Blue-stained granulation tissue after six or 28 days of rCTGF (1 µg/day/sponge) or saline injections. Black = sponge, blue= collagen, red = granulation tissue.

B. Quantitative real-time PCR analysis of mouse Collagen1a2 demonstrates that CTGF exposure for the initial stages (days 0-15) of wound repair yields decreased collagen deposition, normalized to 18S content, whereas prolonged exposure increases collagen transcript levels. n=6 sponges per cohort. * $p<0.001$ Two way ANOVA with Bonferroni post test.

C. rCTGF (1 µg/day/sponge) increases the proliferative index of the granulation tissue as quantified by the threshold values of Ki67 positive areas in 20X representative images of PVA sponges. ANOVA * $p = 0.0392$ vs. saline.

Dose Dependent Response to Endogenous CTGF, Increased Collagen Content within Early Wounds of CTGF$^{+/-}$ Mice

The previous results suggested that CTGF did not affect the wound repair process negatively at the early stages. Its up-regulation during the initial repair process implied CTGF could have a physiological role in healing. To confirm this, we wanted to test the wound repair capabilities of animals lacking CTGF. This was not possible since CTGF null animals die shortly after birth because of respiratory failure [147, 148]. Instead, we used animals containing only one copy of CTGF (CTGF$^{+/-}$, HET) which reach adulthood without apparent phenotype [148].

Full-thickness excisional wounds were created with a biopsy punch [149] onto the backs of WT and HET animals. Animals were sacrificed after 10 and 14 days following surgical intervention. The wound repair capabilities of the mice were assessed with the use of a histopathological scoring system. The collagen content, granulation tissue, and vascularization within the wounds were blindly graded. As seen in Figure 24A, although there were no differences in the amount of granulation tissue, the amount of collagen found in the wounds of the HET mice was greater than that in the WT mice. This data correlate with the results observed whereas increased CTGF exposure during early wound processes had decreased collagen content (Figure 23B). Albeit not statistically significant, there was an apparent decrease in vascular content within the wounds of the HET animals. There were no differences in the ability to repair the wounds at the late time point (day 14, Figure 24B) suggesting a role for CTGF in early wound repair.

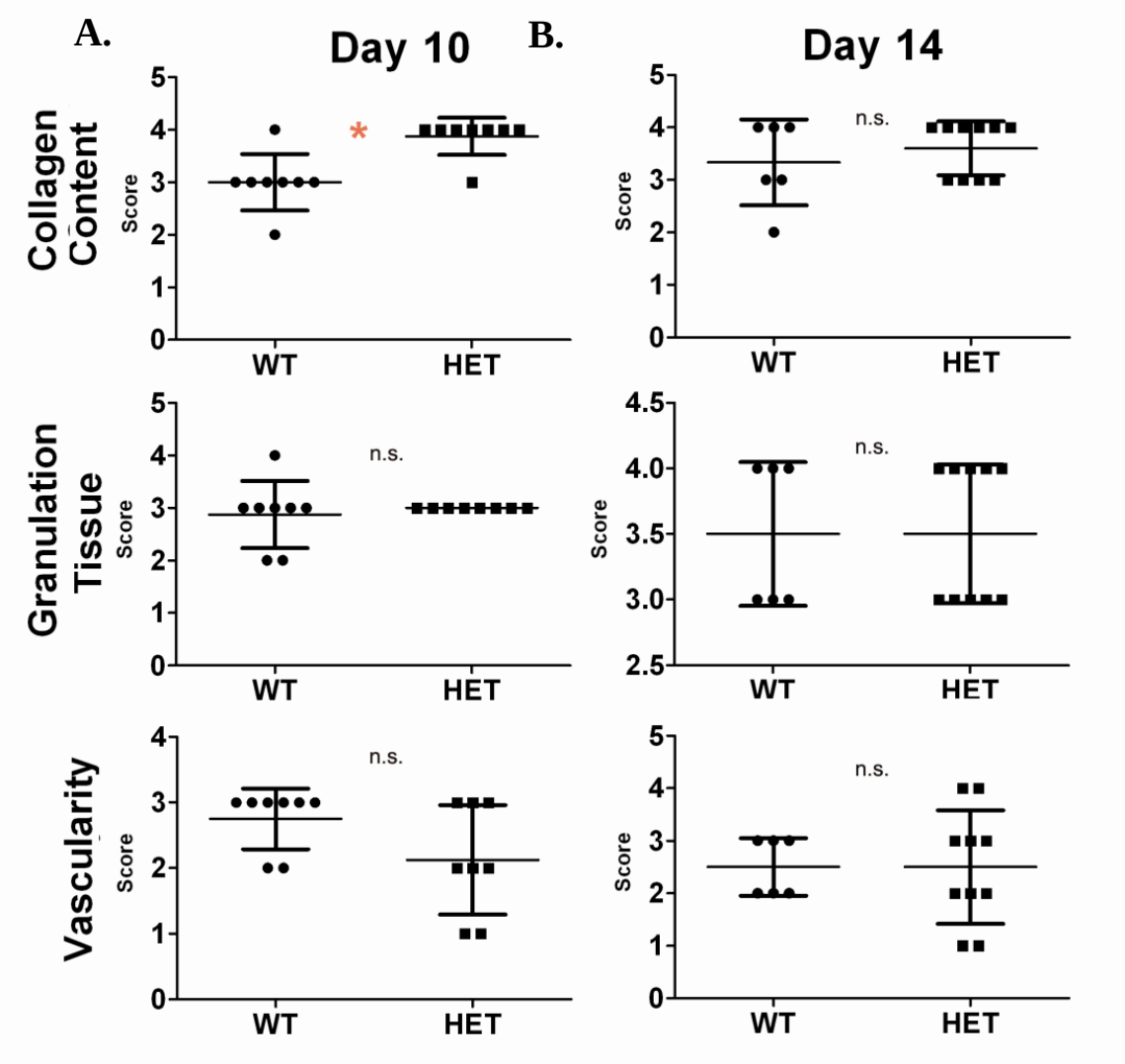

Figure 24. Dose Dependent Response to Endogenous CTGF, Increased Collagen Content within Early Wounds of CTGF$^{+/-}$ Mice

Histopathological scores assessing collagen content, amount of granulation tissue, and vascularity within sections of excisional wounds from CTGF$^{+/+}$ mice (WT) versus CTGF$^{+/-}$ (HET) mice 10 days (A.) and 14 days (B.) after injury. Increased collagen content within 10 day old wounds of HET mice was observed. n≥6 wounds per cohort; paired t-test * p=0.0062, n.s.= not significant.

Discussion

Proteomic analysis of CM from two MSC populations found CTGF to be increased in the group which previously had been shown to improve wound repair [75]. However, most of the literature discusses the regulation of CTGF in fibrotic conditions. The levels of TGF-β have been shown to precede CTGF induction during normal wound repair, suggesting CTGF is downstream of TGF-β signaling [143, 150]. Although addition of CTGF alone can induce collagen deposition, several reports have determined that the fibrotic effects of CTGF are more robust if TGF-β is present in the system [146, 151, 152]. Indeed, administration of a CTGF neutralizing antibody following TGF-β induced fibrosis ameliorates the fibrotic condition in mice [153].

The results do not contradict the published results but rather demonstrate the importance of timing on the role of CTGF in wound repair. The first clue to point in this direction came by realizing the regulation of CTGF by MSCs *in vitro*; the levels of CTGF decrease with increased passage (data not shown). The PVA model of granulation tissue formation was a useful tool which showed the induction of CTGF transcripts spiking seven days post implantation and the protein levels following at 15 days. Importantly, the endogenous CTGF production was very low by 28 days.

The same wound repair model was utilized to demonstrate that high levels of recombinant CTGF at early time points has no deleterious effect on the wound process. Strikingly, early CTGF addition decreased the collagen production in the wounds. As expected, sustained CTGF administration led to increased

granulation tissue deposition. The granulation tissue derived from continuous rCTGF addition was highly proliferative and collagenous. The differences in the effect of rCTGF could also be explained by differences in the levels of TGF-β during the different stages of granulation tissue formation, an important cascade we aim to look at. We speculate that fibroblast activation is only achieved after a certain threshold of CTGF is reached [154].

The use of $CTGF^{+/-}$ animals confirmed a role for endogenous CTGF in early wound repair processes. Analysis of the wounds 10 days following injury determined a change in only one parameter, which correlated with the earlier results. It will be interesting to assess the wound repair capabilities of the HET versus WT CTGF animals at an even earlier time point as it is clear that the differences in repair diminish with time.

These data suggest that the regulation of CTGF in the wound repair process is critical to avoid a pathological, fibrotic condition. The kinetics of tissue repair include three major phases: the inflammatory, the proliferative, and the remodeling/maturation [155]. Our data suggest the physiological expression of CTGF during the proliferative phase. A similar regulation in the levels of CTGF after injury has been documented elsewhere [143]. If CTGF levels persist during the remodeling phase of wound repair, then fibrosis ensues [140-142].

Previous studies have demonstrated a positive role of CTGF in the wound repair process. Recombinant human CTGF (10–100 ng /cm^2) was added to non-human primate burn wounds for 19 days following wounding. Two weeks after CTGF administration, the wound tissue generated orderly healing fibers at the

burn site, accompanied by an increased proliferative response. Compared to the control group, the CTGF treated group had a significantly smaller wound area [156].

Recently, CTGF was added to MSC cultures *in vitro* causing a loss of expression of MSC markers, a decrease in MSC tri-lineage differentiation and an increase in collagen deposition. *In vivo* administration of CTGF favored fibrogenesis rather than ectopic mineralization in rodent connective tissue healing [145]. These results are interesting since they demonstrate a positive role for CTGF in MSC-directed wound repair.

The presence of CTGF in pathological settings has been widely documented thus dissuading investigations on the precise biological function of this molecule. More work on the events affected by CTGF during early wound repair is necessary to fully explore the apparent bimodal activity of this molecule. Ultimately, understanding the physiologic effects of CTGF can lead to its management in the clinic.

CHAPTER V

DISCUSSION AND FUTURE WORK

Conclusions

MSCs remain an intriguing entity. The work contained within this dissertation shed some light on mechanisms dictating MSC biology; however, the light was dim in the grand scheme. It is exciting to think that one day MSCs may be utilized in the clinic to successfully treat a variety of conditions. Understanding the events which dictate their efficacy is of great importance. Many unknowns in this field remain as such.

The work contained in this dissertation demonstrated that MSCs isolated from two different mice strains had differing levels of granulation tissue formation and myocardial repair. Microarray analysis pointed to sFRP2 as the key molecule responsible for these observed results. Indeed, sFRP2 overexpression increased the reparative ability of MSCs. Most importantly, sFRP2 facilitated MSC engraftment and cardiac remodeling and repair in a mouse model of acute MI [75].

Sequence homology between sFRP2 and sFRP1 is relatively high (approximately 70%); yet overexpression of sFRP1 in MSCs (sFRP1-MSCs) was not sufficient to enhance MSC-directed wound repair (Figure 25). Proliferation studies demonstrated sFRP1-MSCs did not have increased turn-over *in vitro* (Figure 25B). Assessment of the effects of sFRP1-MSCs in the PVA model of

granulation tissue formation demonstrated no enhancement in the reparative potential of MSCs due to overexpression of sFRP1 (Figure 25C and 25D). These results further demonstrated the unique nature of sFRP2 and highlighted the importance of the data presented in this dissertation.

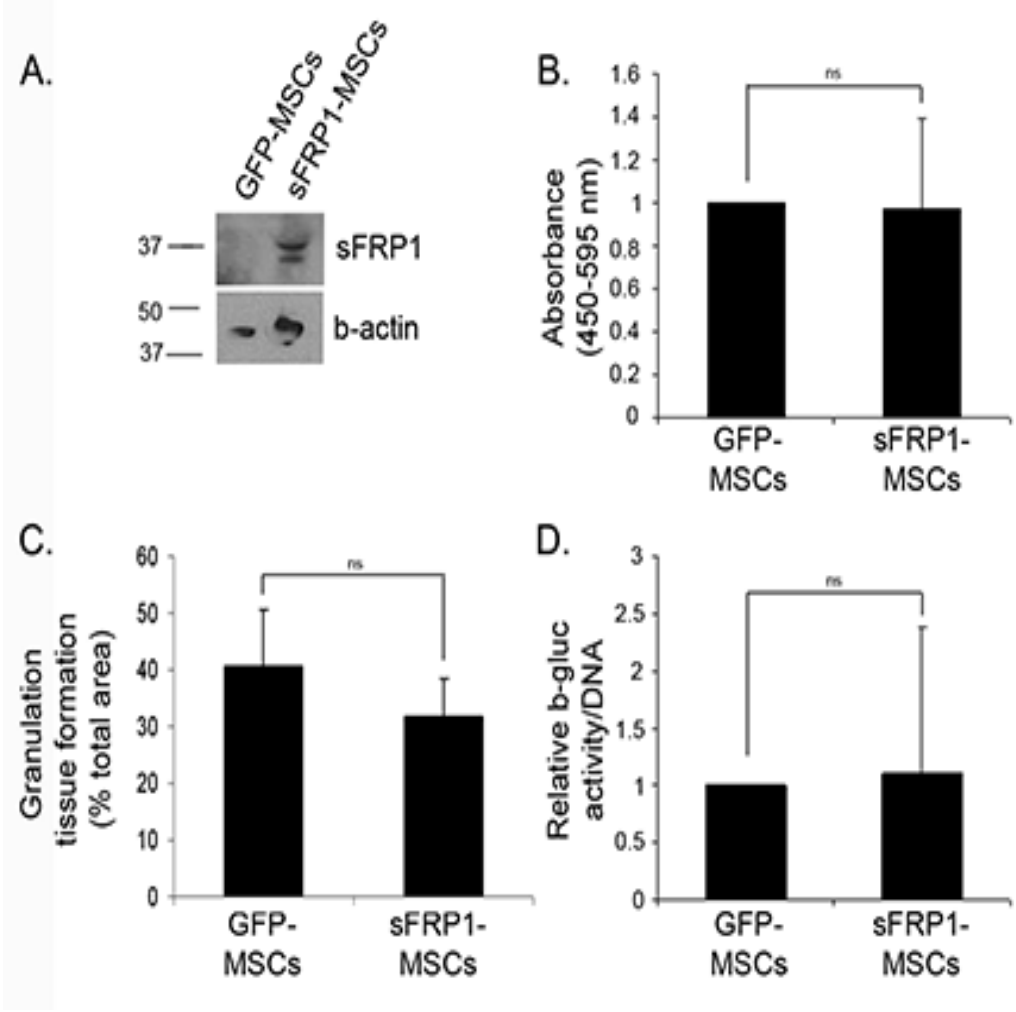

Figure 25. sFRP1 Does Not Enhance MSC Reparative Potential

A. sFRP1 is overexpressed in MSCs as confirmed by Western blot analysis.
B. Proliferation of MSCs is not enhanced by sFRP1 as assessed with a BrdU incorporation ELISA.
C. Morphometric analysis revealed that sFRP1-MSCs do not deposit more granulation tissue in the PVA sponge model.
D. Engraftment of sFRP1-MSCs is not increased *in vivo* in the PVA sponge model as assessed by β-gluc activity. ns= not significant.

The mechanism of action of sFRP2 remains elusive. Is the molecule acting on the wounded microenvironment or on the MSCs? Data from other labs suggest that sFRP2 mediates myocardial survival following injury by inhibiting

Wnt signaling [71, 123]. He *et al*. demonstrated that fibrosis is decreased by sFRP2 by inhibiting pro-collagen maturation through the inhibition of BMP1 proteinase activity [131]. This last claim, however, is disputed by conflicting evidence whereby sFRP2-null mice have decreased fibrosis post-MI [157]. An issue of dosage sensitivity and timing is brought up by these contradictory results. He *et al*. demonstrated that high doses of sFRP2 inhibit, yet low doses enhance, BMP1 activity. Both published results demonstrate that the levels of sFRP2 dramatically increase immediately after MI (days 1-3) and then diminish to homeostatic levels. At the early time points post-MI, sFRP2 exerts its anti-apoptotic role. Deletion of sFRP2 could enhance apoptosis. At later time points post-MI, once sFRP2 levels decrease, it would mostly increase BMP1 activity. In accordance, the decreased fibrosis of the sFRP2-null mice is only significant during late stages of the wound repair process (two weeks post-MI). Together, these data call to mind the importance of dosage and timing in understanding the role of sFRP2.

Our work focused on the effect of sFRP2 on the MSCs themselves. To address this point we thought about the possible outcomes for the MSCs within a wound: senescence, apoptosis, differentiation or self-renewal. Addition of recombinant sFRP2 to both murine and human MSCs increased proliferation by approximately two-fold. Consistent with these results, overexpression of sFRP2 enhanced the *in vitro* proliferation of MSCs approximately three-fold [75]. The increase in proliferation meant that sFRP2 decreased the possibility of the MSCs to enter into a senescent state.

The ability of the MSCs to survive within the wound is critical to their reparative capabilities. Thus, we assessed the levels of apoptosis following serum starvation and hypoxic culture conditions. sFRP2-MSCs had decreased Annexin V positive cells and lower cleaved Caspase 3 levels compared to the GFP-MSC control. These insults were significant since serum starvation and hypoxia are hallmarks of a wound [158]. We assessed whether the effect on apoptosis involved canonical Wnt signaling since sFRP2 had been implicated in the inhibition of this cascade [100, 159]. sFRP2 decreased Wnt signaling in MSCs, as assessed by immuno-blotting for β-catenin as well as functional inhibition of TOP/FOP flash luciferase reporter system [75, 76]. This inhibition correlated with decreased *in vitro* apoptosis observed.

Molecular and biochemical assays of differentiation studies revealed decreased chondrogenic and osteogenic lineage commitment for sFRP2-MSCs compared to GFP-MSC control [76]. Multiple mechanisms, including Wnt and BMP signaling, direct MSC lineage commitment [82, 110, 160, 161]. Our next aim was to determine if the observed decrease in differentiation was due, in part, to direct BMP inhibition by sFRP2. Utilizing a luciferase reporter construct for BMP signaling, we demonstrated that sFRP2 functionally inhibited ID-1 promoter activity. Immunofluorescent analysis of the signaling molecules involved in canonical BMP signaling, phosphorylated SMADS 1, 5 and 8 (pSMAD 1/5/8), showed decreased nuclear staining when the cells were treated with sFRP2. These studies were confirmed with immunoblotting for pSMAD 1/5/8 and taken

together demonstrated direct and specific inhibition of BMP signaling by sFRP2 [76].

Importantly, the decreased *in vitro* differentiation potential of sFRP2-MSCs was translated to decreased ectopic calcification within MSC-treated infarcted hearts. The sFRP2-MSCs remained undifferentiated at higher numbers in this setting [75, 76]. This increase in engraftment translated to an increase in cardiac function post-MSC treatment [75].

The positive effect on myocardial repair of the sFRP2-MSCs is probably due to an increase in levels of favorable wound-repair factors. Our efforts were focused on identifying such trophic factors. The secretome of sFRP2-MSCs was compared to that of the GFP-MSCs, and Connective Tissue Growth Factor (CTGF) was detected. Although tangential to the bulk of our work, studies on CTGF revealed that it has a physiologic role in early wound repair.

The majority of the publications concerning CTGF correlate its expression with pro-fibrotic conditions; however, its temporal regulation following injury suggested it may have a physiologic role in wound repair. Different methods allowed us to demonstrate that CTGF levels rise quickly (7-15 days) following injury and decline thereafter. The endogenous up-regulation of CTGF in early time points following injury suggested it was expressed during the proliferative phase of wound repair. We speculate that the pathologic role of CTGF is conferred upon continued expression during the remodeling phase. Our data demonstrate that the temporal expression of CTGF dictates its effects on wound repair.

Significance

The work described in this dissertation delineated the effects of sFRP2 in MSC biology. sFRP2 increased proliferation, prevented apoptosis and decreased differentiation of MSCs. As a whole these data suggest sFRP2 is a potent factor involved in MSC self-renewal. Our work is the first to identify a MSC self-renewal factor. Increasing MSC self-renewal is critical to enhancing their therapeutic efficacy and therefore the work on sFRP2 is critically important. The significance of this finding can be appreciated by looking at the impact self-renewal factors have had on other stem cell fields. Particularly, the *ex-vivo* expansion of hematopoietic stem cells (HSCs, $CD34^{+}$) through addition of recombinant self-renewal factors is being actively pursued and has yielded important results in several clinical trials of a variety of human diseases [162].

Expansion of the HSC pool requires symmetric self-renewing cell divisions that give rise to two daughter cells that retain HSC function, and Hoxb4, Wnt signaling and Notch signaling are thought to drive this event [163]. Until now, no signaling cascade had been implicated in MSC self-renewal. Careful study of sFRP2 allowed us to identify a role for Wnt signaling in MSC biology. Our data correlate with previously published results which associated increased Wnt activity to tissue specific stem cell dysfunction or aging [97, 98].

Endogenous sFRP2 Expression during Myogenic Repair

sFRP2 was originally cloned from a BM-derived stromal cell line [100]. Our lab first identified this protein when comparing BM-derived MSCs from the

superhealer MRL/MpJ mouse to MSCs (MRL-MSCs) from a wild-type C57-Bl6 mouse; sFRP2 transcripts as well as protein were significantly up-regulated in the MRL-MSCs [75]. These data suggest there is an important role for this protein in successful MSC-derived healing. But is there a role for sFRP2 in non MSC-derived healing?

Endogenous presence of sFRP2 could delineate whether or not it might play a role in wound repair. Studies in the developing chick embryo (*in situ* hybridizations) implicated sFRP2 in myogenesis, given its expression in mesenchyme associated with developing muscles in the limb bud as well as in ventricular myocardium [159]. The expression of sFRP2 mRNA on whole rabbit muscle is highest at embryonic day 21 and quickly decreases to undetectable levels by post-natal day 5 [164]. However, sFRP2 can be detected in expanded myogenic precursors (satellite cells) isolated from uninjured adult muscle. The levels of sFRP2 decrease in the adult muscle satellite cells with age [165]. Interestingly, as early as 24 hours following cardiotoxin injury or muscle denervation the levels of sFRP2 mRNA re-appear [164, 165]. These data demonstrate sFRP2 is involved in myogenesis and/or muscle repair yet also hint to a role in myogenic precursor maintenance.

Anakwe *et al.*, grafted sFRP2-overexpressing cells onto a stage 18-20 chick embryo causing impaired myogenesis [166]. This group demonstrated that the number of pre-myogenic cells (Pax-3 positive cells) was increased in the sFRP2-transfected limbs compared to control limb [166]. More proof on the role of sFRP2 in myogenic precursor maintenance came from a time-course,

expression analysis of cardiotoxin injected muscle. Following injury, sFRP2 was up-regulated at time points that correlate with satellite cell activation and proliferation, and its expression coincided with the increase in Pax-7 [167]. Furthermore sFRP2 inhibits *in vitro* myoblast differentiation of rabbit and mice satellite cells. Its effects are increased if added before the induction of differentiation, and not observed if administered after myogenic commitment has taken place [168]. Although all of the data presented above are circumstantial, taken together with our data on the role of sFRP2 in MSC self-renewal, it is possible sFRP2 plays an important role in myogenic tissue-resident stem cell maintenance.

Future Directions

To address the role of endogenous sFRP2 in tissue repair, we created a tissue-specific inducible transgenic mouse. The fibroblast specific protein 1 (FSP1) Green Fluorescent Protein (GFP) (FSP1.GFP) construct was attained from the laboratory of E. Neilson [169]. Two loxP sites were cloned into the vector sequence, one directly upstream of the GFP start codon and one following its poly A tail [170]. The complete coding sequence for sFRP2 as well as a poly A tail was added downstream of the GFP poly A tail, following the second loxP site. Digestion of the final product with XhoI and FsPI produced a linearized product for injection into zygotes. Figure 26 contains the map of the vector constructed to generate the transgenic mouse line.

Pro-nuclear DNA injections were performed at the Vanderbilt Transgenic Mouse/ES Cell Shared Resource facility. PCR analysis of the ten lines generated uncovered four different mouse lines positive for the transgene. These lines are currently being bred with a Rosa 26 Cre-ER^{T2} mouse line (The Jackson Laboratory No. 008463) which express a conditional recombinase that is retained in the cytoplasm until tamoxifen administration; binding of tamoxifen to the estrogen receptor releases the recombinase to allow it to act upon loxP sites in the nucleus [171].

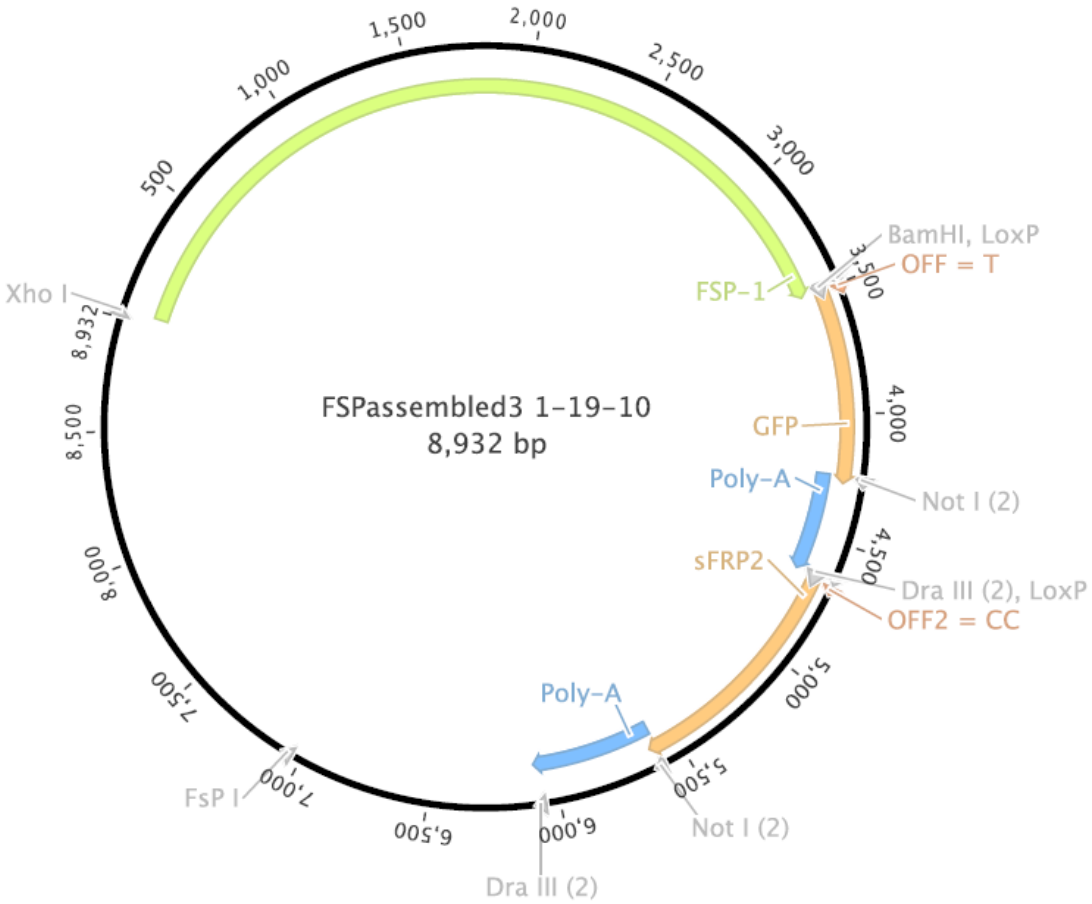

Figure 26. Map of the Floxed GFP Construct for Inducible sFRP2 Expression *in Vivo*

The *in vivo* recombination event is in the process of being confirmed. Once the system is finely tuned, the transgenic mouse line that we created will allow us to induce the expression of sFRP2 in a tissue specific manner. The literature suggests that expression of sFRP2 prior to injury will allow the pool of myogenic progenitors to increase; however its prolonged expression might block lineage commitment of these cells [164]. Understanding the timing and extent of

recombination will be a unique challenge. Nevertheless, this mouse serves as a powerful tool to understand the role of endogenous sFRP2 in tissue repair.

The exact mechanism of action of sFRP2 *in vivo* remains unknown and the work described herein demonstrates the need to further understand this molecule, particularly as it pertains to stem cell biology and wound repair. Although its roles in Wnt and BMP signaling inhibition have been demonstrated by our work and others, we have noticed a dosage issue that must be explored further. It is possible however, that sFRP2 acts on other signaling pathways and may have roles directed by its structural domains [172].

Experiments utilizing small molecule inhibitors of Wnt and BMP signaling may demonstrate that the effects of sFRP2 are indeed due to its dual actions. These inhibitors can be injected following injury by themselves, in conjunction with the MSCs, or used for pre-treatment of the MSCs prior to administration. If indeed concomitant inhibition of Wnt and BMP is the mechanism of action of sFRP2, then these experiments will demonstrate the importance of sFRP2 on the MSCs themselves (autocrine) or on the damaged tissue (paracrine). These experiments might demonstrate that pre-treatment with these inhibitors may yield MSCs with an increased reparative phenotype.

Closing Remarks

Overall, this work delineates the molecular function of sFRP2 in MSC-directed wound repair and more importantly in MSC biology. sFRP2 expression by MSCs enhances their reparative potential; it increases MSC self-renewal by functional inhibition of BMP and Wnt signaling. Further roles for this molecule remain to be determined, however our work shows that sFRP2 could serve as a powerful marker for successful MSC-directed wound repair.

REFERENCES

1. Baddoo, M., et al., *Characterization of mesenchymal stem cells isolated from murine bone marrow by negative selection.* J Cell Biochem, 2003. **89**(6): p. 1235-49.

2. Short, B., et al., *Mesenchymal stem cells.* Arch Med Res, 2003. **34**(6): p. 565-71.

3. Meirelles Lda, S. and N.B. Nardi, *Murine marrow-derived mesenchymal stem cell: isolation, in vitro expansion, and characterization.* Br J Haematol, 2003. **123**(4): p. 702-11.

4. Colter, D.C., et al., *Rapid expansion of recycling stem cells in cultures of plastic-adherent cells from human bone marrow.* Proc Natl Acad Sci U S A, 2000. **97**(7): p. 3213-8.

5. Xu, S., et al., *An improved harvest and in vitro expansion protocol for murine bone marrow-derived mesenchymal stem cells.* Journal of Biomedical Biotechnology, 2010. **2010**: p. 105940.

6. Madonna, R., Y.J. Geng, and R. De Caterina, *Adipose tissue-derived stem cells: characterization and potential for cardiovascular repair.* Arterioscler Thromb Vasc Biol, 2009. **29**(11): p. 1723-9.

7. Harris, D.T., *Cord blood stem cells: a review of potential neurological applications.* Stem Cell Rev, 2008. **4**(4): p. 269-74.

8. Zhang, X., et al., *Isolation and characterization of mesenchymal stem cells from human umbilical cord blood: Reevaluation of critical factors for successful isolation and high ability to proliferate and differentiate to chondrocytes as compared to mesenchymal stem cells from bone marrow and adipose tissue.* J Cell Biochem, 2011.

9. Pozzobon, M., M. Ghionzoli, and P. De Coppi, *ES, iPS, MSC, and AFS cells. Stem cells exploitation for Pediatric Surgery: current research and perspective.* Pediatr Surg Int, 2010. **26**(1): p. 3-10.

10. Tropel, P., et al., *Isolation and characterisation of mesenchymal stem cells from adult mouse bone marrow.* Experimental Cell Research, 2004. **295**(2): p. 395-406.

11. Pittenger, M.F., et al., *Multilineage potential of adult human mesenchymal stem cells.* Science, 1999. **284**(5411): p. 143-7.

12. Delorme, B., et al., *Specific plasma membrane protein phenotype of culture-amplified and native human bone marrow mesenchymal stem cells.* Blood, 2008. **111**(5): p. 2631-5.

13. Dominici, M., et al., *Minimal criteria for defining multipotent mesenchymal stromal cells. The International Society for Cellular Therapy position statement.* Cytotherapy, 2006. **8**(4): p. 315-7.

14. Rombouts, W.J. and R.E. Ploemacher, *Primary murine MSC show highly efficient homing to the bone marrow but lose homing ability following culture.* Leukemia, 2003. **17**(1): p. 160-70.

15. Ortiz, L.A., et al., *Interleukin 1 receptor antagonist mediates the antiinflammatory and antifibrotic effect of mesenchymal stem cells during lung injury.* Proc Natl Acad Sci U S A, 2007. **104**(26): p. 11002-7.

16. Zappia, E., et al., *Mesenchymal stem cells ameliorate experimental autoimmune encephalomyelitis inducing T-cell anergy.* Blood, 2005. **106**(5): p. 1755-61.

17. Orlic, D., et al., *Bone marrow cells regenerate infarcted myocardium.* Nature, 2001. **410**(6829): p. 701-705.

18. Halfon, S., et al., *Markers Distinguishing Mesenchymal Stem Cells from Fibroblasts Are Downregulated with Passaging.* Stem Cells Dev, 2010.

19. Dimitriou, H., et al., *Are mesenchymal stromal cells from children resistant to apoptosis?* Cell Prolif, 2009. **42**(3): p. 276-83.

20. Jones, E., et al., *Large-scale extraction and characterization of CD271+ multipotential stromal cells from trabecular bone in health and osteoarthritis: implications for bone regeneration strategies based on uncultured or minimally cultured multipotential stromal cells.* Arthritis Rheum, 2010. **62**(7): p. 1944-54.

21. Le Douarin, N.M., G.W. Calloni, and E. Dupin, *The stem cells of the neural crest.* Cell Cycle, 2008. **7**(8): p. 1013-9.

22. Dupin, E., G.W. Calloni, and N.M. Le Douarin, *The cephalic neural crest of amniote vertebrates is composed of a large majority of precursors endowed with neural, melanocytic, chondrogenic and osteogenic potentialities.* Cell Cycle, 2010. **9**(2): p. 238-49.

23. Calloni, G.W., et al., *Sonic Hedgehog promotes the development of multipotent neural crest progenitors endowed with both mesenchymal and neural potentials.* Proc Natl Acad Sci U S A, 2007. **104**(50): p. 19879-84.

24. John, N., et al., *TGFbeta-Mediated Sox10 Suppression Controls Mesenchymal Progenitor Generation in Neural Crest Stem Cells.* Stem Cells, 2011.

25. Simmons, P.J. and B. Torok-Storb, *Identification of stromal cell precursors in human bone marrow by a novel monoclonal antibody, STRO-1.* Blood, 1991. **78**(1): p. 55-62.

26. Tavian, M., et al., *The vascular wall as a source of stem cells.* Ann N Y Acad Sci, 2005. **1044**: p. 41-50.

27. Crisan, M., et al., *A perivascular origin for mesenchymal stem cells in multiple human organs.* Cell Stem Cell, 2008. **3**(3): p. 301-13.

28. Gronthos, S., et al., *The STRO-1+ fraction of adult human bone marrow contains the osteogenic precursors.* Blood, 1994. **84**(12): p. 4164-73.

29. Shi, S. and S. Gronthos, *Perivascular niche of postnatal mesenchymal stem cells in human bone marrow and dental pulp.* J Bone Miner Res, 2003. **18**(4): p. 696-704.

30. da Silva Meirelles, L., A.I. Caplan, and N.B. Nardi, *In search of the in vivo identity of mesenchymal stem cells.* Stem Cells, 2008. **26**(9): p. 2287-99.

31. U.S. National Library of Medicine, U.S.N.I.o.H., U.S. Department of Health & Human Services, *Clinicaltrials.gov*, Lester Hill National Center for Biomedical Communications.

32. Devine, M.J., et al., *Transplanted bone marrow cells localize to fracture callus in a mouse model.* J Orthop Res, 2002. **20**(6): p. 1232-9.

33. Shen, F.H., et al., *Systemically administered mesenchymal stromal cells transduced with insulin-like growth factor-I localize to a fracture site and potentiate healing.* J Orthop Trauma, 2002. **16**(9): p. 651-9.

34. Shake, J.G., et al., *Mesenchymal stem cell implantation in a swine myocardial infarct model: engraftment and functional effects.* Ann Thorac Surg, 2002. **73**(6): p. 1919-25; discussion 1926.

35. Shi, M., et al., *Regulation of CXCR4 expression in human mesenchymal stem cells by cytokine treatment: role in homing efficiency in NOD/SCID mice.* Haematologica, 2007. **92**(7): p. 897-904.

36. Wang, Y., Y. Deng, and G.Q. Zhou, *SDF-1alpha/CXCR4-mediated migration of systemically transplanted bone marrow stromal cells towards ischemic brain lesion in a rat model.* Brain Res, 2008. **1195**: p. 104-12.

37. Hung, S.C., et al., *Short-term exposure of multipotent stromal cells to low oxygen increases their expression of CX3CR1 and CXCR4 and their engraftment in vivo.* PLoS ONE, 2007. **2**(5): p. e416.

38. Son, B.R., et al., *Migration of bone marrow and cord blood mesenchymal stem cells in vitro is regulated by stromal-derived factor-1-CXCR4 and hepatocyte growth factor-c-met axes and involves matrix metalloproteinases.* Stem Cells, 2006. **24**(5): p. 1254-64.

39. Chen, Y., et al., *Recruitment of endogenous bone marrow mesenchymal stem cells towards injured liver*. J Cell Mol Med, 2010. **14**(6B): p. 1494-508.

40. Viswanathan, A., et al., *Functional expression of N-formyl peptide receptors in human bone marrow-derived mesenchymal stem cells.* Stem Cells, 2007. **25**(5): p. 1263-9.

41. Sweeney, S.M., et al., *Candidate cell and matrix interaction domains on the collagen fibril, the predominant protein of vertebrates.* J Biol Chem, 2008. **283**(30): p. 21187-97.

42. Lu, C., et al., *MT1-MMP controls human mesenchymal stem cell trafficking and differentiation.* Blood, 2010. **115**(2): p. 221-9.

43. Zhang, W., C. Qin, and Z.M. Zhou, *Mesenchymal stem cells modulate immune responses combined with cyclosporine in a rat renal transplantation model.* Transplant Proc, 2007. **39**(10): p. 3404-8.

44. Laupacis, A., et al., *Cyclosporin A: a powerful immunosuppressant.* Can Med Assoc J, 1982. **126**(9): p. 1041-6.

45. Mitchell, J., et al., *Alpha-smooth muscle actin in parenchymal cells of bleomycin-injured rat lung.* Lab Invest, 1989. **60**(5): p. 643-50.

46. Iyer, S.S. and M. Rojas, *Anti-inflammatory effects of mesenchymal stem cells: novel concept for future therapies.* Expert Opin Biol Ther, 2008. **8**(5): p. 569-81.

47. Shi, Y., et al., *BMP Signaling Is Required for Heart Formation in Vertebrates.* Developmental Biology, 2000. **224**(2): p. 226-237.

48. Hare, J.M., et al., *A randomized, double-blind, placebo-controlled, dose-escalation study of intravenous adult human mesenchymal stem cells (prochymal) after acute myocardial infarction.* J Am Coll Cardiol, 2009. **54**(24): p. 2277-86.

49. Makino, S., et al., *Cardiomyocytes can be generated from marrow stromal cells in vitro.* J Clin Invest, 1999. **103**(5): p. 697-705.

50. Hakuno, D., et al., *Bone marrow-derived regenerated cardiomyocytes (CMG Cells) express functional adrenergic and muscarinic receptors.* Circulation, 2002. **105**(3): p. 380-6.

51. Behfar, A. and A. Terzic, *Derivation of a cardiopoietic population from human mesenchymal stem cells yields cardiac progeny.* Nat Clin Pract Cardiovasc Med, 2006. **3 Suppl 1**: p. S78-82.

52. Jiang, S., et al., *Supportive interaction between cell survival signaling and angiocompetent factors enhances donor cell survival and promotes angiomyogenesis for cardiac repair.* Circ Res, 2006. **99**(7): p. 776-84.

53. Copland, I.B., et al., *Coupling erythropoietin secretion to mesenchymal stromal cells enhances their regenerative properties.* Cardiovasc Res, 2008. **79**(3): p. 405-15.

54. Alvarez-Dolado, M., et al., *Fusion of bone-marrow-derived cells with Purkinje neurons, cardiomyocytes and hepatocytes.* Nature, 2003. **425**(6961): p. 968-73.

55. Iso, Y., et al., *Multipotent human stromal cells improve cardiac function after myocardial infarction in mice without long-term engraftment.* Biochem Biophys Res Commun, 2007. **354**(3): p. 700-6.

56. Satija, N.K., et al., *Mesenchymal stem cells: molecular targets for tissue engineering.* Stem Cells Dev, 2007. **16**(1): p. 7-23.

57. Uren, A., et al., *Secreted frizzled-related protein-1 binds directly to Wingless and is a biphasic modulator of Wnt signaling.* J Biol Chem, 2000. **275**(6): p. 4374-82.

58. Whelan, R.S., V. Kaplinskiy, and R.N. Kitsis, *Cell death in the pathogenesis of heart disease: mechanisms and significance.* Annu Rev Physiol, 2010. **72**: p. 19-44.

59. Shirozu, M., et al., *Characterization of Novel Secreted and Membrane Proteins Isolated by the Signal Sequence Trap Method.* Genomics, 1996. **37**(3): p. 273-280.

60. Tang, Y.L., et al., *Autologous mesenchymal stem cell transplantation induce VEGF and neovascularization in ischemic myocardium.* Regul Pept, 2004. **117**(1): p. 3-10.

61. Yoon, Y.S., et al., *Clonally expanded novel multipotent stem cells from human bone marrow regenerate myocardium after myocardial infarction.* J Clin Invest, 2005. **115**(2): p. 326-38.

62. Wang, Y.Q., et al., *Effect of transplanted mesenchymal stem cells from rats of different ages on the improvement of heart function after acute myocardial infarction.* Chin Med J (Engl), 2008. **121**(22): p. 2290-8.

63. Kinnaird, T., et al., *Marrow-derived stromal cells express genes encoding a broad spectrum of arteriogenic cytokines and promote in vitro and in vivo arteriogenesis through paracrine mechanisms.* Circ Res, 2004. **94**(5): p. 678-85.

64. Matsumoto, R., et al., *Vascular endothelial growth factor-expressing mesenchymal stem cell transplantation for the treatment of acute myocardial infarction.* Arterioscler Thromb Vasc Biol, 2005. **25**(6): p. 1168-73.

65. van der Meer, P., et al., *Erythropoietin in cardiovascular diseases.* Eur Heart J, 2004. **25**(4): p. 285-91.

66. Heeschen, C., et al., *Erythropoietin is a potent physiologic stimulus for endothelial progenitor cell mobilization.* Blood, 2003. **102**(4): p. 1340-6.

67. Liu, X.B., et al., *Angiopoietin-1 protects mesenchymal stem cells against serum deprivation and hypoxia-induced apoptosis through the PI3K/Akt pathway.* Acta Pharmacol Sin, 2008. **29**(7): p. 815-22.

68. Uemura, R., et al., *Bone marrow stem cells prevent left ventricular remodeling of ischemic heart through paracrine signaling.* Circ Res, 2006. **98**(11): p. 1414-21.

69. Wei, C.L., et al., *Transcriptome profiling of human and murine ESCs identifies divergent paths required to maintain the stem cell state.* Stem Cells, 2005. **23**(2): p. 166-85.

70. Dai, J., et al., *Bone morphogenetic protein-6 promotes osteoblastic prostate cancer bone metastases through a dual mechanism.* Cancer Res, 2005. **65**(18): p. 8274 - 8285.

71. Mirotsou, M., et al., *Secreted frizzled related protein 2 (Sfrp2) is the key Akt-mesenchymal stem cell-released paracrine factor mediating myocardial survival and repair.* Proc Natl Acad Sci U S A, 2007. **104**(5): p. 1643-1648.

72. Tsubokawa, T., et al., *Impact of anti-apoptotic and anti-oxidative effects of bone marrow mesenchymal stem cells with transient overexpression of heme oxygenase-1 on myocardial ischemia.* Am J Physiol Heart Circ Physiol, 2010. **298**(5): p. H1320-9.

73. Mangi, A.A., et al., *Mesenchymal stem cells modified with Akt prevent remodeling and restore performance of infarcted hearts.* Nat Med, 2003. **9**(9): p. 1195-201.

74. Horwitz, E.M., et al., *Isolated allogeneic bone marrow-derived mesenchymal cells engraft and stimulate growth in children with osteogenesis imperfecta: Implications for cell therapy of bone.* Proc Natl Acad Sci U S A, 2002. **99**(13): p. 8932-7.

75. Alfaro, M.P., et al., *The Wnt modulator sFRP2 enhances mesenchymal stem cell engraftment, granulation tissue formation and myocardial repair.* Proc Natl Acad Sci U S A, 2008. **105**(47): p. 18366-71.

76. Alfaro, M.P., et al., *sFRP2 suppression of bone morphogenic protein (BMP) and Wnt signaling mediates mesenchymal stem cell (MSC) self-renewal promoting engraftment and myocardial repair.* J Biol Chem, 2010. **285**(46): p. 35645-53.

77. McBrearty, B.A., et al., *Genetic analysis of a mammalian wound-healing trait.* Proc Natl Acad Sci U S A, 1998. **95**(20): p. 11792-7.

78. Heber-Katz, E., *The regenerating mouse ear.* Semin Cell Dev Biol, 1999. **10**(4): p. 415-9.

79. Heber-Katz, E., et al., *The scarless heart and the MRL mouse.* Philos Trans R Soc Lond B Biol Sci, 2004. **359**(1445): p. 785-93.

80. Bedelbaeva, K., et al., *The MRL mouse heart healing response shows donor dominance in allogeneic fetal liver chimeric mice.* Cloning Stem Cells, 2004. **6**(4): p. 352-63.

81. Otto, T.C. and M.D. Lane, *Adipose development: from stem cell to adipocyte.* Crit Rev Biochem Mol Biol, 2005. **40**(4): p. 229-42.

82. Gaur, T., et al., *Canonical WNT signaling promotes osteogenesis by directly stimulating Runx2 gene expression.* J Biol Chem, 2005. **280**(39): p. 33132-40.

83. Luo, Q., et al., *Connective tissue growth factor (CTGF) is regulated by Wnt and bone morphogenetic proteins signaling in osteoblast differentiation of mesenchymal stem cells.* J Biol Chem, 2004. **279**(53): p. 55958-68.

84. Yano, F., et al., *The canonical Wnt signaling pathway promotes chondrocyte differentiation in a Sox9-dependent manner.* Biochem Biophys Res Commun, 2005. **333**(4): p. 1300-8.

85. Gregory, C.A., et al., *Dkk-1-derived synthetic peptides and lithium chloride for the control and recovery of adult stem cells from bone marrow.* J Biol Chem, 2005. **280**(3): p. 2309-23.

86. Kawano, Y. and R. Kypta, *Secreted antagonists of the Wnt signalling pathway.* J Cell Sci, 2003. **116**(Pt 13): p. 2627-34.

87. Krummel, T.M., et al., *Transforming growth factor beta (TGF-beta) induces fibrosis in a fetal wound model.* J Pediatr Surg, 1988. **23**(7): p. 647-52.

88. Cooney, R., et al., *Tumor necrosis factor mediates impaired wound healing in chronic abdominal sepsis.* J Trauma, 1997. **42**(3): p. 415-20.

89. Pittenger, M.F. and B.J. Martin, *Mesenchymal stem cells and their potential as cardiac therapeutics.* Circ Res, 2004. **95**(1): p. 9-20.

90. Shtutman, M., et al., *The cyclin D1 gene is a target of the beta-catenin/LEF-1 pathway.* Proc Natl Acad Sci U S A, 1999. **96**(10): p. 5522-7.

91. Van Raay, T.J., et al., *Frizzled 5 signaling governs the neural potential of progenitors in the developing Xenopus retina.* Neuron, 2005. **46**(1): p. 23-36.

92. Jho, E.H., et al., *Wnt/beta-catenin/Tcf signaling induces the transcription of Axin2, a negative regulator of the signaling pathway.* Mol Cell Biol, 2002. **22**(4): p. 1172-83.

93. Lescher, B., B. Haenig, and A. Kispert, *sFRP-2 is a target of the Wnt-4 signaling pathway in the developing metanephric kidney.* Dev Dyn, 1998. **213**(4): p. 440-51.

94. Veeman, M.T., et al., *Zebrafish prickle, a modulator of noncanonical Wnt/Fz signaling, regulates gastrulation movements.* Curr Biol, 2003. **13**(8): p. 680-5.

95. Gregory, C.A., et al., *The Wnt signaling inhibitor dickkopf-1 is required for reentry into the cell cycle of human adult stem cells from bone marrow.* J Biol Chem, 2003. **278**(30): p. 28067-78.

96. Phinney, D.G. and D.J. Prockop, *Concise review: mesenchymal stem/multipotent stromal cells: the state of transdifferentiation and modes of tissue repair--current views.* Stem Cells, 2007. **25**(11): p. 2896-902.

97. Liu, H., et al., *Augmented Wnt signaling in a mammalian model of accelerated aging.* Science, 2007. **317**(5839): p. 803-6.

98. Brack, A.S., et al., *Increased Wnt signaling during aging alters muscle stem cell fate and increases fibrosis.* Science, 2007. **317**(5839): p. 807-10.

99. Cselenyi, C.S. and E. Lee, *Context-dependent activation or inhibition of Wnt-beta-catenin signaling by Kremen.* Sci Signal, 2008. **1**(8): p. pe10.

100. Rattner, A., et al., *A family of secreted proteins contains homology to the cysteine-rich ligand-binding domain of frizzled receptors.* Proc Natl Acad Sci U S A, 1997. **94**(7): p. 2859-2863.

101. Wawrzak, D., et al., *Wnt3a binds to several sFRPs in the nanomolar range.* Biochem Biophys Res Commun, 2007. **357**(4): p. 1119-23.

102. Dufourcq, P., et al., *Regulation of endothelial cell cytoskeletal reorganization by a secreted frizzled-related protein-1 and frizzled 4- and frizzled 7-dependent pathway: role in neovessel formation.* Am J Pathol, 2008. **172**(1): p. 37-49.

103. Schofield, R., *The stem cell system.* Biomed Pharmacother, 1983. **37**(8): p. 375-80.

104. Reya, T. and H. Clevers, *Wnt signalling in stem cells and cancer.* Nature, 2005. **434**(7035): p. 843-50.

105. McReynolds, L.J., et al., *Smad1 and Smad5 differentially regulate embryonic hematopoiesis.* Blood, 2007. **110**(12): p. 3881-90.

106. Suzuki, T. and S. Chiba, *Notch signaling in hematopoietic stem cells.* Int J Hematol, 2005. **82**(4): p. 285-94.

107. Gaur, T., et al., *Secreted frizzled related protein 1 regulates Wnt signaling for BMP2 induced chondrocyte differentiation.* J Cell Physiol, 2006. **208**(1): p. 87-96.

108. Goldring, M.B., K. Tsuchimochi, and K. Ijiri, *The control of chondrogenesis.* J Cell Biochem, 2006. **97**(1): p. 33-44.

109. Manton, K.J., et al., *Disruption of heparan and chondroitin sulfate signaling enhances mesenchymal stem cell-derived osteogenic differentiation via bone morphogenetic protein signaling pathways.* Stem Cells, 2007. **25**(11): p. 2845-54.

110. Denker, A.E., et al., *Chondrogenic differentiation of murine C3H10T1/2 multipotential mesenchymal cells: I. Stimulation by bone morphogenetic protein-2 in high-density micromass cultures.* Differentiation, 1999. **64**(2): p. 67-76.

111. Gregory, K.E., et al., *The prodomain of BMP-7 targets the BMP-7 complex to the extracellular matrix.* J Biol Chem, 2005. **280**(30): p. 27970 - 27980.

112. Finch, P.W., et al., *Purification and molecular cloning of a secreted, Frizzled-related antagonist of Wnt action.* Proc Natl Acad Sci U S A, 1997. **94**(13): p. 6770-5.

113. Ezan, J., et al., *FrzA/sFRP-1, a secreted antagonist of the Wnt-Frizzled pathway, controls vascular cell proliferation in vitro and in vivo.* Cardiovasc Res, 2004. **63**(4): p. 731-8.

114. Hoang, B., et al., *Primary structure and tissue distribution of FRZB, a novel protein related to Drosophila frizzled, suggest a role in skeletal morphogenesis.* J Biol Chem, 1996. **271**(42): p. 26131-7.

115. Thorne, C.A., et al., *Small-molecule inhibition of Wnt signaling through activation of casein kinase 1alpha.* Nat Chem Biol, 2010. **6**(11): p. 829-36.

116. Komori, T., et al., *Targeted disruption of Cbfa1 results in a complete lack of bone formation owing to maturational arrest of osteoblasts.* Cell, 1997. **89**(5): p. 755-64.

117. Ducy, P., *Cbfa1: a molecular switch in osteoblast biology.* Dev Dyn, 2000. **219**(4): p. 461-71.

118. Lee, K.S., S.H. Hong, and S.C. Bae, *Both the Smad and p38 MAPK pathways play a crucial role in Runx2 expression following induction by transforming growth factor-beta and bone morphogenetic protein.* Oncogene, 2002. **21**(47): p. 7156-63.

119. Collavin, L. and M.W. Kirschner, *The secreted Frizzled-related protein Sizzled functions as a negative feedback regulator of extreme ventral mesoderm.* Development, 2003. **130**(4): p. 805-16.

120. Zilberberg, L., et al., *A rapid and sensitive bioassay to measure bone morphogenetic protein activity.* BMC Cell Biol, 2007. **8**: p. 41.

121. Yu, P.B., et al., *Dorsomorphin inhibits BMP signals required for embryogenesis and iron metabolism.* Nat Chem Biol, 2008. **4**(1): p. 33-41.

122. Breitbach, M., et al., *Potential risks of bone marrow cell transplantation into infarcted hearts.* Blood, 2007. **110**(4): p. 1362-9.

123. Zhang, Z., et al., *Secreted frizzled related protein 2 protects cells from apoptosis by blocking the effect of canonical Wnt3a.* J Mol Cell Cardiol, 2009. **46**(3): p. 370-7.

124. Melkonyan, H.S., et al., *SARPs: A family of secreted apoptosis-related proteins.* Proceedings of the National Academy of Sciences, 1997. **94**(25): p. 13636-13641.

125. Sasai, Y., et al., *Xenopus chordin: a novel dorsalizing factor activated by organizer-specific homeobox genes.* Cell, 1994. **79**(5): p. 779-90.

126. De Robertis, E.M. and H. Kuroda, *Dorsal-ventral patterning and neural induction in Xenopus embryos.* Annu Rev Cell Dev Biol, 2004. **20**: p. 285-308.

127. Lee, H.X., et al., *Embryonic dorsal-ventral signaling: secreted frizzled-related proteins as inhibitors of tolloid proteinases.* Cell, 2006. **124**(1): p. 147-59.

128. Misra, K. and M.P. Matise, *A critical role for sFRP proteins in maintaining caudal neural tube closure in mice via inhibition of BMP signaling.* Dev Biol, 2010. **337**(1): p. 74-83.

129. Gnecchi, M., et al., *Paracrine mechanisms in adult stem cell signaling and therapy.* Circ Res, 2008. **103**(11): p. 1204-19.

130. Caplan, A.I. and J.E. Dennis, *Mesenchymal stem cells as trophic mediators.* J Cell Biochem, 2006. **98**(5): p. 1076-84.

131. He, W., et al., *Exogenously administered secreted frizzled related protein 2 (Sfrp2) reduces fibrosis and improves cardiac function in a rat model of myocardial infarction.* Proc Natl Acad Sci U S A, 2010. **107**(49): p. 21110-5.

132. Estrada, R., et al., *Secretome from mesenchymal stem cells induces angiogenesis via Cyr61.* J Cell Physiol, 2009. **219**(3): p. 563-71.

133. Salasznyk, R.M., et al., *Comparing the protein expression profiles of human mesenchymal stem cells and human osteoblasts using gene ontologies.* Stem Cells Dev, 2005. **14**(4): p. 354-66.

134. Polacek, M., et al., *The secretory profiles of cultured human articular chondrocytes and mesenchymal stem cells: implications for autologous cell transplantation strategies.* Cell Transplant, 2010.

135. Higdon, R., et al., *Randomized sequence databases for tandem mass spectrometry peptide and protein identification.* OMICS, 2005. **9**(4): p. 364-79.

136. Elias, J.E., et al., *Comparative evaluation of mass spectrometry platforms used in large-scale proteomics investigations.* Nat Methods, 2005. **2**(9): p. 667-75.

137. Ma, Z.Q., et al., *IDPicker 2.0: Improved protein assembly with high discrimination peptide identification filtering.* J Proteome Res, 2009. **8**(8): p. 3872-81.

138. Shi-Wen, X., A. Leask, and D. Abraham, *Regulation and function of connective tissue growth factor/CCN2 in tissue repair, scarring and fibrosis.* Cytokine Growth Factor Rev, 2008. **19**(2): p. 133-44.

139. Rachfal, A.W. and D.R. Brigstock, *Structural and functional properties of CCN proteins.* Vitam Horm, 2005. **70**: p. 69-103.

140. Ito, Y., et al., *Expression of connective tissue growth factor in human renal fibrosis.* Kidney Int, 1998. **53**(4): p. 853-61.

141. di Mola, F.F., et al., *Connective tissue growth factor is a regulator for fibrosis in human chronic pancreatitis.* Ann Surg, 1999. **230**(1): p. 63-71.

142. Igarashi, A., et al., *Connective tissue growth factor gene expression in tissue sections from localized scleroderma, keloid, and other fibrotic skin disorders.* J Invest Dermatol, 1996. **106**(4): p. 729-33.

143. Igarashi, A., et al., *Regulation of connective tissue growth factor gene expression in human skin fibroblasts and during wound repair.* Mol Biol Cell, 1993. **4**(6): p. 637-45.

144. Leask, A. and D.J. Abraham, *The role of connective tissue growth factor, a multifunctional matricellular protein, in fibroblast biology.* Biochem Cell Biol, 2003. **81**(6): p. 355-63.

145. Lee, C.H., et al., *CTGF directs fibroblast differentiation from human mesenchymal stem/stromal cells and defines connective tissue healing in a rodent injury model.* J Clin Invest, 2010. **120**(9): p. 3340-9.

146. Frazier, K., et al., *Stimulation of fibroblast cell growth, matrix production, and granulation tissue formation by connective tissue growth factor.* J Invest Dermatol, 1996. **107**(3): p. 404-11.

147. Ivkovic, S., et al., *Connective tissue growth factor coordinates chondrogenesis and angiogenesis during skeletal development.* Development, 2003. **130**(12): p. 2779-91.

148. Crawford, L.A., et al., *Connective tissue growth factor (CTGF) inactivation leads to defects in islet cell lineage allocation and beta-cell proliferation during embryogenesis.* Mol Endocrinol, 2009. **23**(3): p. 324-36.

149. Draper, B.K., et al., *Topical epiregulin enhances repair of murine excisional wounds.* Wound Repair Regen, 2003. **11**(3): p. 188-97.

150. Ujike, K., et al., *Kinetics of expression of connective tissue growth factor gene during liver regeneration after partial hepatectomy and D-galactosamine-induced liver injury in rats.* Biochem Biophys Res Commun, 2000. **277**(2): p. 448-54.

151. Mori, T., et al., *Role and interaction of connective tissue growth factor with transforming growth factor-beta in persistent fibrosis: A mouse fibrosis model.* J Cell Physiol, 1999. **181**(1): p. 153-9.

152. Bonniaud, P., et al., *Adenoviral gene transfer of connective tissue growth factor in the lung induces transient fibrosis.* Am J Respir Crit Care Med, 2003. **168**(7): p. 770-8.

153. Ikawa, Y., et al., *Neutralizing monoclonal antibody to human connective tissue growth factor ameliorates transforming growth factor-beta-induced mouse fibrosis.* J Cell Physiol, 2008. **216**(3): p. 680-7.

154. Chen, Y., et al., *Matrix contraction by dermal fibroblasts requires transforming growth factor-beta/activin-linked kinase 5, heparan sulfate-containing proteoglycans, and MEK/ERK: insights into pathological scarring in chronic fibrotic disease.* Am J Pathol, 2005. **167**(6): p. 1699-711.

155. Arnold, F. and D.C. West, *Angiogenesis in wound healing.* Pharmacol Ther, 1991. **52**(3): p. 407-22.

156. Liu, L.D., et al., *The repairing effect of a recombinant human connective-tissue growth factor in a burn-wounded rhesus-monkey (Macaca mulatta) model.* Biotechnol Appl Biochem, 2007. **47**(Pt 2): p. 105-12.

157. Kobayashi, K., et al., *Secreted Frizzled-related protein 2 is a procollagen C proteinase enhancer with a role in fibrosis associated with myocardial infarction.* Nat Cell Biol, 2009. **11**(1): p. 46-55.

158. Thackham, J.A., D.L.S. McElwain, and R.J. Long, *The use of hyperbaric oxygen therapy to treat chronic wounds: A review.* Wound Repair and Regeneration, 2008. **16**(3): p. 321-330.

159. Ladher, R.K., et al., *Cloning and Expression of the Wnt Antagonists Sfrp-2 and Frzb during Chick Development.* Developmental Biology, 2000. **218**(2): p. 183-198.

160. Boland, G.M., et al., *Wnt 3a promotes proliferation and suppresses osteogenic differentiation of adult human mesenchymal stem cells.* Journal of Cellular Biochemistry, 2004. **93**(6): p. 1210-1230.

161. Bowers, R.R. and M.D. Lane, *A role for bone morphogenetic protein-4 in adipocyte development.* Cell Cycle, 2007. **6**(4): p. 385-9.

162. Kelly, S.S., et al., *Ex vivo expansion of cord blood.* Bone Marrow Transplant, 2009. **44**(10): p. 673-81.

163. Eckfeldt, C.E., E.M. Mendenhall, and C.M. Verfaillie, *The molecular repertoire of the 'almighty' stem cell.* Nat Rev Mol Cell Biol, 2005. **6**(9): p. 726-37.

164. Levin, J.M., et al., *SFRP2 expression in rabbit myogenic progenitor cells and in adult skeletal muscles.* J Muscle Res Cell Motil, 2001. **22**(4): p. 361-9.

165. Scime, A., et al., *Transcriptional profiling of skeletal muscle reveals factors that are necessary to maintain satellite cell integrity during ageing.* Mech Ageing Dev, 2010. **131**(1): p. 9-20.

166. Anakwe, K., et al., *Wnt signalling regulates myogenic differentiation in the developing avian wing.* Development, 2003. **130**(15): p. 3503-14.

167. Zhao, P. and E.P. Hoffman, *Embryonic myogenesis pathways in muscle regeneration.* Developmental Dynamics, 2004. **229**(2): p. 380-392.

168. Descamps, S., et al., *Inhibition of myoblast differentiation by Sfrp1 and Sfrp2.* Cell Tissue Res, 2008. **332**(2): p. 299-306.

169. Iwano, M., et al., *Evidence that fibroblasts derive from epithelium during tissue fibrosis.* J Clin Invest, 2002. **110**(3): p. 341-50.

170. Abremski, K., et al., *Bacteriophage P1 Cre-loxP site-specific recombination. Site-specific DNA topoisomerase activity of the Cre recombination protein.* J Biol Chem, 1986. **261**(1): p. 391-6.

171. Ventura, A., et al., *Restoration of p53 function leads to tumour regression in vivo.* Nature, 2007. **445**(7128): p. 661-5.

172. Bovolenta, P., et al., *Beyond Wnt inhibition: new functions of secreted Frizzled-related proteins in development and disease.* J Cell Sci, 2008. **121**(Pt 6): p. 737-46.